Multi-Loading Ligands to Transport Copper

Dorothy Christina Rankin Henry

Doctor of Philosophy

School of Chemistry

University of Edinburgh

May 2007

Abstract

This thesis concerns the design and evaluation of the properties of new types of metal extractants for use in the mining industry. Current reagents and industrial solvent extraction processes are discussed in Chapter 1. In order to improve established extraction operations, ligands which increase mass transport efficiency are considered. The new ligands are diacids and can thus form neutral complexes with divalent metals with a 1 : 1 ligand to metal stoichiometry, improving on the 2 : 1 stoichiometry achieved by conventional reagents which operate in pH-controlled solvent extraction processes. In addition, in order to address new, high tenor feed solutions resulting from the mining of sulfidic ores, this improved stoichiometry should be coupled with the ability to extract metal cations and their attendant anions cooperatively in a loading process which does not change the pH of the aqueous feed.

Chapter 2 addresses the improvement in mass transport using the diacidic imine ligand, 4-*t*-butyl-2-{[(*E*)-5-*t*-butyl-2-hydroxy-phenylimino]methyl}-phenol (**1**). This prototype ligand is shown to form complexes with nickel in the desired 1 : 1 ligand to metal ratio. X-ray structure determination of crystals of the nickel complex obtained by slow evaporation of a methanol solution shows this to be a tetranuclear complex $[Ni_4(\mathbf{1}–2H)_4(MeOH)_4]$, with interesting magnetic properties. The strength of **1** as an extractant for nickel into chloroform was found to be too low ($pH_{½}$ *ca.* 6.7) to be used commercially for recovery from mixed Ni(II)/Fe(III) feeds. However, it is potentially much more practicable for the recovery of copper ($pH_{½}$ *ca.* 3). EPR experiments support formation of dinuclear copper(II) complexes $[Cu_2(\mathbf{1}–2H)_2]$, in chloroform with μ–phenoxy bridges between the copper(II) ions. Addition of 3-*iso*-propyl-2-pyrazol-5-one to chloroform solutions of **1** results in extraction of copper(II) as the mononuclear ternary complex [Cu(**1**–2H)(3-*iso*-propyl-2-pyrazol-5-one)] with a useful reduction of the $pH_{½}$ value to *ca.* 1.6.

Modification of **1** by substitution *ortho* to the hydroxyl group on one or both aromatic rings of either a *N*-piperidinomethyl or bis(*n*-hexyl)aminomethyl group to generate potential metal *salt* extractants is discussed in chapter 3. Solvent extraction

experiments have shown that the piperidinomethyl-substituted ligand, 4-*t*-butyl-2-{[(*E*)-5-*t*-butyl-2-hydroxy-phenylimino]-methyl}-6-piperidinyl-phenol (**5**), extracts *both* copper(II) cations and sulfate counter anions in a pH range which is applicable to processing high tenor feeds from pressure leaching of sulfidic ores. Loading data are consistent with the formation of a 2 : 2 : 1 assembly, $[Cu_2(\mathbf{5}–H)_2(SO_4)]$, and with the sulfate ion being located within the inner coordination sphere of the copper(II) centre. The effects of addition of the auxiliary ligand 3-*iso*-propyl-2-pyrazol-5-one on the behaviour of **5** as an extractant are reported. Unlike **1**, see above, no increase in strength of copper(II) extraction is recorded and in general the addition has an adverse effect on sulfate loading.

In order to establish whether **5** or structurally related analogues could be used as industrial reagents, a series of experiments was carried out to probe solubility, stability and selectivity. As a means of increasing solubility in water-immiscible solvents, the nonyl-substituted analogue, 4-nonyl-2-{[(*E*)-5-nonyl-2-hydroxy-phenylimino]-methyl}-6-piperidinyl-phenol (**10**) was synthesised. This modification resulted in a decrease in $pH_{½}$ for copper(II) sulfate extraction, improving the potential recovery from high tenor, low pH, feeds. However, the stability to hydrolysis, although improved in comparison to **5**, is unsuitable for use in a commercial process. Also there is no selectivity of copper when iron is present in the feed and **10** selectively extracts chloride over sulfate when both are present in equal concentration.

Acknowledgements

First and foremost, my most sincere thanks go to Professor Peter Tasker. He has been a great support and inspiration throughout my PhD studies. Thank you for your time and patience throughout the past few years - I could never have got here without you!

Next I must thank my fellow Tasker group members. Having also been a Masters Project student in the group "one or two" years ago, there are many who've come and gone in the time I've been around! Those who I'd like to mention in particular are Dave, Stuart, Jenny, Rachel, Arjan, Ross F. and Ross G. - you lot made my lab time fun!

The crystallographers have been very helpful too - my appreciation to both Fraser White and Dr Simon Parsons for their time and patience with not always the most simple of structures! Their company on many Friday nights in KB bar has also been a highlight of the past few years.

For EPR assistance I would like to thank both Professor Lesley Yellowlees and Paul Murray - their knowledge knows no bounds! Many thanks also to Professor Andrew Harrison for his work on the magnetism of the cubane.

Many thanks to the technicians, Alan Taylor for his mass spectrometry skills, and John Millar for his NMR expertise, and more importantly to them both for their respective chats whenever I passed! Lorna Eades has been most helpful with ICP-OES problems and thanks to her especially for getting the online booking system up and running.

Now we come to the friends I've made in my time in the Joseph Black Building. Since this is the ten year anniversary of the year I first set foot here, there are more than I can possibly do justice to here. However, some stick out from the last couple of years: Anne-Marie Fuller, Maria Kaisheva, Fiona Mackay, Anna Peacock (Wineapple to those in the know), Craig McGowan, Iain Smellie, Andy Welland,

Tom Young and the unforgettable Mourad Chennaoui. Thank you all for a fantastic social side to the PhD experience, it's been a blast!

To my wonderful family (who there are also too many of to thank here), thank you for all your love and support throughout the many, many years I've been a student! Of special importance are my Grannies. And also my Papa who unfortunately isn't here to see me become a doctor at last, even if it is a different kind of doctor! But most important of all are my Mum, Dad and wee sisters Susan and Cara - I love you all very much and just knowing you're there at the other end of the phone/road whenever I need you makes all the difference. Thank you.

So, Dr Iain Inverarity, what to say about you?! You've got me this far. Who else could have made me go into that box room and batter out more pages for poor Peter to have to read? I'm not sure. Thank you for your support throughout this whole writing experience, even when you had just as important things to be doing yourself. Our time together so far has been great, and to steal just one line from your thesis...long may it continue.

Contents

Preface and Declaration i
Abstract ii
Acknowledgements iv
Contents vi
Ligands x
Abbreviations xi

1 CHAPTER 1 1
1.1 Thesis Aims 3
1.2 Copper 3
1.3 Nickel 4
1.4 Metallurgy 5
1.5 Pyrometallurgy[9] 6
1.6 Hydrometallurgy 9
1.6.1 Cation-exchange extraction of copper 11
1.6.2 Phenolic oxime extractants for copper 13
1.7 Mass Transport Efficiency of Solvent Extraction 15
1.8 Metal Salt Extractants 17
1.9 High Transport Efficiency of Metal Salts 21
1.10 Reagent Design Criteria 22
1.11 Systems Chosen for Study 23
1.12 Analysis of Extracted Species 25
1.12.1 Inductively Coupled Plasma-Optical Emission Spectroscopy[27] 26
1.12.2 Electron Paramagnetic Resonance (EPR)[28] 27
1.13 Thesis Outline 29
1.14 References 30

2 CHAPTER 2 32
2.1 Introduction 34
2.2 Ligand synthesis and characterisation 39
2.2.1 Crystal structure of ligand 1 40
2.3 Preparation and characterisation of metal complexes 42
2.4 Nickel complex formation and solvent extraction by ligand 1 45
2.4.1 Crystallography 46
2.4.2 Magnetism 56
2.4.3 Solvent extraction 58
2.5 Copper complex formation and solvent extraction by ligand 1 61
2.5.1 Solvent extraction 62
2.5.2 Electron paramagnetic resonance (EPR) 65
2.5.3 Mononuclear complexes containing an auxiliary ligand 67
2.6 Conclusions 72
2.7 References 74

3 CHAPTER 3 78
3.1 Introduction 80
3.2 Ligand synthesis and characterisation 84
3.3 Metal complex synthesis and characterisation 91
3.4 Solvent extraction 95
3.4.1 Stripping 96
3.4.2 Loading 103
3.4.3 EPR 108
3.4.4 Mononuclear complexes containing an auxiliary ligand 111
3.4.5 'Dual-Host' studies 116
3.4.6 Cooperativity of copper/anion binding 120
3.5 Conclusions 124
3.6 References 125

4 CHAPTER 4 126

4.1 Introduction 128

4.2 Synthesis and characterisation of ligands 130

4.3 Solvent extraction 132

4.3.1 Stripping 132

4.3.2 Loading 133

4.3.3 EPR of extracted species 136

4.4 Stability 138

4.4.1 Strip/load cycles 138

4.4.2 Ligand stability to hydrolysis 140

4.5 Selectivity 143

4.5.1 Copper(II) and iron(III) 143

4.5.2 Sulfate and chloride 143

4.6 Conclusions 145

4.7 References 147

5 CHAPTER 5 148

5.1 Instrumentation 150

5.2 Ligand Synthesis 152

5.3 Metal complex synthesis 177

5.4 Liquid : liquid extraction experiments 180

5.4.1 Stripping 180

5.4.2 Loading 181

5.4.3 Load/Strip Cycles 182

5.4.4 Selectivity of copper(II)/ iron(III) 182

5.4.5 Selectivity of sulfate/chloride 182

5.5 X-ray Crystallography 183

5.6 EPR 183

6 CHAPTER 6 185

Conclusions 186

7 CHAPTER 7.....189

Appendix CD contents.....190

Ligands

- Ligand **1** is discussed in Chapter 2

1

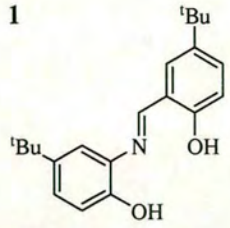

- Ligands **2-8** are discussed in Chapter 3

2

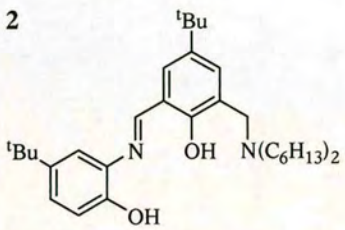

3

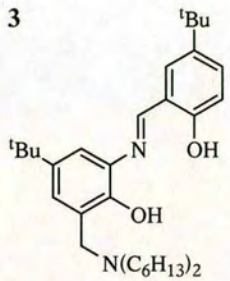

4

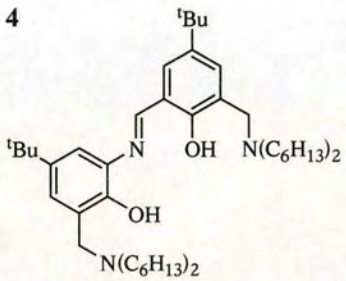

5

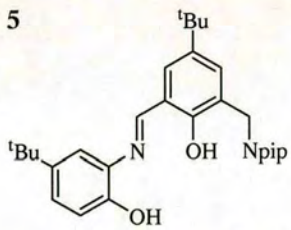

6

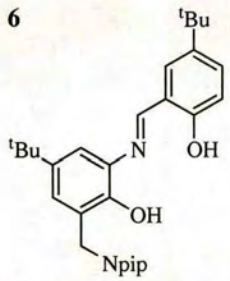

7

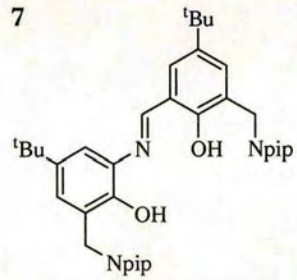

8

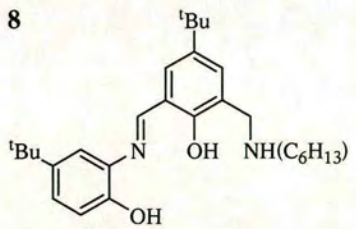

- Ligands **9** and **10** are discussed in Chapter 4

9

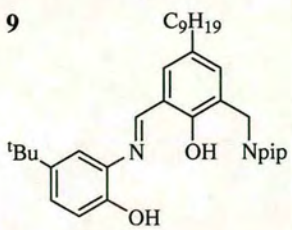

10

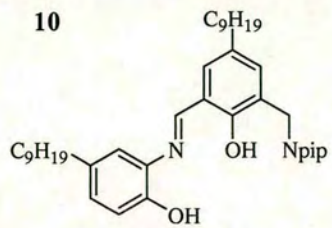

Abbreviations

δ	chemical shift
°	degrees
°C	degree centigrade
$	dollars
<	less than
≤	less than or equal to
>	more than
≥	more than or equal to
%	percent
±	plus or minus
~	approximately
√	square route
ν	wavenumber (IR)
μ_B	effective magnetic moment
aq	aqueous phase
Å	Angstrom
Ar	aromatic (NMR)
aux	auxiliary ligand
Boc	Boc anhydride (di-*t*-butyldicarbonate)
BM	Bohr magneton
bs	broad singlet (NMR)
C	coulomb
ca.	*circa* (approximately)
$CDCl_3$	deuterated chloroform
cf.	compare
CHN	elemental analysis
cis	*cisoid*
cm^{-1}	wavenumber
conc.	concentrated
CSD	Cambridge Structural Database
d	doublet (NMR)
D	distribution coefficient
D_2O	deuterated water
DCM	dichlormethane
dd	doublet of doublets (NMR)
dihex	dihexylamino
e.g.	for example
eds.	editor(s)
emu	electromagnetic unit
ES	Electrospray
et al.	*et alli* (and others)
EtOH	ethanol
EPR	Electron Paramagnetic Resonance
Equ.	Equation
equi	equimolar
ΔE	difference in energy

FAB	Fast Atom Bombardment
fac	*facial*
G	gauss
g	gram
g	g-factor, or spectroscopic splitting factor
$g\ l^{-1}$	grams per litre
HCl	hydrochloric acid
h	hour
h	Planck's constant
Hz	Hertz
I	Nuclear spin quantum number
i.e.	that is
ICP-OES	Inductively Coupled Plasma Optical Emission Spectroscopy
in situ	in the natural place
in vacuo	under vacuum
IR	Infrared
J	coupling constant (NMR)
J	joule
K	Kelvin
$kJ\ mol^{-1}$	kilojoules per mole
lit.	literature
m	multiplet (NMR)
M	Molar
m	*meta*
m/z	mass per unit charge
Me	methyl
Mer	*meridional*
mg	milligrams
MHz	Mega Hertz
min	minute
ml	millilitre
mmHg	millimetres of mercury
mmol	millimoles
mol	moles
$mol\ dm^{-3}$	moles per decimetre cubed
$mol\ g^{-1}$	moles per gram
MS	Mass Spectrometry
M_s	spin quantum number
MW	molecular weight
nm	nanometre
NMR	Nuclear Magnetic Resonance
NOBA	3-Nitrobenzyl Alcohol
o	*ortho*
OAc	acetate
org	organic phase
p	*para*
pH	$-\log_{10}[H^+]$
$pH_{½}$	pH when log D = 0

$\Delta pH_{½}$	difference in $pH_{½}$
Ph	phenyl
pip	piperidine
p*K*a	$-\log_{10}$[acid dissociation constant]
pls	pregnant leach solution
ppm	parts per million
q	quartet (NMR)
r	radius
s	singlet (NMR)
s	seconds
t	triplet (NMR)
t	tertiary
θ	Weiss temperature
^{t}Bu	tertiary butyl
T	temperature
T	tesla
TFA	trifluoroacetic acid
trans	*transoid*
US	United States of America
ν	microwave frequency
via	by way of
vs.	versus

CHAPTER 1

1 CHAPTER 1 1

1.1 Thesis Aims 3

1.2 Copper 3

1.3 Nickel 4

1.4 Metallurgy 5

1.5 Pyrometallurgy[9] 6

1.6 Hydrometallurgy 9

1.6.1 Cation-exchange extraction of copper 11

1.6.2 Phenolic oxime extractants for copper 13

1.7 Mass Transport Efficiency of Solvent Extraction 15

1.8 Metal Salt Extractants 17

1.9 High Transport Efficiency of Metal Salts 21

1.10 Reagent Design Criteria 22

1.11 Systems Chosen for Study 23

1.12 Analysis of Extracted Species 25

1.12.1 Inductively Coupled Plasma-Optical Emission Spectroscopy[27] 26

1.12.2 Electron Paramagnetic Resonance (EPR)[28] 27

1.13 Thesis Outline 29

1.14 References 30

1.1 Thesis Aims

This thesis aims to develop novel reagents for the extraction of copper and nickel. Industry uses liquid-liquid solvent extraction to separate and concentrate metals of value from their mined ores. In order to improve upon conventional extractants used commercially, their mass transport efficiency is addressed. Extending this concept towards the transport of the cation of choice along with its attendant anion(s) to extract a metal salt is another key target.

1.2 Copper

Copper is an important element in the modern world. It is used extensively in a wide range of applications; in electronics in its pure elemental form; as an alloy for use in structural engineering, household products and coinage; and copper compounds are used in scientific applications such as catalysis, biostatic surfaces and fungicides.[1]

The price of copper is on the increase. In the first 8 months of 2006, the average copper price was US$ 6,490 a tonne, an increase of 89% compared to the corresponding period in 2005.[2] Globally, over 16 million tonnes of copper were produced in 2006. However, any disruption in supply can prove costly and further boost the copper price. For example, in July 2006 the Escondida mine in Chile ceased production due to industrial action, resulting in an estimated loss of production of 45,000 tonnes of copper.[2] In the same month, the largest copper mine in the world, Chuquicamata, also in Chile, suffered a disruption due to a rockslide which damaged vital equipment. The estimated loss of production was around 30,000 tonnes of copper.[2] Losses in production such as these, with others always possible, help to maintain high copper prices. The price of copper has risen so consistently over the years that, in 1982, the US government stopped making one-cent coins from copper and they now contain mostly zinc (99.2%). Consequently, pre-1982 pennies are now worth two cents, double their face value![3]

The worldwide demand for copper has increased in line with production, with a forecast global consumption of 17.9 million tonnes in 2007, an annual increase of 4.2%.[2] This growth is driven mainly by China, which continues its industrialisation,

urbanisation and expansion of electric power grids. In particular, huge infrastructure projects such as the Three Gorges Dam, the 2008 Beijing Olympics and the 2010 World Expo demand more copper than China can produce.[1]

In order to maintain a strong copper market, it is important that manufacturers improve efficiency and lower the cost of production. In 2007, the media are widely publicising Climate Change, increasing pressure on industry to develop less wasteful, more environmentally friendly processes.

1.3 Nickel

Nickel is another very useful metal. The addition of nickel, even in small quantities, significantly increases the durability, strength and resistance to corrosion of steel, and the manufacture of stainless steel accounts for 65% of the total nickel produced worldwide.[4] Of the remaining thirty-five percent, 20% is used for other steel and non-ferrous alloys, often for highly specialized industrial, aerospace and military applications. About 9% is used in plating and 6% in other uses including coins and a variety of nickel based chemicals.[4]

In 2006, the average price of nickel was US$ 20,300 per tonne, 38% higher than in 2005.[2] This increase in price is, as for copper, due to disruption in supply, declining stocks and increase in demand from China. Of the 1.3 million tonnes of nickel produced globally in 2005, only about 20% was produced in Asia, compared with consumption of almost 50% of the world's nickel (Figure 1.1).

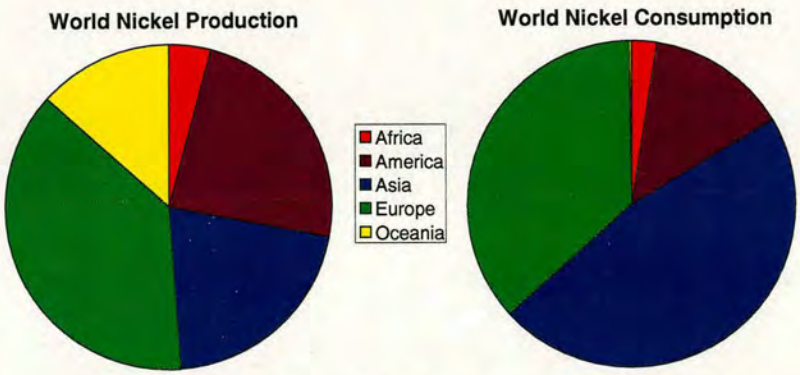

Figure 1.1: World production and consumption of nickel.[5]

The exceptionally high price of nickel is also affecting the United States Mint. One US 10¢ coin (nickel) contains 75% copper and 25% nickel, making the melting down of coins to sell the metal for profit a real possibility. In order to avoid this practise, in December 2006, the US Mint implemented new interim rules which criminalise the melting and export of pennies and nickels.[6]

The same industrial challenges which concern copper companies also affect nickel producers. New methods which are less expensive, but with less environmental impact for the production of both metals are urgently required.

1.4 Metallurgy

The earth's atmosphere was originally mainly composed of SO_2 and CO_2. At this time, metal ores formed as metal sulfides. As photosynthesis took over, the atmosphere changed and when oxygen became one of its main components, exposed metal sulfides were oxidised to produce oxidic ores. This left metal deposits having three layers: a sulfidic lower layer, a mixed sulfidic/oxidic ("transition ore") middle layer and a superficial oxidic layer.[7]

Metallurgy is defined as "The branch of applied science concerned with the production of metals from their ores, the purification of metals, the manufacture of alloys, and the use and performance of metals in engineering practise."[8] Generally, extractive metallurgy involves industrial processes in which ores containing low concentrations of a metal are processed to obtain it in a pure form. The earliest evidence of metallurgical processing is of copper smelting in around 4000 BC.[7] Today, techniques such as pyrometallurgy and hydrometallurgy make up the world's processing of metal ores.

There are four "unit operations" usually involved in a metallurgical process:[9]

- Concentration – of the desired metal from the ore deposit,
- Separation – of the desired metal from other metals present in the ore,
- Reduction – generation of M^0 from M^{n+},
- Refining – when very high purity metal is required.

1.5 Pyrometallurgy[9]

The earliest processing of metal ores was carried out *via* simple reduction by heating (or smelting) the ore, often in the presence of a reducing agent such as carbon.[7] An example of modern pyrometallurgical processing is the extraction of copper from its sulfidic ore (*e.g.* chalcopyrite, $CuFeS_2$), involving four steps (Figure 1.2).

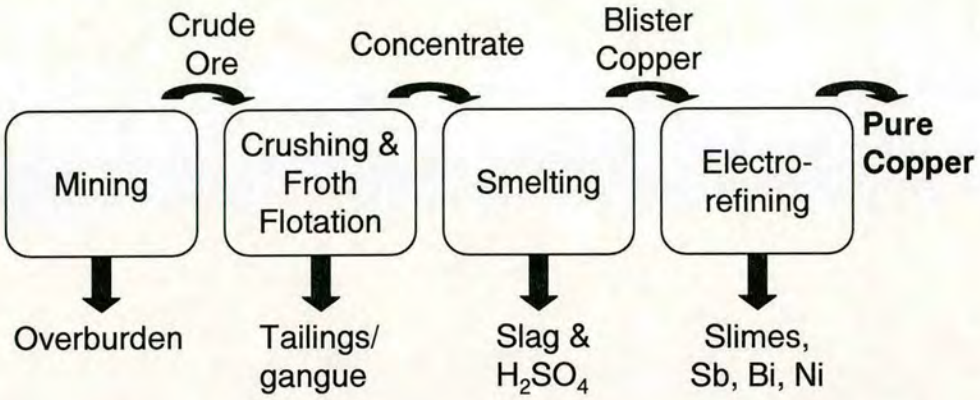

Figure 1.2: Flowsheet for recovery of copper *via* pyrometallurgy.[9]

First, the ore is mined and crushed, before undergoing a process of concentration *via* froth flotation. This involves the separation of the sulfide particles from silicate waste material, or gangue. The sulfide particles are preferentially selected by a flotating agent or collector, which float them in an oil froth which is removed from the separator. The silicate wastes, or "gangue", are wetted by water and drawn off from the bottom of the separator. The copper concentrate is then smelted in two steps, beginning with the generation of a "matte" containing Cu_2S in an oxygen flash furnace. The concentrate, sand and oxygen are blown into a furnace at *ca.* 1300°C, causing the reaction seen below, which is driven by the production of thermodynamically stable SO_2.[10]

$$2CuFeS_2 + 2O_2 \rightarrow Cu_2S + 2FeO + 3SO_2$$

The matte is dense and can therefore be drawn off from the bottom of the furnace, the SO_2 is vented off from the top and the iron oxides are removed as slag by addition of silica flux:

$$2FeO + SiO_2 \rightarrow Fe_2SiO_4.$$

The matte is then converted to copper by controlled oxidation, generating sulfur dioxide:

$$Cu_2S + O_2 \rightarrow 2Cu + SO_2.$$

This copper is 98% pure "blister copper" which is caste into "blister anodes" and refined using electrolysis. These anodes are set in cells containing an acidic copper sulfate electrolyte. As current is applied, copper dissolves from the anode and deposition occurs on the stainless steel cathode. The reactions involved at the electrodes are seen below. The pure copper cathodes are then sold or melted and cast prior to sale. The impurities at the anode either dissolve in the electrolyte or sink to the bottom of the cell as "slime".

$$\text{Anode:} \quad Cu^0 \rightarrow Cu^{2+} + 2e^-$$

$$\text{Cathode:} \quad Cu^{2+} + 2e^- \rightarrow Cu^0$$

The pyrometallurgical process has been improved and modernised and is used on a huge scale. This continual upgrading has led to a steady decrease in operating costs for traditional smelter/refinery operations and hence lower metal price. Any hydrometallurgical process must work at a comparable low or lower cost in order to compete in the modern metal market.

Despite improvements in the pyrometallurgical process, there are still a number of disadvantages.[11] The capital cost of smelter and refinery complexes is high, at US$ 3,000- 5,000 of investment per annual tonne of copper.[11] Impurities are a problem in smelting operations, with limited ability to treat concentrates with high levels of impurity. The emission of toxic gases such as sulfur dioxide is also of great concern, with ever more environmental awareness throughout the world. Even systems which

do fix the SO_2 as sulfuric acid then have the problem of market saturation, with less demand for it as more is produced. Finally, with high-grade metal ores becoming less available, processing of low-grade ores must be tackled which often is not cost effective in large scale pyrometallurgical processes.

Therefore, although pyrometallurgy is a proven successful metal extraction method, alternative methods are required to meet environmental regulations and to process low-grade ores at minimal cost.

1.6 Hydrometallurgy

Hydrometallurgy is currently used mainly in the recovery of copper, nickel, cobalt, lead, zinc, aluminium, titanium, uranium and gold.[12] The benefits of hydrometallurgy include reduced costs since it does not require the high temperatures used in pyrometallurgy and fewer transport costs as plants are much smaller and so can be situated in the region where the raw material is mined.[10] These factors also reduce the environmental impact of metal processing. Low grade ores can also be extracted.[12]

A typical flowsheet for hydrometallurgical extraction of metals is shown in Figure 1.3. The leaching step involves transferring the desired metal into an aqueous solution. Once the metal of value is present in an aqueous phase, its separation from other metals and concentration is achieved *via* liquid-liquid solvent extraction. This technology is a robust, continuous process which uses mixer settlers first developed for the nuclear industry.[9]

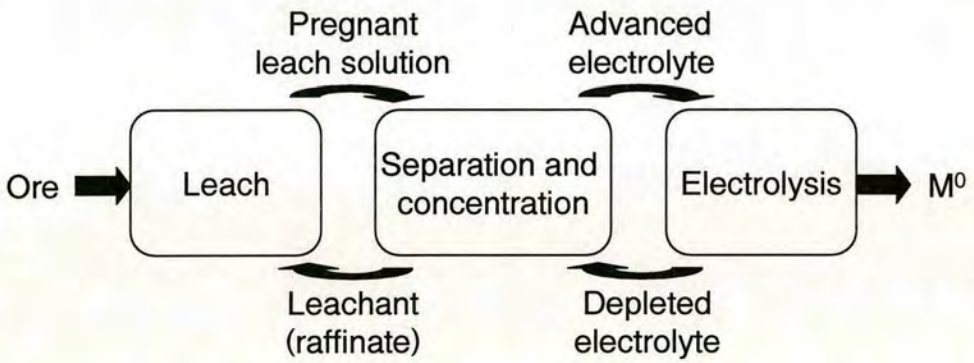

Figure 1.3: The basic flowsheet for extractive hydrometallurgy which allows complexing agents to achieve the operations of separation and concentration.

Various reagents can be used in the separation and concentration operations of a solvent extraction system. *Anion exchange reagents*[13] complex metal anions and transfer them into water-immiscible solvents, usually as contact ion-pairs. An example is the extraction of $FeCl_4^-$ using tetraalkylammonium salts:

$$FeCl_4^- + [R_4N]Cl_{(org)} \rightleftharpoons [R_4N][FeCl_4]_{(org)} + Cl^-.$$

These reagents are used commercially to recover kinetically inert precious metals as their chlorometallate complexes from acidic media. However, few details of the actual reagents used in industry have been published and the design of reagents for selective transfer of the desired metal of value remains challenging.[14]

An alternative extraction process is the use of *solvating reagents*.[9] These are neutral molecules which impart organic solubility to metal salts by displacing some or all of the water molecules in the coordination sphere of the metal cation or its complexes. For example, using tri-*n*-butyl phosphate (TBP) as a solvating reagent, uranium(IV) can be extracted from nitrate solutions:

$$UO_2^{2+} + 2NO_3^- + 2TBP_{(org)} \rightleftharpoons [UO_2(NO_3)_2(TBP)_2]_{(org)}.$$

Both the solvating reagent (TBP) and the attendant nitrate anion address the inner coordination sphere of the uranium. Stripping and loading are achieved by altering the positioning of the equilibrium by controlling the concentration of the coordinating anion in the aqueous phase.

Cation exchange reagents generate neutral, organic-soluble metal complexes by addressing the inner coordination sphere of the metal. Usually, an acidic ligand is used to generate an anionic donor and the loading-stripping equilibrium is pH-dependent:

$$n\mathbf{L}_{(org)} + M^{n+} \rightleftharpoons [M(\mathbf{L}\text{-}H)_n]_{(org)} + nH^+.$$

1.6.1 Cation-exchange extraction of copper

The cation-exchange method of solvent extraction is illustrated for the production of copper from oxidic ores in the flow diagram shown in Figure 1.4.

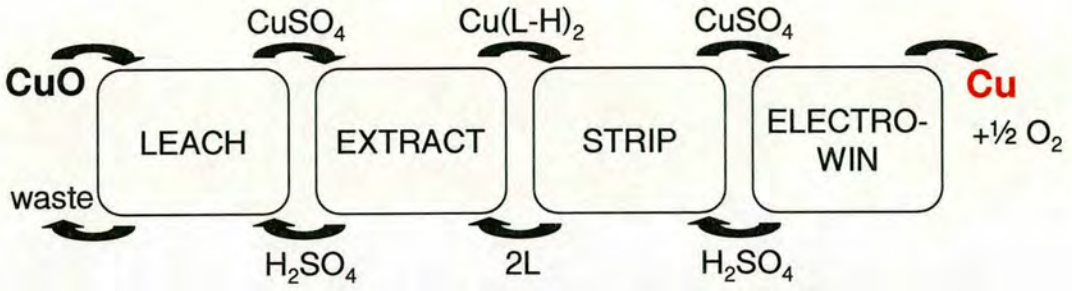

Figure 1.4: Production of copper from oxidic ores.

Leaching involves the dissolution of the metal of value, copper, usually with sulfuric acid, requiring only mild conditions and relatively low cost equipment. Sulfuric acid is passed through a "heap pad" of oxidic ore and transfers most of the metals present into an aqueous solution known as the pregnant leach solution (pls) which typically contains around 3-10 g L^{-1} of copper(II) and a significant quantity of Fe(III) (and Fe(II)).[9] New and alternative leaching processes will be discussed in more detail in Section 1.8.

In the extraction step the metal is selectively transported into a water-immiscible organic phase using a hydrophobic ligand. Particularly important in this stage is the formation of a neutral metal-ligand complex for the desired solubility in the organic phase. The transfer of the Cu^{2+} ion from the aqueous to the organic phase involves a cation exchange reagent:

$$Cu^{2+} + 2\mathbf{L} \rightleftharpoons [Cu(\mathbf{L}\text{-}H)_2] + 2H^+.$$

Once the organic phase is loaded with copper, it is separated from the aqueous phase. It is then contacted with an aqueous sulfate solution at low pH to strip the copper and regenerate the ligand. The resulting pure copper sulfate solution is used in the final electrowinning stage to produce conductivity grade copper and sulfuric acid, which

is recycled for use in the stripping step. This step is equivalent to the final stage in the pyrometallurgical process discussed in the previous section.

In the copper recovery process, the control of loading and stripping involves "pH-swing" equilibria based on an acidic extractant $\mathbf{L}_{(org)}$ and aqueous load and strip solutions with relatively high and low pH values respectively (Figure 1.5).

Leach	$CuO_{(s)} + H_2SO_{4\,(aq)}$	$\longrightarrow CuSO_{4\,(aq)} + H_2O_{(l)}$
Extract	$CuSO_{4\,(aq)} + 2\,\mathbf{L}_{(org)}$	$\longrightarrow [Cu(\mathbf{L}\text{-}H)_2]_{(org)} + H_2SO_{4\,(aq)}$
Strip	$[Cu(\mathbf{L}\text{-}H)_2]_{(org)} + H_2SO_{4\,(aq)}$	$\longrightarrow CuSO_{4\,(aq)} + 2\,\mathbf{L}_{(org)}$
Electrowin	$CuSO_{4\,(aq)} + H_2O_{(l)}$	$\longrightarrow Cu^0_{(s)} + \frac{1}{2}\,O_{2\,(g)} + H_2SO_{4\,(aq)}$
Overall	$\mathbf{CuO_{(s)}}$	$\longrightarrow \mathbf{Cu^0_{(s)} + \frac{1}{2}\,O_{2\,(g)}}$

Figure 1.5: Materials balance for solvent extraction in the production of copper from oxidic ores using a "pH swing" extractant, **L**.

The remarkable materials balance associated with the process outlined in Figures 1.4 and 1.5 is important both environmentally and economically, and hence this methodology accounts for the production of over 2.3 million tonnes of copper per annum, around one fifth of the total world production.[15] However, such favourable material balances do not necessarily follow when different types of extractant and different types of leaching processes are used.

There are a number of benefits of hydrometallurgy over pyrometallurgy:[10, 16]

- the excellent materials balances obtained, when compared to the generation of slag and sulfuric acid, and the consumption of SiO_2 (flux),
- the minimal energy input as opposed to the high energy consumption of a smelting plant,
- the smaller plant size, allowing closer proximity to the mine site, resulting in less transportation cost and,
- the ability to process low-grade ores, which is often not cost effective in large-scale pyrometallurgical processes.

1.6.2 Phenolic oxime extractants for copper

The reagents used in the flowsheets outlined in Figures 1.4 and 1.5 are phenolic oximes. The majority of commercial activity is currently based on the reagents shown in Figure 1.6.[9] The phenolic hydroxyl group provides the acidic proton for the "pH swing" controlled extraction equilibrium:

$$2\mathbf{L}_{(org)} + M^{2+} \rightleftharpoons [M(\mathbf{L}\text{-}H)_2]_{(org)} + 2H^+.^{12}$$

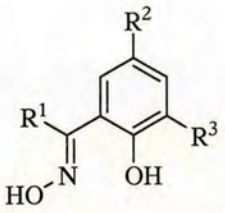

R^1	R^2	R^3	Commercial Name
H	C_9H_{19}	H	P50
$C_6H_5CH_2$	C_9H_{19}	H	P17
CH_3	C_9H_{19}	H	LIX84
C_6H_5	$C_{12}H_{25}$	H	LIX64
C_6H_5	C_9H_{19}	H	HS-LIX 65N
C_6H_5	C_9H_{19}	Cl	LIX70
H	$C_{12}H_{25}$	H	LIX860

Figure 1.6: Some phenolic aldoximes and ketoximes used commercially.[9]

Solubility in hydrocarbon solvents is imparted by multi-branched, mixed isomer alkyl groups in the R^2 position. The extractants are often slightly too "strong" for efficient stripping of the copper back into the aqueous phase and are therefore used in the presence of a modifier.[17] These are either long chain alcohols or esters of long chain carboxylic acids.

Upon deprotonation of the phenolic protons, a neutral 2 : 1 complex is formed. In the solid state, H-bonding between the oxime OH groups and phenolic oxygen atoms within a complex unit is observed, leading to *pseudo*-macrocyclic complexes as

shown for P50 in Figure 1.7. Some free ligands also exist in this *pseudo*-macrocyclic structure in solution.[17]

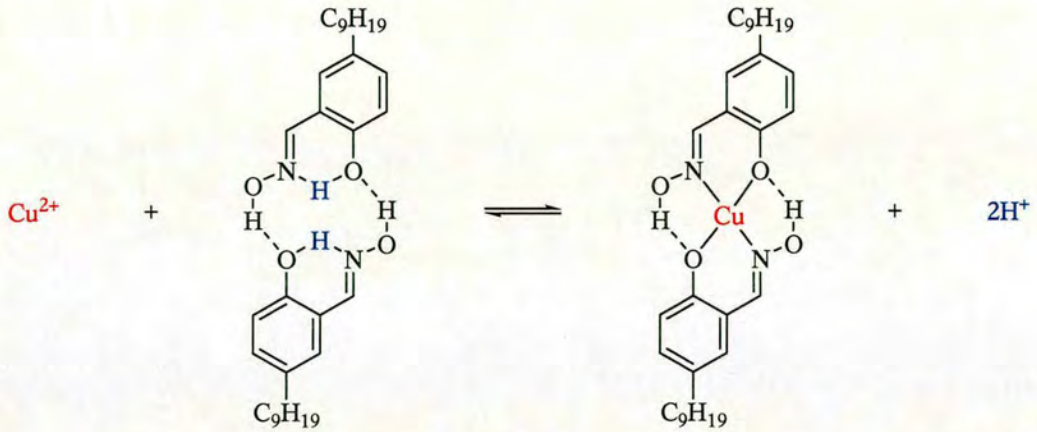

Figure 1.7: Preorganisation of the phenolic oxime, P50 and its complexation to copper.

The strength of binding of ligands of this type is determined by measuring the $pH_{½}$, the pH at which half of the theoretical maximum copper loading into the organic phase occurs.[12] A low $pH_{½}$ indicates a stable complex and hence a strong extractant. This value is usually determined by plotting pH against the percentage of copper loaded into the organic phase. Due to the characteristic shape of these graphs, they are known as S-curves. A plot of various S-curves for the extraction of a range of metals with P50 oxime can be seen in Figure 1.8. Typical values for copper(II) extraction lie in the pH range 0.0-2.0.[18] Such a $pH_{½}$ range is ideal for optimum copper recovery as generally the feed has a pH of $\approx$ 2.0 and the spent electrolyte used for stripping is at pH $\approx$ 0.0. The higher $pH_{½}$'s for the other metals ensure selectivity for copper in this pH range.

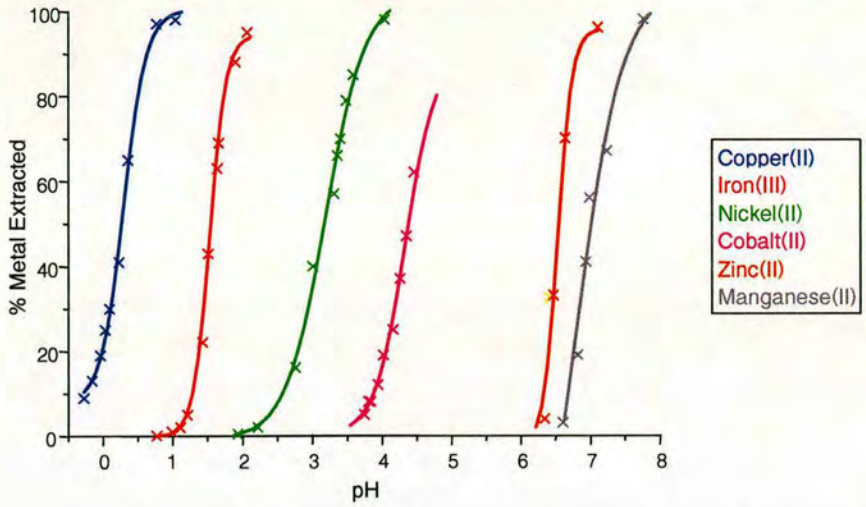

Figure 1.8: S-curves for the extraction of a range of metals using P50 in kerosene.[12]

In most respects pH-swing extractants of the phenolic oxime type have almost ideal properties for their application in copper recovery from heap leach operations involving oxidic ores.

The work described in this thesis is aimed at developing alternative reagents which would be more efficient in two respects:

- delivery of higher transport efficiency (Section 1.7) and
- recovery of copper from new leaching processes which deliver much higher tenor feeds (Cu content > 30 g l^{-1}) or do not consume acid in the leaching process (Section 1.8).

1.7 Mass Transport Efficiency of Solvent Extraction

As seen in Figure 1.7, the ligand to metal stoichiometry for commercial copper extractants is 2 : 1. This means that for every mole of metal produced, two moles of ligand are required. Since these ligands contain bulky alkyl groups which impart their organic solubility, a large mass of compound is required per mole of cation extracted. This is known as the "mass transport efficiency" of the ligand.

To improve on this efficiency, new ligands can be designed which can achieve the same strength of binding ($pH_{½}$) whilst reducing the total mass of reagent used. To meet these criteria, extractants which can complex one metal cation per ligand,

altering the stoichiometry from 2 : 1 to 1 : 1, or n : n could be envisaged. Since most metals processed in this way, such as copper, are divalent, this new class of ligand must therefore have two deprotonatable sites in order to yield a neutral complex. If these new ligands include a donor atom capable of bridging two copper centres, neutral complexes with a 2 : 2 ligand to metal ratio, *i.e.* "double loading" systems could be formed (Figure 1.9).

Figure 1.9: Possible equilibrium equation for a tridentate ligand forming a neutral 2 : 2 complex with a divalent metal, M.

Previous work in the Tasker group by Wood *et al.* used hydrazone ligands (Figure 1.10, (i)) to achieve this 2 : 2 ligand to copper stoichiometry, resulting in an improvement in mass transport efficiency over commercial copper extractants.[19] In this thesis, Schiff base imine ligands such as that shown in Figure 1.10 (ii) will be used to replicate the diacidic binding site and form neutral complexes in the organic phase.

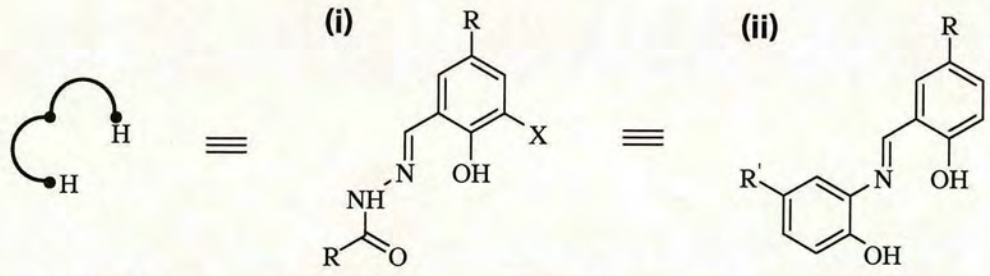

Figure 1.10: (i) General structure of the hydrazone ligands used in previous work at Edinburgh[19] and, (ii) general structure of the tridentate ligands designed for use in this study.

The key target of this thesis is to extend the use of tridentate "ion-exchange" reagents capable of double loading to reagents which transport metal *salts* (Section 1.8).

1.8 Metal Salt Extractants

The processing of copper oxidic ores is a well established and understood industrial process, which has been operating successfully for a number of years (Section 1.6). However, until recently, sulfidic ores have primarily been treated using pyrometallurgical methods. This is because the processes used in the hydrometallurgical treatment of oxidic ores result in slow and incomplete leaching when addressing sulfidic minerals such as chalcopyrite ($CuFeS_2$). These issues have been studied extensively over the last 10-15 years and there are now a number of leaching processes which can be operated on a commercial scale, or nearing the final stages of their development. These have been reviewed in a recent paper.[11]

One of the most successful new systems is the Total Pressure Oxidation process. It uses high temperature and pressure oxidation to oxidise all sulfide minerals to sulfates and sulfuric acid, e.g.

$$CuFeS_2 + O_2 + 2H_2SO_4 \rightarrow CuSO_4 + FeSO_4 + 2H_2O + 2S.$$

At the Bagdad plant in Arizona, around 16,000 tonnes of copper per annum are processed in this way, from concentrates which were previously smelted. The total oxidation conditions also produce around 140 short tons of acid per day:

$$S + 1½O_2 + H_2O \rightarrow H_2SO_4,$$

which in Bagdad is used in another leach process. This would however, be a large amount of acid to sell on, and therefore total pressure oxidation processes should ideally be applied where the acid can be used beneficially on-site or nearby.

Another technology being effectively implemented is the BioCOP™ process, developed by the BHP Billiton biotechnologies group based in Johannesburg, South Africa. It uses thermophile bacteria to oxidise sulfide minerals to metal sulfates and sulfuric acid at 65-80 °C. The chemistry of microbial oxidation of sulfides is closely related to that of ferric ion oxidation in acidic solutions:

$$CuFeS_2 + 4Fe^{3+} \rightarrow 5Fe^{2+} + Cu^{2+} + 2S.$$

The microorganisms play a catalytic role in oxidising ferrous ion to ferric ion, thus regenerating the oxidant while also oxidising sulfur to sulfate, generating acid:

$$2Fe^{2+} + 2H^{+} + \tfrac{1}{2}O_2 \rightarrow 2Fe^{3+} + H_2O,$$
$$2S + 3O_2 + 2H_2O \rightarrow 2H_2SO_4.$$

This process has recently been employed in Chile, with the installation of a 20,000 tonnes per annum plant close to the Chuquicamata mine. It also produces excess sulfuric acid, although there is less available for secondary use as some must be neutralised as part of the process.

These novel recovery processes tend to generate higher tenor feeds than those arising from heap leaching of oxidic ores, with pregnant leach solutions containing 30-90 g L^{-1}.[20] Sulfuric acid build-up at the front-end of the circuit is a concern when processing such high tenor feeds, as explained in Figures 1.11 and 1.12.

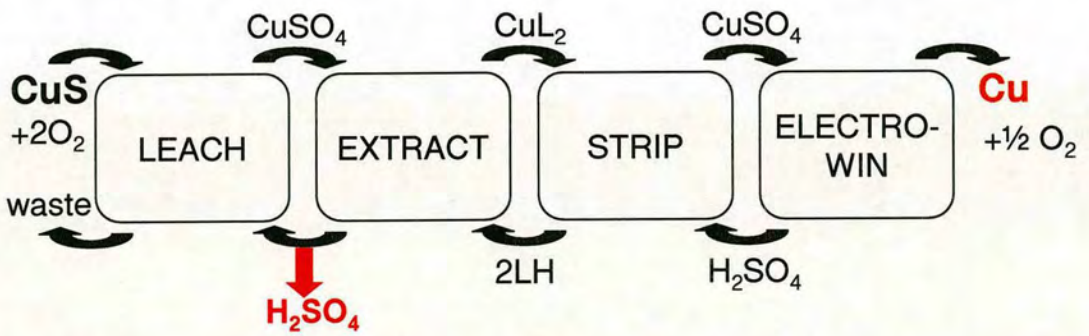

Figure 1.11: Production of copper from sulfidic ores.

Leach	$CuS_{(s)} + 2\,O_{2\,(g)}$	⟶	$CuSO_{4\,(aq)}$
Extract	$CuSO_{4\,(aq)} + 2\,\mathbf{L}_{(org)}$	⟶	$[Cu(\mathbf{L}\text{-}H)_2]_{(org)} + \mathbf{H_2SO_{4\,(aq)}}$
Strip	$[Cu(\mathbf{L}\text{-}H)_2]_{(org)} + H_2SO_{4\,(aq)}$	⟶	$CuSO_{4\,(aq)} + 2\,\mathbf{L}_{(org)}$
Electrowin	$CuSO_{4\,(aq)} + H_2O_{(l)}$	⟶	$Cu^0_{(s)} + ½\,O_{2\,(g)} + H_2SO_{4\,(aq)}$
Overall	$\mathbf{CuS_{(s)} + {}^3/_2\,O_{2\,(g)} + H_2O_{(l)}}$	⟶	$\mathbf{Cu^0_{(s)} + H_2SO_{4\,(aq)}}$

Figure 1.12: Sulfuric acid build-up during copper extraction from sulfidic ores.

With conventional pH-swing extractants, for every metal extracted, two protons are released into the aqueous phase causing a build-up of acid. In recovery from oxidic ores this acid is reused in the leaching step. When processing sulfidic ores the acid must either be recovered *via* an expensive acid recovery process or neutralised with base, which generates a salt waste which subsequently has to be removed.[21]

To avoid the release of sulfuric acid in the front end of the circuit during the extractions, ditopic ligand systems (Figure 1.13) have been designed which transport both the metal cation and its attendant anion into the organic phase.[21] These can exist in a zwitterionic form, where both positive and negative sites are present on the same molecule, resulting in an overall charge-neutral species. The ligand can then extract the metal cation (into the blue, anionic section of the ligand) and its associated anion(s) (into the red, cationic site) simultaneously.

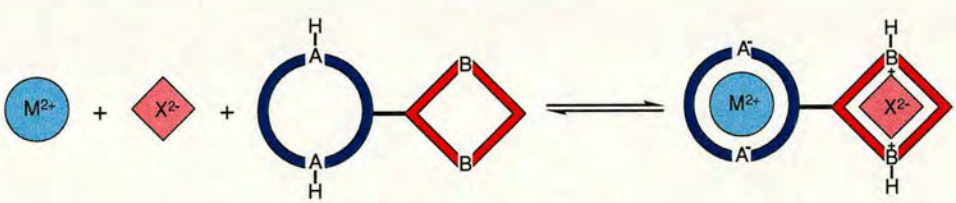

Figure 1.13: Ditopic system forming neutral complexes [MLX] of a metal salt in a zwitterionic (2+/2-) ligand.

In the stripping stage, the cation is stripped as before, using sulfuric acid at low pH, reprotonating the A^- donor and producing a pure metal sulfate solution. The anion

can then be stripped using an aqueous base (BOH). This results in the regeneration of the ligand and, if designed well, a marketable salt by-product in the back end of the circuit. The pure metal sulfate solution can then be used in a conventional electrowinning step to give pure metal and regenerate the sulfuric acid needed for stripping the metal. The overall materials balance for this system can be seen in Figure 1.14.

Leach	$MS_{(s)} + 2O_{2(g)}$	$\longrightarrow MSO_{4(aq)}$
Extract	$MSO_{4(aq)} + L_{(org)}$	$\longrightarrow MLSO_{4(org)}$
Strip cation	$MLSO_{4(org)} + H_2SO_{4(aq)}$	$\longrightarrow MSO_{4(aq)} + [LH_2]SO_{4(org)}$
Strip anion	$[LH_2]SO_{4(org)} + 2BH_{(aq)}$	$\longrightarrow L_{(org)} + B_2SO_{4(aq)} + H_2O_{(l)}$
Electrowin	$MSO_{4(aq)} + H_2O_{(l)}$	$\longrightarrow M_{(s)} + \frac{1}{2}O_{2(g)} + H_2SO_{4(aq)}$
Overall	$\mathbf{MS_{(s)} + 1\frac{1}{2}O_{2(g)} + 2BH_{(aq)}}$	$\longrightarrow \mathbf{M_{(s)} + B_2SO_{4(aq)}}$

Figure 1.14: Materials balance for recovery of a base metal from a sulfide ore *via* "metal salts" solvent extraction.

A simple system which fulfils these criteria uses the zwitterionic form of "salen"-type (salen^{2-} = *N,N'*-(salicylidene)ethylenediaminato dianion) ligands developed by Galbraith *et al.* at Edinburgh University (Figure 1.15). They have been shown to form metal sulfate complexes which, upon contact with base, lose the sulfate anion as shown in Figure 1.14 above. They also show loading and stripping pH-profiles for copper chloride and sulfate suitable for use in industrial systems.[21]

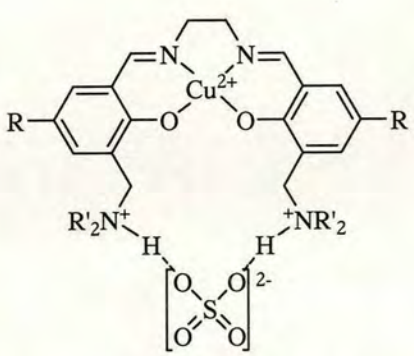

Figure 1.15: An example of a copper(II) sulfate complex of a ditopic ligand with "salen" metal-binding site.[21]

1.9 High Transport Efficiency of Metal Salts

If we take a system such as that discussed in Section 1.7, which forms 2 : 2 ligand to metal complexes, and append anion binding sites then an overall neutral complex with formula $[M_2L_2X_2]$ could be formed, as seen in Figure 1.16.

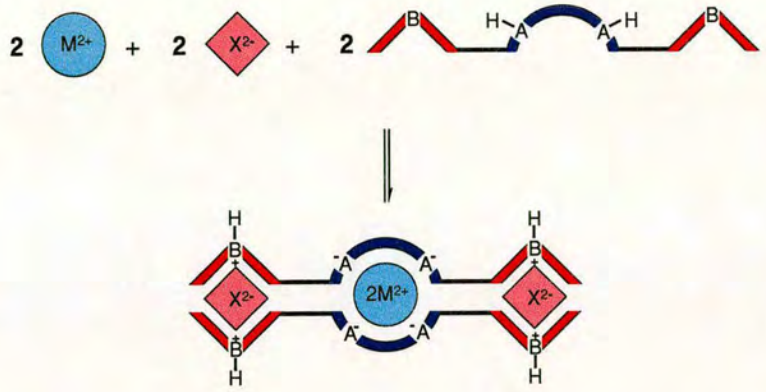

Figure 1.16: A tritopic system, overall complex $[M_2L_2X_2]$.

In order to achieve this, ligands such as that seen in Figure 1.17 have been synthesised and are discussed in Chapter 3. The deprotonatable sites A-H, which form the cation binding site are the phenols, and the two anion binding sites, B, are shown as X and X' in the structure.

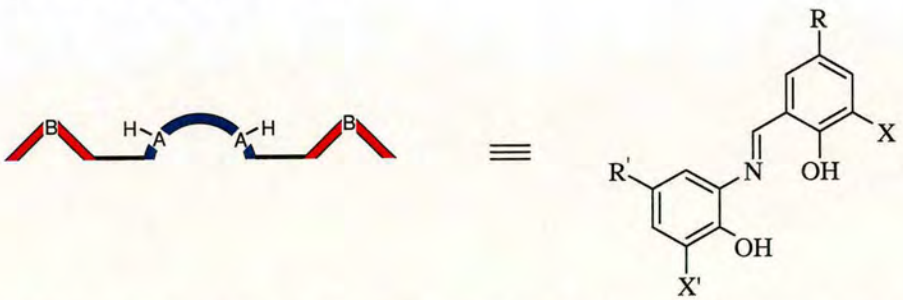

Figure 1.17: General structure of potential tritopic ligands for use as metal salt extractants.

An alternative approach to extracting metal salts is to use a combination of ligands to perform the individual tasks (Figure 1.18). Using a metal extractant (blue) and an anion encapsulating ligand (red) in a blend may in some instances perform the same operation as ligands such as those seen above.[22, 23]

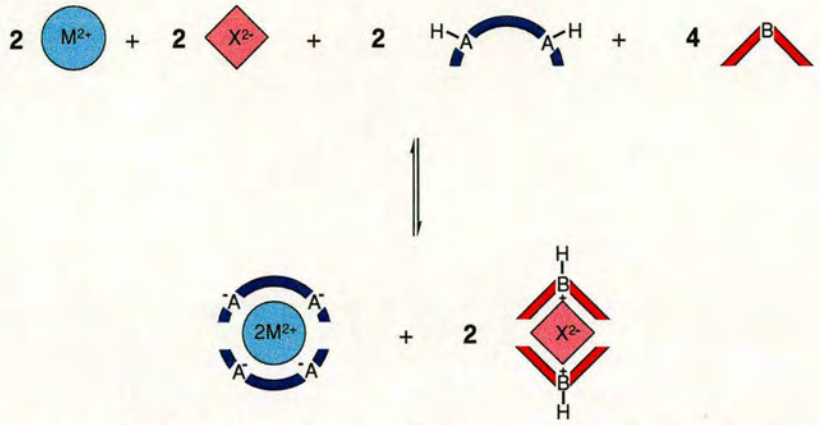

Figure 1.18: "Dual-host" method for extracting metal salts, using separate ligands to extract the cation and anions.

If these two separated host ligands were made from cheap and simple synthetic steps, it may be that this "dual-host" approach is a more attractive industrial process. This concept will be explored in Chapter 3, Section 3.4.5.

1.10 Reagent Design Criteria

The aim of this thesis is to design and investigate the properties of ligands which can achieve favourable ligand to metal stoichiometries and possibly also function as metal *salt* extractants. The combination of these goals should identify reagent types which could address high tenor feed solutions of metal without the need for pH adjustment. Whilst it is not the primary objective of this work to develop candidate reagents for commercial use it is pertinent to be aware of the criteria which a new extractant must meet in order to compete commercially:

Safety- The ligand needs to satisfy all safety requirements and environmental regulations.

Selectivity- The ligand must be selective for the metal of choice over a number of other metals likely to be present in the feed solution. Anion selectivity is also an important factor in the design of metal-salt extractants.

Separation- Rapid disengagement of the two phases in the extraction and stripping stages of a solvent extraction process is essential to ensure clean separation of the organic phase.

Solubility- The ligand and the resultant complex need to be soluble in water-immiscible solvents and to have negligible solubility in the aqueous phase. This is usually achieved *via* the incorporation of long, branched alkyl chains into the ligand structure and formation of neutral species upon complexation.

Speed- The extraction needs to take place quickly, as slow kinetics of either complex formation or phase transfer reduces the efficiency of the process.

Stability- The ligand needs to show both hydrolytic stability and resistance to oxidation.

Strength- The strength of an extractant must be sufficient to allow successful extraction, but must not be too strong, rendering the stripping stage unfeasible.

Synthesis- The ligand synthesis needs to be simple and inexpensive to make large scale production industrially viable.

System- Ideally, a new extractant could be implemented into a current solvent extraction process without need for extensive site modification. Increasingly, the "systems engineering" approach looks to ensure that the total system has minimal environmental impact, rather than considering each individual component.[24]

1.11 Systems Chosen for Study

Keeping these design criteria in mind, we must first design a ligand with a suitable metal binding site. From the outset, the aim was to design ligands capable of coordinating to divalent nickel and copper. 6-coordinate nickel(II) forms stable octahedral coordination geometry, while it tends to prefer square planar complexes when 4-coordinate. Copper(II), forms distorted octahedral complexes and regular

square planar complexes. Therefore, a ligand for the extraction of either metal should ideally have the ability to form 4-coordinate square planar complexes with divalent metals.

Nickel(II) and copper(II) are borderline Lewis acids which will therefore prefer complexation by borderline Lewis bases or a combination of hard and soft Lewis bases.[25, 26] Oxygen is a relatively hard Lewis base and would therefore tend to coordinate to hard acids such as iron(III). However, taking a combination of oxygen and nitrogen donors should produce stable copper/nickel(II) complexes. As discussed earlier, deprotonatable donors are also essential, which led us to choose phenols as the oxygen donors, with an imine nitrogen as the third donor.

The chelate effect states that a metal complex with multidentate ligands has much greater stability than one with analogous single donors.[7] The multidentate ligands cause a rise in entropy of reaction, which results in a more favourable complexation. If the metal ion is contained within 5- or 6-membered chelate rings, steric effects will also dictate that more stable complexes are formed. Therefore, multidentate ligands should promote the complexation of metal ions, transporting them from the aqueous phase into the water-immiscible organic phase.

The anion binding sites must contain protonatable donors, and can be chosen to impart either increased solubility or, conversely, promote crystallisation. Therefore, two amines were chosen for use in this thesis: *N*-ethoxymethyldi-*n*-hexylamine and 1-ethoxymethylpiperidine.

Having prepared the ligands in Figure 1.19, the aim was to establish a proof of concept that they can

- give higher metal transport efficiency than conventional cation-exchange reagents such as P50, and
- transport both metal cation and attendant sulfate anion into an organic phase.

It was intended that once systems were identified which meet these criteria some testing to check that they also meet the criteria listed in Section 1.10 would be undertaken to define whether they were suitable for commercial development.

The ligands synthesised for this thesis are shown in the table below (Figure 1.19).

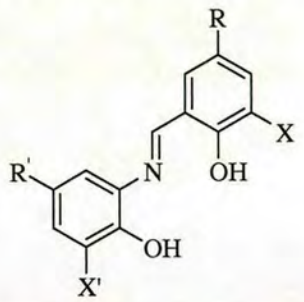

Ligand	R	R'	X	X'
1	^{t}Bu	^{t}Bu	H	H
2	^{t}Bu	^{t}Bu	$CH_2N(C_6H_{13})_2$	H
3	^{t}Bu	^{t}Bu	H	$CH_2N(C_6H_{13})_2$
4	^{t}Bu	^{t}Bu	$CH_2N(C_6H_{13})_2$	$CH_2N(C_6H_{13})_2$
5	^{t}Bu	^{t}Bu	$CH_2N(C_5H_{10})$	H
6	^{t}Bu	^{t}Bu	H	$CH_2N(C_5H_{10})$
7	^{t}Bu	^{t}Bu	$CH_2N(C_5H_{10})$	$CH_2N(C_5H_{10})$
8*	^{t}Bu	^{t}Bu	$CH_2NH(C_6H_{13})$	H
9	C_9H_{19}	^{t}Bu	$CH_2N(C_5H_{10})$	H
10	C_9H_{19}	C_9H_{19}	$CH_2N(C_5H_{10})$	H

Figure 1.19: Reference numbers for ligands synthesised and used in this thesis.

1.12 Analysis of Extracted Species

In order to understand speciation in the solution phase, both ICP-OES and EPR spectroscopy are used. ICP provides quantitative analysis of the metal and sulfur content of a solution, whilst EPR can identify the number of paramagnetic species. A combination of these two techniques therefore provides a good indication of the species extracted by our ligands into the organic phase.

* Ligand 8 was not synthesised, it is the result of metal complex recrystallisation (Section 3.3).

1.12.1 Inductively Coupled Plasma-Optical Emission Spectroscopy (ICP-OES)[27]

In order to identify the composition of a sample in solution, ICP-OES takes advantage of the fact that each chemical element emits light in characteristic wavelengths when placed in a very high energised state. It is a spectroscopic method which uses a high temperature (*ca.* 6500 K) plasma as the excitation source, which is powered by a radiofrequency generator. The solution of interest is first drawn into a nebuliser, which forms a homogeneous aerosol in the spray chamber, separating droplets by size with smaller drops being carried to the plasma and the larger ones drained away. The aerosol is vapourised, atomized and ionized, then electronically excited by the plasma. The constituent atoms then emit their signature light wavelengths which are sampled through a narrow entrance slit and dispersed with a grating polychromator. The resolved radiation is measured with a photomultiplier tube which converts the optical signal into an electric signal to be stored as a computer file. The overall process can be seen in Figure 1.20.

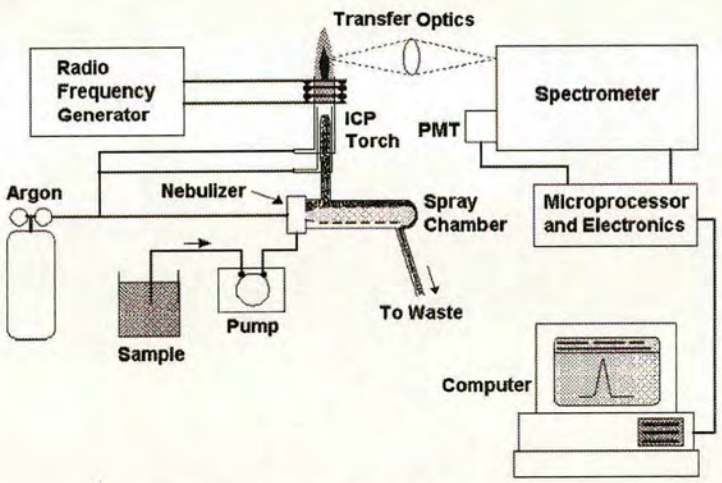

Figure 1.20: The ICP-OES spectrometer.

ICP-OES is used throughout the work in this thesis for the quantitative analysis of copper, nickel and sulfur in solution. Both organic and aqueous samples were studied.

1.12.2 Electron Paramagnetic Resonance (EPR)[28]

EPR is a spectroscopic technique which detects chemical species that have unpaired electrons. Since an unpaired electron's spin magnetic moment is very sensitive to local magnetic fields, such as other nuclei within a compound, EPR can provide detailed structural information.

Application of a strong magnetic field, B_0, to a paramagnetic species results in the magnetic moment of the unpaired electron aligning itself parallel (M_s = -½) or antiparallel (M_s = +½) to the external field (Figure 1.21). These distinct energy levels allow for absorption of electromagnetic radiation to occur. The energy separation between the two states is defined as:

$$\Delta E = h\nu = g\mu_B B_0,$$

where: ΔE is the energy difference between the two states,

h is Planck's constant,

ν is the microwave frequency,

g is the g-factor, or spectroscopic splitting factor = 2.0023 for a free electron,

μ_B is the Bohr magneton = 9.2731×10^{-28} J G^{-1}.

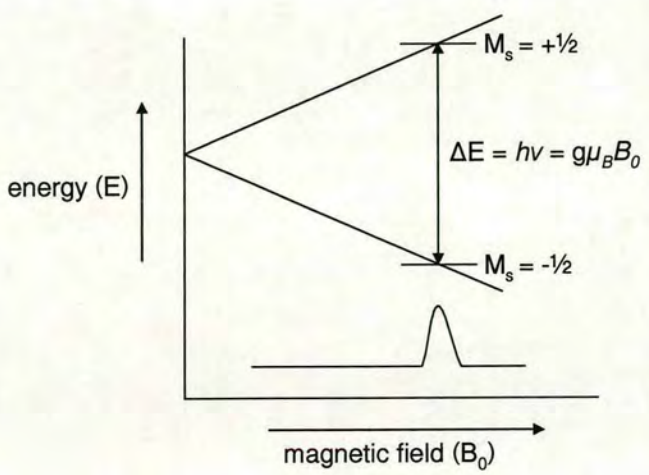

Figure 1.21: Variation of the spin state energies as a function of the applied magnetic field.

In an EPR experiment, the paramagnetic centre is placed in a magnetic field and the electron is caused to resonate between the two states. By measuring the energy it absorbs as it does this, an EPR spectrum can be plotted.

In order to obtain specific structural information of a compound, hyperfine couplings can be measured. This is the interaction between the unpaired electron and any nuclei within the complex, which produces a local magnetic field at the electron and results in splitting of the EPR signal. The number of peaks resulting from this splitting depends on the nuclear spin quantum number (I) of the nuclei, and the number of nuclei (n):

$$\text{Number of peaks in EPR spectrum} = 2nI + 1.$$

Thus, one copper(II) ion with $I = 3/2$ gives rise to four peaks in an EPR spectrum. The presence of a second nuclei, such as nitrogen for which $I = 1$, will split each copper peak into a further three peaks.

In dinuclear complexes, strong antiferromagnetic interactions can occur between the two copper(II) centres, resulting in diamagnetic behaviour and the absence of an EPR signal.[29-32] This effect is, however, dependent on the coupling mechanism and the nature of the bridge between the copper(II) centres.[33] EPR is consequently an invaluable tool in establishing the stoichiometry of extracted species in the organic phase of extraction experiments.

1.13 Thesis Outline

Chapter 2 discusses the extraction chemistry of the metal-only extractant, ligand **1** (Figure 1.19). The chapter is introduced with a review of the previous research involving this type of Schiff Base ligand. Ligand synthesis and characterisation follows, along with some interesting nickel extraction, complexation and crystallographic studies. The extraction of copper is studied and further investigated with EPR. Finally, the addition of an auxiliary ligand yields remarkable results.

Chapter 3 extends the ligand **1** work towards the field of metal-salt extraction. Ligands **2-8** are synthesised and characterised, with some additional crystallographic results. Ligand **5** proves to possess the most interesting coordination and extraction chemistry and hence is studied in some detail, involving EPR, further auxiliary ligand studies, investigation into the "dual-host" possibility and some comparison of copper salt extraction.

Chapter 4 looks to investigate the possible commercial application of the ligands studied thus far. Ligands **9** and **10** are synthesised to improve upon solubility. A number of experiments are carried out on **10** in order to establish its stability and selectivity.

Chapter 5 contains the preparative methods of all compounds synthesised, including full characterisation. The extraction techniques are also detailed.

1.14 References

1 A. Cole, *Metal Bulletin Monthly*, 2004, **copper**, 6.

2 W. Millsteed, K. Penney, W. Mollard, R. Kendall and K. Huggan, *Australian Commodities*, 2006, **13**, 519.

3 '*The Composition of the Cent*', The United States Mint, 2001.

4 '*London Metal Exchange (www.lme.co.uk/nickel.asp)* ', 2007.

5 *International Nickel Study Group, World Nickel Statistics*, 2007, **16**.

6 '*United States Mint Moves to Limit Exportation & Melting of Coins*', The United States Mint, 2006.

7 D. F. Shriver, P. W. Atkins and C. H. Langford, '*Inorganic Chemistry*', Oxford University Press, Oxford, 2nd edn., 1994.

8 '*The New Penguin English Dictionary*', ed. R. Allen, Penguin Books, 2001.

9 P. A. Tasker, P. G. Plieger and L. C. West, *Comprehensive Coordination Chemistry II*, 2004, **9**, 759.

10 T. W. Swaddle, '*Inorganic Chemistry: An Industrial and Environmental Perspective.*' San Diego, California, 1996.

11 D. Dreisinger, *Hydrometallurgy*, 2006, **83**, 10.

12 J. Szymanowski, '*Hydroxyoximes and Copper Hydrometallurgy*', CRC Press, London, 1993.

13 M. Nicol, C. A. Flemming and J. S. Preston, *Comprehensive Coordination Chemistry I*, 1987, **6**, 779.

14 F. L. Bernardis, R. A. Grant and D. C. Sherrington, *Reactive and Functional Polymers*, 2005, 205.

15 A. G. Smith, P. A. Tasker and D. J. White, *Coordination Chemistry Reviews*, 2003, **241**, 61.

16 F. Habashi, *Minerals Engineering*, 1994, **7**, Chapter 2.

17 J. Szymanowski, *Critical Reviews in Analytical Chemistry*, 1995, **25**, 143.

18 G. A. Kordosky, *Journal of the Minerals, Metals and Materials Society*, 1992, **44**, 40.

19 J. L. Wood, '*Multi-Loading Ligand Assemblies to Transport Copper*', PhD thesis, University of Edinburgh, 2005.

20 K. C. Sole, *Solvent Extraction and Ion Exchange*, 2002, **20**, 601.

21 S. G. Galbraith, '*Ditopic Ligands for the Selective Solvent Extraction of Transition Metal Sulfates*', PhD thesis, University of Edinburgh, 2004.

22 K. Kavallieratos and B. A. Moyer, *Chemical Communications*, 2001, 1620.

23 K. Kavallieratos, R. A. Sachleben, G. J. Van Berkel and B. A. Moyer, *Chemical Communications*, 2000, 187.

24 '*The Industrial Green Game: Implications for Environmental Design and Management*', ed. D. J. Richards, National Academy Press, Washington D. C., 1997.

25 R. G. Pearson, *Journal of the American Chemical Society*, 1963, **85**, 3533.

26 R. G. Pearson and J. Songstad, *Journal of the American Chemical Society*, 1967, **89**, 1827.

27 A. Settle, '*Handbook of Instrumental Techniques for Analytical Chemistry*', Prentice Hall, PTR, 1997.

28 B. A. Goodman and J. B. Raynor, *Advances in Inorganic Chemistry and Radiochemistry*, 1970, **13**, 135.

[29] N. R. Sangeetha, K. Baradi, R. Gupta, C. K. Pal, V. Manivannan and S. Pal, *Polyhedron*, 1999, **18**, 1425.

[30] F. Tuna, L. Patron, Y. Journaux, M. Andruh, W. Plass and J.-C. Trombe, *Journal of the Chemical Society, Dalton Transactions*, 1999, 539.

[31] O. Cozar, L. David, V. Chis, G. Damian, M. Todica and C. Agut, *Journal of Molecular Structure*, 2001, **563-564**, 371.

[32] P. Zanello, S. Tamburini, P. A. Vigato and G. A. Mazzocchin, *Coordination Chemistry Reviews*, 1987, **77**, 165.

[33] J. J. Grzybowski, P. H. Merrell and F. L. Urbach, *Inorganic Chemistry*, 1978, **17**, 3078.

CHAPTER 2

2 CHAPTER 2 32

2.1 Introduction 34

2.2 Ligand synthesis and characterisation 39

2.2.1 Crystal structure of ligand 1 40

2.3 Preparation and characterisation of metal complexes 42

2.4 Nickel complex formation and solvent extraction by ligand 1 45

2.4.1 Crystallography 46

2.4.2 Magnetism 56

2.4.3 Solvent extraction 58

2.5 Copper complex formation and solvent extraction by ligand 1 61

2.5.1 Solvent extraction 62

2.5.2 Electron paramagnetic resonance (EPR) 65

2.5.3 Mononuclear complexes containing an auxiliary ligand 67

2.6 Conclusions 72

2.7 References 74

2.1 Introduction

The majority of commercial copper solvent extraction processes employ phenolic oxime complexing agents.[1, 2] P50, derived from 5-nonylsalicylaldehyde, is one of the industrial extractants of choice. In non-polar organic solvents, it forms a hydrogen bonded dimer which can undergo cation exchange upon contact with a copper(II)-containing aqueous solution *via* loss of the phenolic protons to form a square planar complex with a 2 : 1 ligand to metal ratio (Figure 2.1). The system's mass transport efficiency is determined by this stoichiometry.

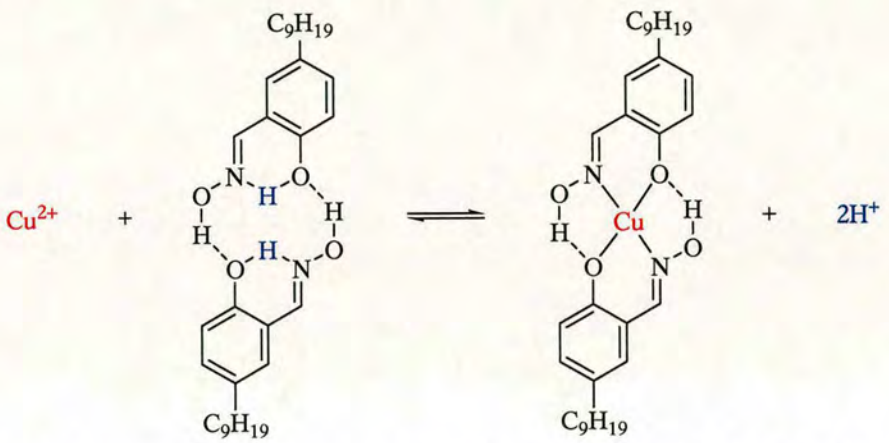

Figure 2.1: Preorganisation of P50 oxime and intermolecular H-bonding in its copper(II) complex.

One approach to improving the performance of these successful extractants is to increase the mass transport efficiency by increasing the ligand-copper stoichiometry from 2 : 1 to 1 : 1. In order to do this and generate a neutral complex the extractant must have two deprotonatable sites. It must also have a molecular weight of less than that of the P50 dimer.

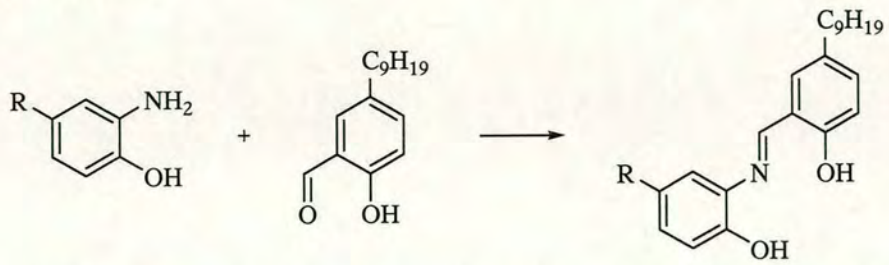

Scheme 2.1: Prototype diacid imine ligand for solvent extraction studies derived from 5-nonylsalicylaldehyde (P50 aldehyde).

Another feature which makes P50 oxime commercially viable is that it is synthesised from cheap, readily available starting materials. Consequently it would be sensible to use the same precursor, P50 aldehyde (Scheme 2.1), in the new reagent and condense it with an amine which also contains an acidic donor atom. The example shown in Scheme 2.1 would provide a tridentate NO_2^{2-} donor set which could achieve the desired 1 : 1 stoichiometry on complex formation. This could either give a mononuclear complex with a neutral monodentate ligand X or a dinuclear complex in which one of the phenolate oxygen atoms provides a bridge between the two copper cations (the example shown in Figure 2.2 uses the phenolate oxygen atom from the benzylidene unit).

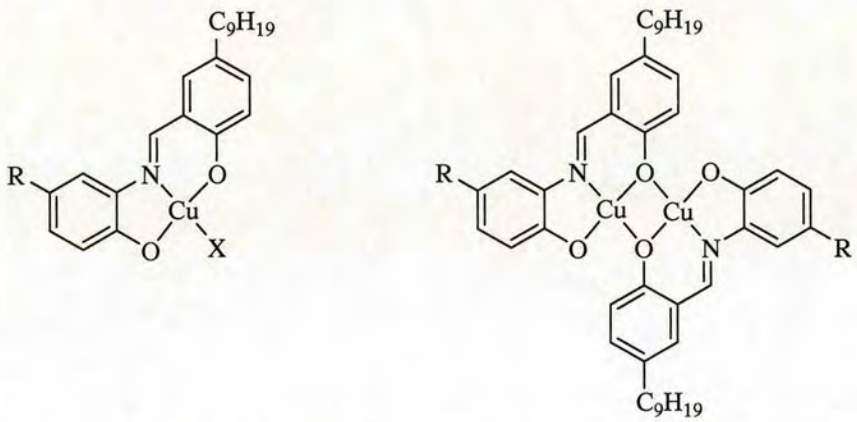

Figure 2.2: Mono- and di-nuclear copper(II) complexes of the prototype ligand which both show 1 : 1 ligand : copper stoichiometry.

Imines of this type have not, to date, been developed for use in industrial solvent extraction processes. Bis-imines of the salen-type have been much studied[3] as quadridentate ligands in coordination chemistry and recent derivatives with pendant 3-dialkylaminomethyl groups (Figure 2.3) have been studied by the Tasker group in Edinburgh as extractants for both copper and nickel salts.[4, 5] Their ease of synthesis and high solubility in water immiscible solvents encouraged us to consider the tridentate analogues in this project. Chapter 3 deals with derivatives of the prototype ligand which can transport metal *salts*.

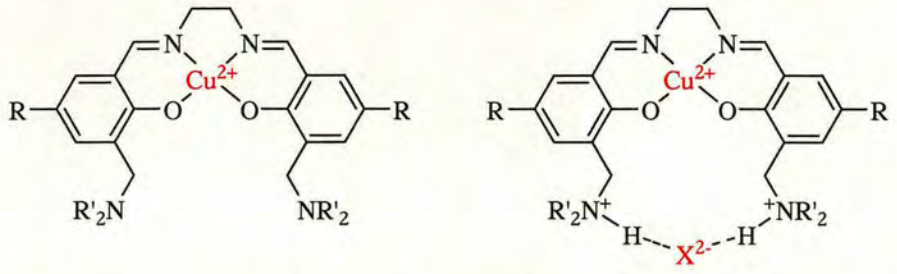

Figure 2.3: "Copper-only" and "copper salt" complexes of salen-type ligands with pendant dialkylaminomethyl substituents.

A large volume of work has been carried out over the last fifty years on the coordination chemistry of aromatic imines derived from salicylaldehyde and related keto phenols. A series of papers by Ledbetter considers the tautomerism of *N*-(*o*- and *p*-hydroxybenzylidene) anils in various solvents, following on from the work of Schmidt *et al.*.[6-10] A series of spectroscopic methods was used to study the solvent and substituent effects on the prevalence of each of the two tautomers (Figure 2.4), including the diphenolic analogue (X = *o*-OH, Y = H) of interest in this thesis.

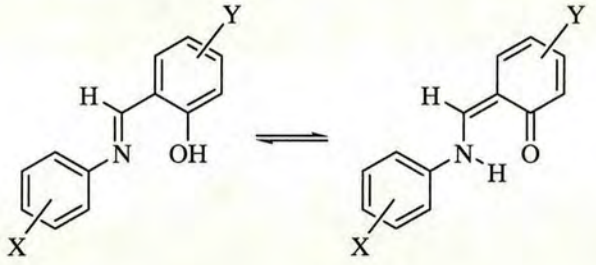

Figure 2.4: Tautomers of *N*-(*o*-hydroxybenzylidene) anil.

Studies of intramolecular hydrogen bonding between the phenolic proton and the imine nitrogen have been carried out, recording the effect on the ligand reduction potentials.[11] More recently, vibrational spectroscopic and computational methods have been employed to investigate this further.[12] Santhi *et al.* have assessed Schiff base compounds of this type for use as fluorescent markers for biological applications and their suitability as laser dyes.[13] They have also been considered as corrosion inhibitors and have been shown to be useful in the protection of copper, iron, zinc and steel.[14-19] The crystal structure of *N*-(2-hydroxyphenyl)salicylaldimine

has been published, confirming the presence of not only the OH···N intramolecular hydrogen bond but also OH···O bonds.[20]

The coordination chemistry of these ligands has been studied extensively with a diverse range of metals in different coordination states. A considerable range of binding modes has been reported, for example with B,[21] Al,[22] V,[23] Cr, Mo and W,[24, 25] Fe,[26] Co,[27, 28] Ni and Cu,[29] Ge,[30] Zr,[31] Sn,[32-35] Re,[36-38] Mn,[39, 40] Pb,[41, 42] and U[43-45]. These papers do not consider potential applications of the complexes or their use in metal recovery. However, a number of other studies have been carried out in this area. The fluorescent properties and use in fluorimetry of complexes with aluminium, gallium, indium, beryllium and scandium have been studied, in order to assess their future use as analytical probes for these metals, finding them to be useful at micromolar levels of metal ions.[46] The magnetic properties of Schiff base complexes of iron and copper have also been investigated. Both studies indicate that binuclear complexes may be present, and that substitution on one or both of the aromatic rings can influence the magnetic behaviour of a given complex.[47, 48] A variety of biological studies into the use of Schiff bases and their metal complexes for antitumour,[49] antimicrobial and anti-inflammatory activity[50] have taken place. It was discovered that the antimicrobial activity of the organic ligands increased several-fold on chelation as compared to the ligand molecule alone, whereas the anti-inflammatory activity of some ligands was lost upon complexation. In addition, these complexes were investigated as possible mimics of copper(II) sites in galactose oxidase.[51] Metal complexes of this class of ligand with copper, vanadium and ruthenium have been investigated for use as catalysts for a range of organic molecule transformations.[52-56] More recently, research has been done on aluminium and gallium complexes for their potential application as small molecule organic light emitting diodes (SMOLEDs), taking advantage of the high luminescence quantum efficiency and relatively low manufacturing cost of this type of molecule.[57, 58]

Ligands of this type have been used in solvent extraction to analyse the metal content of an aqueous solution.[59] The solution was contacted with a water immiscible solvent containing the ligand which extracted the metal ions from the aqueous solution. The

solutions were then separated and the organic layer analysed for metal content. They concluded that a 1 : 1 ligand to metal complex was formed in the organic layer and complexation of nickel(II) was found to be optimal at pH greater than 8. This work encourages further study into this class of compound for their potential use in solvent extraction due to their proven metal coordination properties. More recently, a comparable study into the analysis of aqueous solutions containing trace amounts of copper has been carried out *via* solvent extraction.[60] However, the ligands used in this study contain at least one pyridine ring and therefore have a different donor set to the proposed O,N,O coordination site for metal complexation.

Solvent extractants used in metallurgy generally contain pendant alkyl groups in order to increase their solubility in organic solvents. It is therefore proposed that the prototype ligand will be di-*tert*-butyl substituted, *para* to the hydroxyl groups. Few literature references relating to alkyl-functionalised structures exist, although Sridharan *et al.* have published two papers on the synthesis of Schiff base ligands with pendant tertiary butyl groups. The first involves the synthesis *via* the condensation of the benzilidene and anil units, each containing alkyl groups, in an alcoholic solvent[61] followed by their subsequent conversion to benzoxazoles, while the second is concerned with the microwave-assisted solvent-free condensation.[62] Consequently, accessible routes to alkyl-functionalised Schiff base ligands have been established.

Therefore, this chapter focuses on the synthesis and characterisation of the Schiff base ligand (the di-*tert*-butyl substituted *N*-(*o*-hydroxybenzylidene)*o*-hydroxyanil, **1**). The preparation of copper(II) and nickel(II) complexes is reported and extraction of copper(II) into chloroform has been studied under conditions which allowed the speciation in the water-immiscible solvent to be defined.

2.2 Ligand synthesis and characterisation

Ligand **1** was prepared in two steps. First, 2-hydroxy-5-*t*-butylbenzaldehyde was obtained by a method based on the industrial process developed by Levin and co-workers[63] using a magnesium-mediated formylation. The resulting aldehyde was treated with 2-amino-4-*t*-butylphenol in a Schiff base condensation at room temperature in methanol to form the ligand **1** (Scheme 2.2).

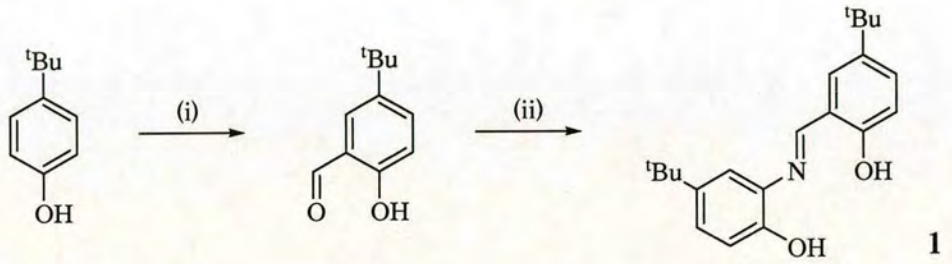

Scheme 2.2: Synthesis of Ligand **1** (i) $Mg(OMe)_2$, paraformaldehyde, toluene, (ii) 2-amino-4-*t*-butylphenol, methanol.

1 was characterised by ^1H and ^{13}C NMR spectroscopy, CHN analysis, IR and FAB mass spectrometry. ^1H NMR spectroscopy proved to be a particularly useful tool for confirming that the Schiff base reaction was complete and for indicating purity of the product. The aldehyde peak has a characteristic signal at $\delta \sim 10.0$ and the imine is seen at $\delta \sim 9.0$. Consequently, the disappearance of the aldehyde peak confirmed the reaction had gone to completion.

2.2.1 Crystal structure of ligand 1

Ligand **1** formed orange square plates of crystallographic quality when recrystallised from methanol. Each asymmetric unit contains one molecule of ligand and one methanol molecule. The structure is shown in Figure 2.5. The molecule is not entirely planar as the two benzene rings are inclined at an angle of 32.52(9)°.

There is an intramolecular H-bond between the phenolic hydrogen atom on O1 and the nitrogen atom, N2, with a distance of 1.706(5)° between H and N2. The hydrogen atom on each methanol is also H-bonded to O1, while the methanolic oxygen (O3) is H-bonded to an adjacent ligand's hydrogen atom on O2.

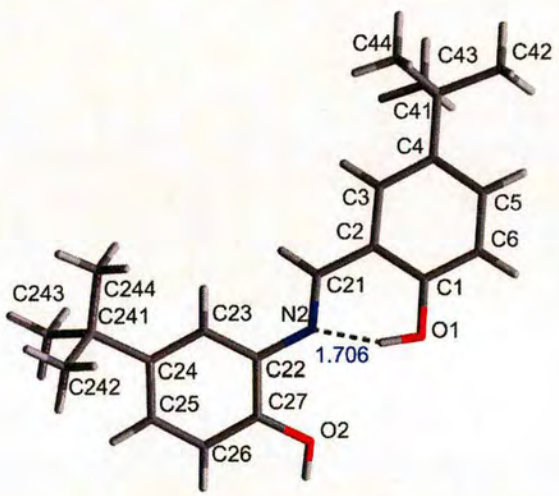

Figure 2.5: Crystal structure of ligand **1** showing the atom labelling scheme used in tables of bond lengths and angles (available in detail on the appendix CD) and the intramolecular H-bonding contact between the H on O1 and N2 (1.706(5) Å).

The O1, N2, O2 angle is 90.42(8)°, indicating that the ligand is preorganised for formation of square planar complexes (Figure 2.6). Placing a metal, M on the midpoint between the two O donors would result in M-O and M-N bond lengths of 1.86 Å and 1.75 Å respectively.

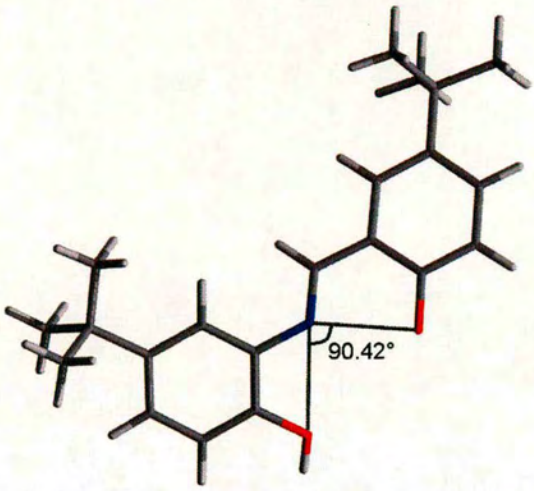

Figure 2.6: Coordination polyhedron reflex angle of ligand **1**.

2.3 Preparation and characterisation of metal complexes

Preparation of neutral metal complexes involved mixing stoichiometric amounts of metal acetate (Ni or Cu) and ligand **1** in methanol, in the expectation that the ligand will be doubly deprotonated under these conditions, hence:

$$nM(OAc)_2 + n\mathbf{1} \rightarrow [M_n(\mathbf{1}\text{-}2H)_n] + 2nH^+$$

Immediate precipitation was observed. The precipitate was washed with ammonia to remove any acetic acid and analysed by mass spectrometry. The spectra showed peaks for the molecular ions at 763 for the Ni complex and 773 for the Cu complex, and are consistent with the formation of a 2 : 2 ligand to metal complex $[M_2(\mathbf{1}\text{-}2H)_2]$. It proved impossible to isolate crystals of these 2 : 2 complexes in order to confirm the structure by X-ray diffraction studies. However, previous work with hydrazones has suggested that 2 : 2 complexes such as A in Figure 2.7 are formed under similar conditions.[64] Ligand **1** could generate a very similar NO_2^{2-} donor set geometry with the aminophenolate unit in B replacing the hydrazonato unit.

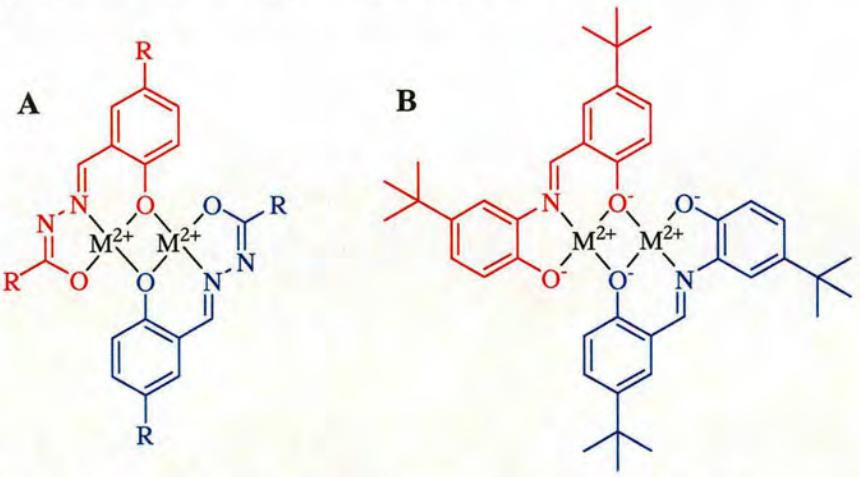

Figure 2.7: Structure of 2 : 2 complex (A) proposed previously[64] and analogous complex (B) formed by ligand **1**.

Formation of this neutral dinuclear complex would require the two phenolic protons on each ligand to be lost upon complexation. In the proposed structure (B) in Figure 2.7, the phenolate oxygen from the aldehyde component (O1 in the crystal structure of **1**, see Figure 2.5) bridges the two metal centres, forming a six-membered ring.

Searching of the CSD for the NO_3 binding motif found that nickel adopts this configuration more often than copper (15 hits *vs*. 8 hits respectively).[65]

C

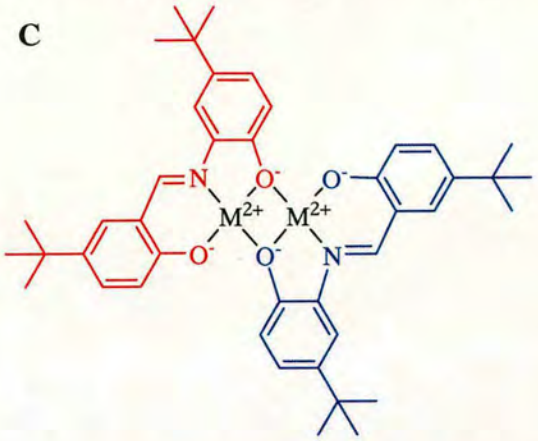

Figure 2.8: Alternative metal complex structure.

In structure C in Figure 2.8, the bridging oxygen is the phenolate oxygen in the anil component (O2 in the crystal structure of **1**). The incorporation of the bridging atom into a five-membered chelate ring increases strain on the bridging oxygen, with M-O bonds not in alignment with the sp^2 lone pairs. Searching the crystal database for these configurations reveals no hits for either copper or nickel when bridged in this way, whereas there are 2 or 3 respectively where the phenolate in the benzylidene component bridges the metals. Consequently it was assumed that binding mode B would predominate in complexes of **1**. However, recent results in a parallel project[66] have shown that this may not necessarily be the case. An analogue of **1** bearing a 3-carboxylato substituent (see D in Figure 2.9) gives a 2 : 2 ligand to copper(II) complex which has the structure shown in Figure 2.8 with the anil phenolate oxygen atoms forming the bridges. The 3-carboxylic acid groups form intermolecular contacts to copper atoms in neighbouring complexes resulting in 5-coordinate copper centres.

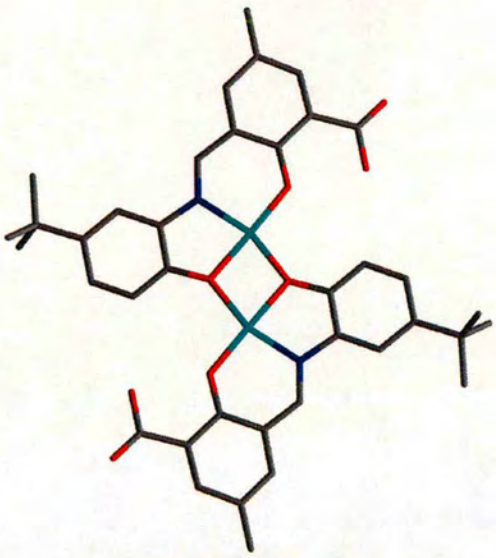

D

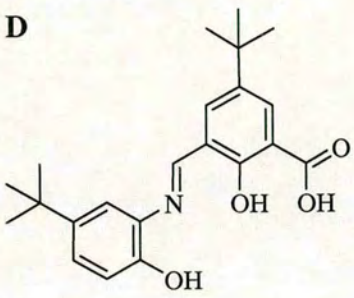

E

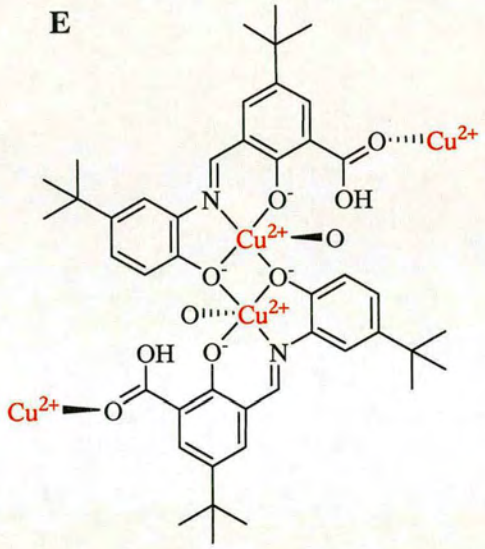

Figure 2.9: X-ray crystal structure[66] of a dinuclear copper complex of the 3-carboxylic acid derivative of **1** shown in D. Intermolecular bonds to copper atoms in neighbouring units from the 3-carboxylic acid groups are omitted from the crystal structure but shown in E.

2.4 Nickel complex formation and solvent extraction by ligand 1

Reaction of **1** with nickel(II) acetate gave a yellow/brown complex which separates readily from solution. The mass spectrum of the product showed a peak at 673, consistent with the formation of a neutral 2 : 2 complex $[Ni_2(\mathbf{1}\text{-}2H)_2]$. The C=N peak in the IR spectrum is shifted to lower energy confirming that the ligand present had been converted to a new species and the imine nitrogen is coordinated to the nickel. CHN microanalysis and determination of the nickel content by ICP-OES supports formation of a 1 : 1 ligand to metal stoichiometry in the complex. These data support formation of the yellow-brown complex as $[Ni_2(\mathbf{1}\text{-}2H)_2]$.

The sections which follow (2.4.1 - 2.4.2) consider the structure and magnetic properties of an unexpected 4 : 4 nickel complex of **1**, whilst the remainder (2.4.3) of the chapter is concerned with the use of **1** as a pH-swing extractant.

2.4.1 Crystallography

The dinuclear nickel complex formed with ligand **1** was dissolved in chloroform and left to evaporate in the presence of methanol over a period of several weeks. The dark green cubic crystals which formed were suitable for X-ray crystallography. They contain a 4 : 4 complex of nickel to ligand **1** (Figure 2.10). The change in colour indicates that this is a different species from the yellow complex prepared earlier. Each nickel is bound to the NO_2^{2-} unit from one ligand and the phenolate oxygens from the anil units of 2 other ligands. A methanol occupies the 6th site to give a pseudo-octahedral structure for each nickel atom.

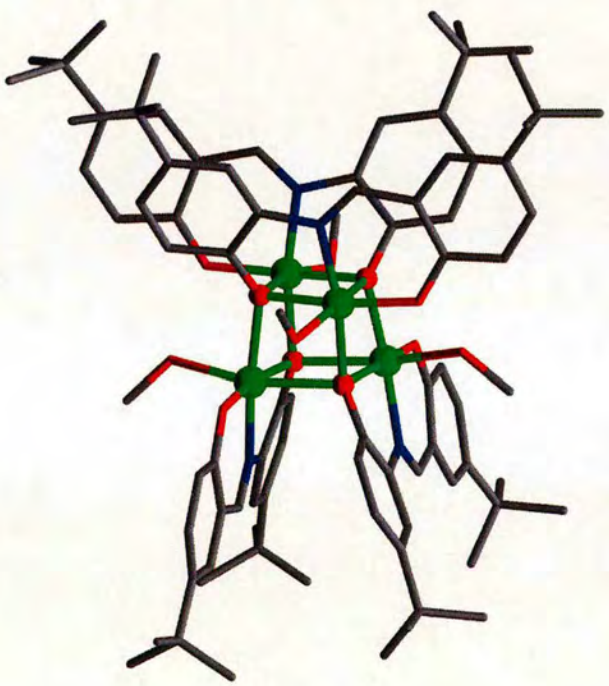

Figure 2.10: Solid state structure of $[Ni_4(\mathbf{1}\text{-}2H)_4(MeOH)_4]$. Grey= C, Red= O, Blue= N, Green= Ni. Hydrogens are removed for clarity.

Searching the CSD (Figure 2.11) for instances of bridging phenolate oxygens revealed that bridging between three metals (Cu, 6; Ni, 7)[67-79] is much less common than bridging between two (Cu, 558; Ni, 228). In the ligand **1** complex, the

deprotonated phenol from the anil unit on each ligand acts as the bridging donor between three nickel(II) atoms. This can be seen more clearly in Figure 2.12.

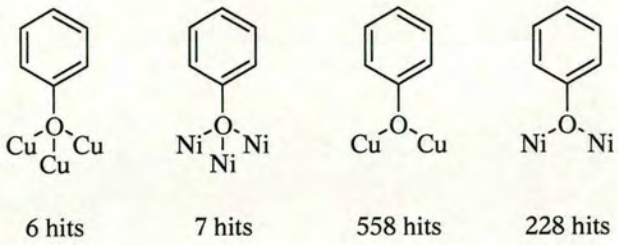

Figure 2.11: Search criteria for CSD search for bridging phenolate oxygens.

A comparison of the structures of the free and complexed ligand shows that it is nearer planarity in the complex; the angle of inclination between the benzene rings decreases from 33° to 17°. This is most probably a consequence of the preference of six coordinate nickel(II) for regular octahedral geometry. Planarity of the NiO_2N unit defined by one of the ligands will be enhanced if the ligand itself is planar so that all atoms in the chelate rings (with the exception of the bridging phenolate) are sp^2 hybridised.

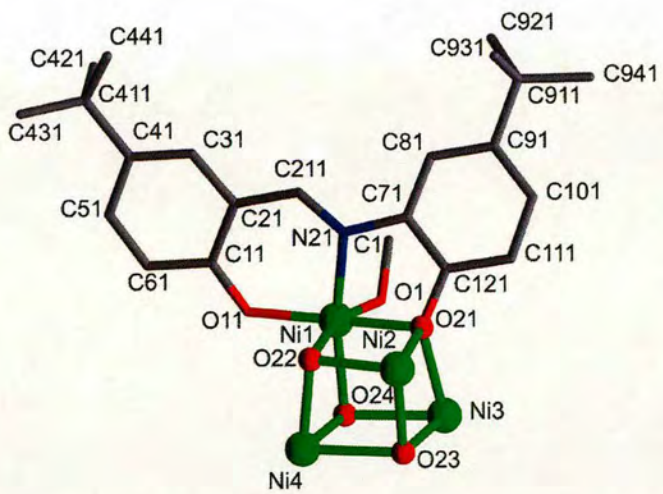

Figure 2.12: Core of the $[Ni_4(1\text{-}2H)_4(MeOH)_4]$ complex showing the ligand chelating Ni1 and the atom labelling scheme used in tables 2.1-2.4.

For a tridentate ligand bound to an octahedral metal, there are two possible geometric isomers (Figure 2.13). *Fac* isomers occupy one face of the octahedron, with all three donor atoms adjacent to one another, hence the name, facial. *Mer* isomers however, can be considered as lying on the meridian of a sphere as they place the three donors and the metal atom in the same plane. Ligand **1** forms the *mer* isomer; donors are on one plane of the nickel octahedron, with two other bridging oxygens and the methanol molecule filling the other plane. This is due to the reasonably rigid donor set of the ligand and its overall planarity, resulting in its preference to bind in this way.

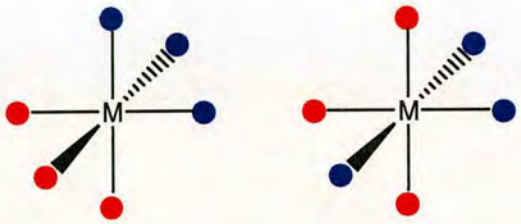

Figure 2.13: Possible geometrical isomers of an octahedral complex.

Table 2.1 and 2.2 show some of the bond lengths and angles in the coordination spheres of the nickel atoms in $[Ni_4(\mathbf{1}\text{-}2H)_4(MeOH)_4]$. From the free ligand structure (Section 2.2.1), ideal M-O and M-N bond lengths obtained by placing the metal on the midpoint between the two O donors would be 1.86 Å and 1.75 Å respectively. The observed bond lengths in the complex are longer but more consistent with those expected for nickel complexes of this type.[80] This increase is likely to result from having to accommodate a large metal ion between the donor atoms, forcing them further apart, when compared to the much smaller protons present in the free ligand. Furthermore, this results in an increase in the angles within the 6-membered chelate rings of the complexed ligand compared to the free ligand (Table 2.2). In contrast, in the 5-membered chelate rings, most of the angles are decreased with respect to the free ligand. These angles are reduced due to ring strain enforced by the 5-membered ring, where both the N and O donors from one ligand must coordinate to the same nickel.

Length of bond between:	Ni1	Ni2	Ni3	Ni4	Mean
Ni-N	1.972(4)	1.978(4)	1.974(4)	1.982(4)	**1.977**
Ni-$O_{terminal}$	1.973(3)	1.948(3)	1.954(3)	1.956(4)	**1.958**
Ni-O_{bridge}	2.051(3)	2.064(3)	2.053(3)	2.048(3)	**2.054**
Ni-O_{bridge}'(cis)	2.217(3)	2.185(3)	2.204(3)	2.216(3)	**2.206**
Ni-O_{bridge}"(trans)	2.055(3)	2.062(3)	2.085(3)	2.041(3)	**2.061**
Ni-$O_{methanol}$	2.098(3)	2.107(4)	2.105(3)	2.087(3)	**2.099**
C-$O_{terminal}$	1.323(6)	1.308(6)	1.322(6)	1.344(6)	**1.324**
C-O_{bridge}	1.359(6)	1.368(6)	1.348(6)	1.366(6)	**1.360**

Table 2.1: Bond lengths (Å) in $[Ni_4(1\text{-}2H)_4(MeOH)_4]$.

	6-membered ring			5-membered ring	
Angle	O-C-C	C-C-C	C-C-N	O-C-C	C-C-N
Ligand	121.4(2)	120.50(18)	120.8(2)	118.6(2)	117.1(2)
Complex (Ni1)	123.6(5)	124.6(5)	127.1(4)	119.3(5)	114.4(4)
(Ni2)	125.5(5)	124.0(5)	124.9(5)	117.4(5)	115.9(4)
(Ni3)	123.6(4)	126.0(4)	124.2(4)	120.7(4)	112.9(4)
(Ni4)	126.2(4)	124.0(5)	126.1(5)	117.8(4)	116.3(4)
Complex mean	124.73	124.65	125.58	118.80	114.88

Table 2.2: Bond angles (°) in free ligand **1** compared to those in $[Ni_4(1\text{-}2H)_4(MeOH)_4]$.

On comparing the Ni-O bond lengths for each nickel, the shortest and therefore strongest bond is between nickel and the terminal phenolate oxygen within the 6-membered chelate ring. This is because the phenolate is bound to only one nickel centre and is therefore unconstrained, allowing it to bind in its preferential sp^2 configuration. It is also negatively charged, making it a better donor than the other monodentate ligand, the methanol. The longest bonds are found between nickel and the oxygen atom *cis* to its nitrogen donor. These oxygens are bound to a carbon and three nickel centres. They are therefore highly strained, tridentate donors and have sp^3 hybridisation. This bond is longer than any other Ni-O bond involving a bridging oxygen due to the monodentate methanol molecule *trans* to it. The methanol can form a short, strong bond, allowing elongation of the Ni-O_{bridge} bond to relieve some of the strain. Also of note is the difference in C-O bond lengths in each ligand coordinated to nickel (Table 2.1). When each of the anil phenolate oxygens bridges between three nickel atoms, the C-O bond is longer than when the benzylidene phenolate forms a terminal Ni-O bond to a single nickel. This suggests that bridging

phenolates have sp^3 bonds with carbon, whereas those which coordinate to just one nickel have shorter, more sp^2-like bonds.

Regular octahedra have 6 identical donors, each with the same bond length from the central atom and with regular 90° angles between bonds. Clearly, since each nickel has an NO_5 donor set, this is not a regular octahedron. Also, the bond lengths, as discussed above, are not all equal, due to the variation in donor and/or hybridisation. Table 2.3 lists the angles around each nickel atom as defined by its donor set. There is a wide range of deviation from 90°; the smallest angle is 77.81° and the largest is 100.76°. This irregularity results in the formation of a skewed octahedron at each nickel(II) centre and consequently influences the shape of the central Ni_4O_4 cube.

Angle at Ni defined by:	Ni1	Ni2	Ni3	Ni4	Mean
N, $O_{terminal}$	94.48(15)	94.09(15)	94.11(15)	94.70(15)	**94.35**
N, O_{bridge}	82.31(14)	82.82(14)	82.75(15)	82.91(15)	**82.70**
N, O_{bridge}' (cis)	96.21(14)	96.43(15)	96.00(14)	97.58(13)	**96.56**
N, O_{bridge}'' (trans)	168.94(14)	168.50(14)	168.45(15)	168.70(15)	**168.65**
N, $O_{methanol}$	91.90(15)	91.33(15)	92.32(15)	90.11(14)	**91.42**
$O_{terminal}$, O_{bridge}	170.18(13)	170.59(15)	169.99(14)	170.67(14)	**170.36**
$O_{terminal}$, O_{bridge}'	92.94(13)	92.86(14)	92.97(13)	93.63(14)	**92.90**
$O_{terminal}$, O_{bridge}''	96.44(13)	97.41(13)	97.36(13)	96.57(13)	**96.95**
$O_{terminal}$, $O_{methanol}$	99.98(14)	99.14(15)	100.76(15)	99.91(14)	**99.95**
O_{bridge}, O_{bridge}'	78.25(12)	78.71(12)	77.97(12)	77.81(12)	**78.19**
O_{bridge}, O_{bridge}''	86.63(12)	85.81(12)	85.72(12)	86.08(13)	**86.06**
O_{bridge}, $O_{methanol}$	89.43(13)	89.84(13)	88.90(13)	89.14(13)	**89.33**
O_{bridge}', O_{bridge}''	81.46(12)	82.94(12)	82.07(12)	82.48(12)	**82.24**
O_{bridge}', $O_{methanol}$	164.16(13)	165.22(13)	163.39(13)	163.84(13)	**164.15**
O_{bridge}'', $O_{methanol}$	87.99(13)	86.95(13)	86.91(13)	87.21(13)	**87.27**

Table 2.3: Bond angles (°) at nickel(II) atoms in $[Ni_4(1\text{-}2H)_4(MeOH)_4]$.

An ideal cube would have eight identical atoms at each corner, identical bond lengths along each side of the cube and right angles between bonds. As the cube has both nickel and oxygen atoms at its corners it forms an irregular shape. Table 2.4 shows the bond lengths defining the sides of the cube and the angles at each corner atom. The angles range from 77.81 to 102.36°, with a mean of 89.58°. The angles greater than 90° are at oxygen atom corners whereas the nickel atoms form angles less than 90°. In order for the oxygen atoms to coordinate to three nickel atoms efficiently, the

angles of the bonds should be as close to 109° as possible. To achieve this, the oxygens therefore move in towards the centre of the cube. This in turn causes the nickel atoms to move outwards, decreasing the angles defined by them. There is some variation from the mean bond length of 2.106 Å; the shortest bond is 2.041 Å while the longest is 2.217 Å. These irregularities highlight the deviance from exact geometry, resulting in an overall distorted cube.

Atoms	Angle
Ni1-O21-Ni2	102.23(14)
Ni2-O21-Ni3	92.14(13)
Ni1-O21-Ni3	96.07(13)
Ni1-O22-Ni2	100.75(13)
Ni2-O22-Ni4	97.27(13)
Ni1-O22-Ni4	92.66(12)
Ni3-O23-Ni2	96.76(14)
Ni2-O23-Ni4	92.08(12)
Ni3-O23-Ni4	101.82(14)
Ni3-O24-Ni1	92.37(12)
Ni1-O24-Ni4	97.38(13)
Ni3-O24-Ni4	102.36(14)
O21-Ni1-O22	78.25(12)
O22-Ni1-O24	81.46(12)
O21-Ni1-O24	86.63(12)
O21-Ni2-O22	78.71(12)
O22-Ni2-O23	85.81(12)
O21-Ni2-O23	82.94(12)
O21-Ni3-O23	85.72(12)
O23-Ni3-O24	77.97(12)
O21-Ni3-O24	82.07(12)
O22-Ni4-O23	82.48(12)
O23-Ni4-O24	77.81(12)
O22-Ni4-O24	86.08(13)
Mean	89.58

Bond	Length
Ni1-O21	2.051(3)
Ni1-O22	2.217(3)
Ni1-O24	2.055(3)
Ni2-O21	2.185(3)
Ni2-O22	2.064(3)
Ni2-O23	2.062(3)
Ni3-O21	2.085(3)
Ni3-O23	2.053(3)
Ni3-O24	2.204(3)
Ni4-O22	2.041(3)
Ni4-O23	2.216(3)
Ni4-O24	2.048(3)
Mean	2.106

Table 2.4: Bond angles (°) and lengths (Å) present in the Ni_4O_4 central cube of $[Ni_4(1\text{-}2H)_4(MeOH)_4]$.

There is one instance of a Ni_4O_4 complex in the literature, which also has an NO_5 environment around each nickel(II) centre.[79] The complex has the molecular formula $[(LH)_2Ni_4(OCH_3)_2(OAc)_2(CH_3OH)_2]$. The ligand involved, L, (Figure 2.14) is capable of coordinating to two nickel atoms and hence formation of the tetranuclear complex involves two ligands. The oxygens forming the central cube with nickel are two methoxides and the two central phenolates from the ligand, each of these bridges

between three nickels as with the ligand **1** complex. To complete the octahedral geometry, each nickel is also coordinated to either an acetate (Ni1 and Ni4) or methanol (Ni2 and Ni3).

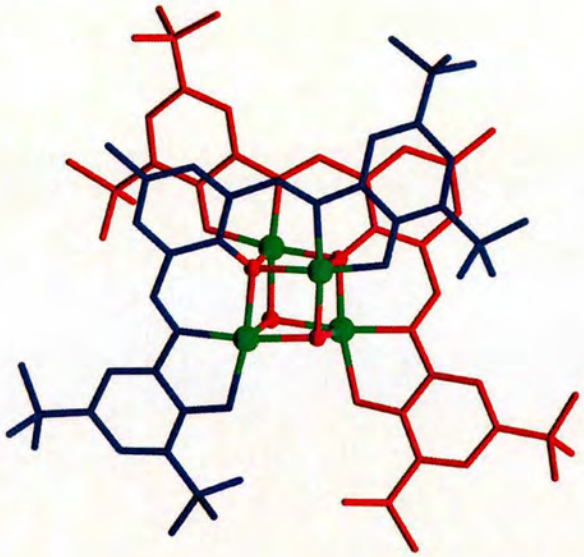

F

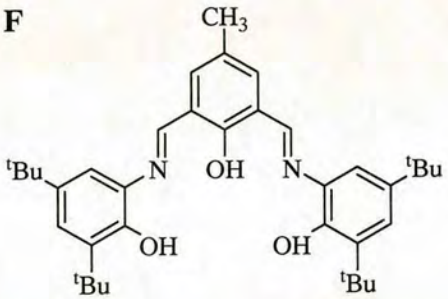

G

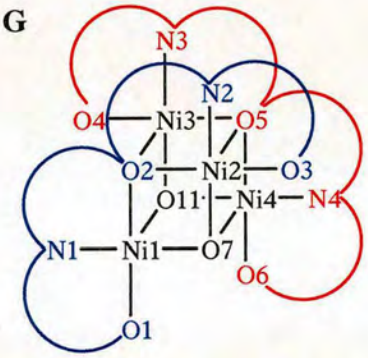

Figure 2.14: Ligand (F) used in literature $[(LH)_2Ni_4(OCH_3)_2(OAc)_2(CH_3OH)_2]$ and an illustration (G) of how the binding of two ligands to four metals forms a central cube. O7 and O11 are from methoxide groups. The additional solvent molecules attached to each nickel (acetate on Ni1 and 4, methanol on Ni2 and 3) have been omitted for clarity.[79]

Each nickel(II) centre has a partial donor set from one ligand defining a plane of its octahedron and each of the two ligands addresses opposite faces of the central cube. The nickel centres can therefore be considered to be in a *mer* configuration, as for the ligand **1** complex. The planarity of each of the NO_2 donor sets from the ligand necessitates binding in this way. However, there is some deviation from planarity in each of the ligands. The ligand coordinated to Ni1 and Ni2 has angles of inclination of 23.34° and 32.33° between the planes of the central benzene ring and those on

either side. The corresponding angles on the second ligand, coordinated to Ni3 and 4, are 26.24° and 21.24°. Therefore, the ligand must undergo a twist from planarity in order to address both nickel atoms, forming two 5-membered and two 6-membered chelate rings. The angles within these rings are shown in Table 2.5 and compared to the mean angles in the ligand **1** complex. The angles in the 5-membered rings were found to be very similar, which is as expected due to the same donor set and ligand configuration. In contrast, the 6-membered rings show a variety of differences. The angles involving the bridging phenolate oxygens are much smaller than previously, due to their coordination to three nickel(II) centres. This subsequently causes an increase in the remaining angles in the 6-membered ring.

	6-membered ring			5-membered ring	
Angle	**O-C-C**	**C-C-C**	**C-C-N**	**O-C-C**	**C-C-N**
Complex (Ni1)	119.7(8)	125.4(8)	127.5(8)	117.9(8)	114.1(8)
(Ni2)	121.4(8)	125.2(9)	127.3(9)	120.8(8)	113.0(8)
(Ni3)	121.8(8)	125.2(8)	127.0(9)	119.9(8)	113.3(8)
(Ni4)	119.9(8)	125.6(8)	127.9(8)	116.9(8)	115.7(8)
Complex mean	120.70	125.35	127.43	118.88	114.03
Ligand 1 complex	124.73	124.65	125.58	118.80	114.88

Table 2.5: Bond angles (°) in $[(LH)_2Ni_4(OCH_3)_2(OAc)_2(CH_3OH)_2]$ compared to those in $[Ni_4(\mathbf{1}\text{-}2H)_4(MeOH)_4]$.

The Ni-N and Ni-O bond lengths in this complex are of similar length to those found in the ligand **1** complex (Table 2.6). The longest Ni-O bond is from the oxygen *cis* to the nitrogen donor. The shortest bond is from the terminal phenolate from the ligand. This bond is however, longer than its equivalent in the ligand **1** complex. Since the ligand coordinates to two metal ions, there is increased strain on the ligand structure which causes this bond to extend.

Length of bond between:	Ni1	Ni2	Ni3	Ni4	Mean
Ni-N	1.989(8)	1.984(8)	1.994(7)	1.979(8)	**1.986**
Ni-$O_{terminal}$	2.089(7)	1.970(6)	1.969(6)	2.126(6)	**2.039**
Ni-O_{bridge}	2.081(7)	2.050(6)	2.054(7)	2.069(6)	**2.064**
Ni-O_{bridge}'(cis)	2.050(7)	2.229(7)	2.221(7)	2.055(7)	**2.139**
Ni-O_{bridge}"(trans)	2.052(6)	2.025(7)	2.051(6)	2.042(6)	**2.043**
Ni-$O_{methanol/acetate}$	2.112(7)	2.123(7)	2.108(7)	2.093(7)	**2.109**
C-O (O1,O3,O4,O6)	1.384(11)	1.315(11)	1.324(11)	1.392(10)	**1.354**
C-O (O2,O5)	1.357(12)	1.357(12)	1.335(11)	1.335(11)	**1.346**

Table 2.6: Bond lengths (Å) in $[(LH)_2Ni_4(OCH_3)_2(OAc)_2(CH_3OH)_2]$. The figures in red represent one ligand while those in blue represent the other.

The ligand **1** complex showed a considerable deviation from regular octahedral geometry around each nickel and consequently a distorted central Ni_4O_4 cube. Table 2.7 and 2.8 give details of the bond lengths and angles which define these geometries for the $[(LH)_2Ni_4(OCH_3)_2(OAc)_2(CH_3OH)_2]$ complex, showing that the same general trends are present.

Angle at Ni defined by:	Ni1	Ni2	Ni3	Ni4	Mean
N, $O_{terminal}$	80.9(3)	83.9(3)	83.5(3)	80.2(3)	**82.13**
N, O_{bridge}	88.4(3)	90.9(3)	90.6(3)	89.4(3)	**89.83**
N, O_{bridge}' (cis)	100.1(3)	97.0(3)	97.0(3)	99.8(3)	**98.48**
N, O_{bridge}" (trans)	170.6(3)	174.3(3)	172.1(3)	171.2(3)	**172.05**
N, $O_{methanol/acetate}$	90.5(3)	88.6(3)	89.5(3)	89.8(3)	**89.60**
$O_{terminal}$, O_{bridge}	167.9(3)	174.4(3)	173.7(3)	168.7(3)	**171.18**
$O_{terminal}$, O_{bridge}'	93.7(3)	96.9(3)	96.7(3)	93.9(3)	**95.30**
$O_{terminal}$, O_{bridge}"	108.4(3)	101.3(3)	103.7(3)	108.5(3)	**105.48**
$O_{terminal}$, $O_{methanol/acetate}$	89.6(3)	96.4(3)	94.5(3)	90.7(3)	**92.80**
O_{bridge}, O_{bridge}'	82.3(3)	81.8(2)	81.9(2)	83.4(3)	**82.35**
O_{bridge}, O_{bridge}"	82.5(3)	83.9(3)	82.2(3)	82.0(3)	**82.65**
O_{bridge}, $O_{methanol/acetate}$	96.4(3)	85.4(3)	87.5(3)	93.7(3)	**90.75**
O_{bridge}', O_{bridge}"	80.9(3)	80.2(3)	79.0(2)	81.1(3)	**80.30**
O_{bridge}', $O_{methanol/acetate}$	169.3(3)	166.1(2)	167.6(2)	170.0(3)	**168.25**
O_{bridge}", $O_{methanol/acetate}$	88.4(3)	93.1(3)	93.3(3)	89.0(3)	**90.95**

Table 2.7: Bond angles (°) at nickel(II) atoms in $[(LH)_2Ni_4(OCH_3)_2(OAc)_2(CH_3OH)_2]$.

Atoms	Angle
Ni1-O2-Ni2	95.1(3)
Ni2-O2-Ni3	98.1(3)
Ni1-O2-Ni3	95.7(3)
Ni2-O5-Ni3	97.7(3)
Ni2-O5-Ni4	94.4(3)
Ni3-O5-Ni4	96.5(3)
Ni1-O7-Ni2	96.7(3)
Ni2-O7-Ni4	101.3(3)
Ni1-O7-Ni4	98.1(3)
Ni1-O11-Ni3	102.2(3)
Ni1-O11-Ni4	98.6(3)
Ni3-O11-Ni4	97.5(3)
O2-Ni1-O7	82.5(3)
O7-Ni1-O11	80.9(3)
O2-Ni1-O11	82.3(3)
O2-Ni2-O5	81.8(2)
O2-Ni2-O7	83.9(3)
O5-Ni2-O7	80.2(3)
O2-Ni3-O5	81.9(2)
O2-Ni3-O11	79.0(2)
O5-Ni3-O11	82.2(3)
O5-Ni4-O7	83.4(3)
O5-Ni4-O11	82.0(3)
O7-Ni4-O11	81.1(3)
Mean	89.71

Bond	Length
Ni1-O2	2.081(7)
Ni1-O7	2.052(6)
Ni1-O11	2.050(7)
Ni2-O2	2.050(6)
Ni2-O5	2.229(7)
Ni2-O7	2.025(7)
Ni3-O2	2.221(7)
Ni3-O5	2.054(6)
Ni3-O11	2.051(6)
Ni4-O5	2.069(6)
Ni4-O7	2.055(7)
Ni4-O11	2.042(6)
Mean	2.082

Table 2.8: Bond angles (°) and lengths (Å) present in the Ni_4O_4 central cube of $[(LH)_2Ni_4(OCH_3)_2(OAc)_2(CH_3OH)_2]$.

2.4.2 Magnetism

The Ni_4O_4 cubane unit in the structure of $[Ni_4(\mathbf{1}\text{-}2H)_4(MeOH)_4]$ provides some possibilities for unusual properties due to the proximity of the metal centres. The measurements described below were carried out by Professor Andrew Harrison.

Magnetisation data were taken for $[Ni_4(\mathbf{1}\text{-}2H)_4(MeOH)_4]$ using a $MPMS_2$ SQUID magnetometer (Quantum Design). A powdered sample (9.7 mg) was loaded in a gelatine capsule and wedged into a polyethylene straw using pieces of another, similar straw. This was loaded in the instrument and data taken in a field of 0.01 T over the temperature range 1.8 – 300 K. Data were corrected for the diamagnetic contribution from the sample holder, as well as from the constituent atoms using Pascal's constants.[81] The remaining molar susceptibility, χ_m, together with the effective moment ($(8\,\chi_m\,T)^{1/2}$), are plotted in Figure 2.15. At relatively high temperature, $(8\chi_mT)^{1/2}$ is close to the value of $\sqrt{8}$ Bohr magnetons, anticipated for spin-only S = 1 centres. However, on cooling, this value initially rises, before dropping slightly below 5 K. Taken together, these observations indicate that the Ni_4 cluster has predominantly ferromagnetic exchange, and that weaker, antiferromagnetic coupling (either within or between Ni_4 units) eventually reduce such magnetic polarization on cooling further. Data were fitted to the Curie-Weiss expression from temperatures above 20 K:

$$\chi_m = C/(T-\theta)$$

where the optimized Curie constant C was found to be 1.28(2) emu mol^{-1} K^{-1}, and the optimized Weiss temperature θ was found to be 9.45(17) K. The former value corresponds to an effective moment of 3.19 Bohr magnetons per Ni atom.

A more detailed analysis of such data would require a model to be established of the dominant exchange pathways, and a set of energy levels calculated for the various possible spin-states, followed by a calculation of the susceptibility of the cluster using a second-order van Vleck equation.[82] However, the potential complexity of the

exchange pathways, linked to the likelihood of significant ligand-field effects, discouraged us from taking this part of the analysis further.

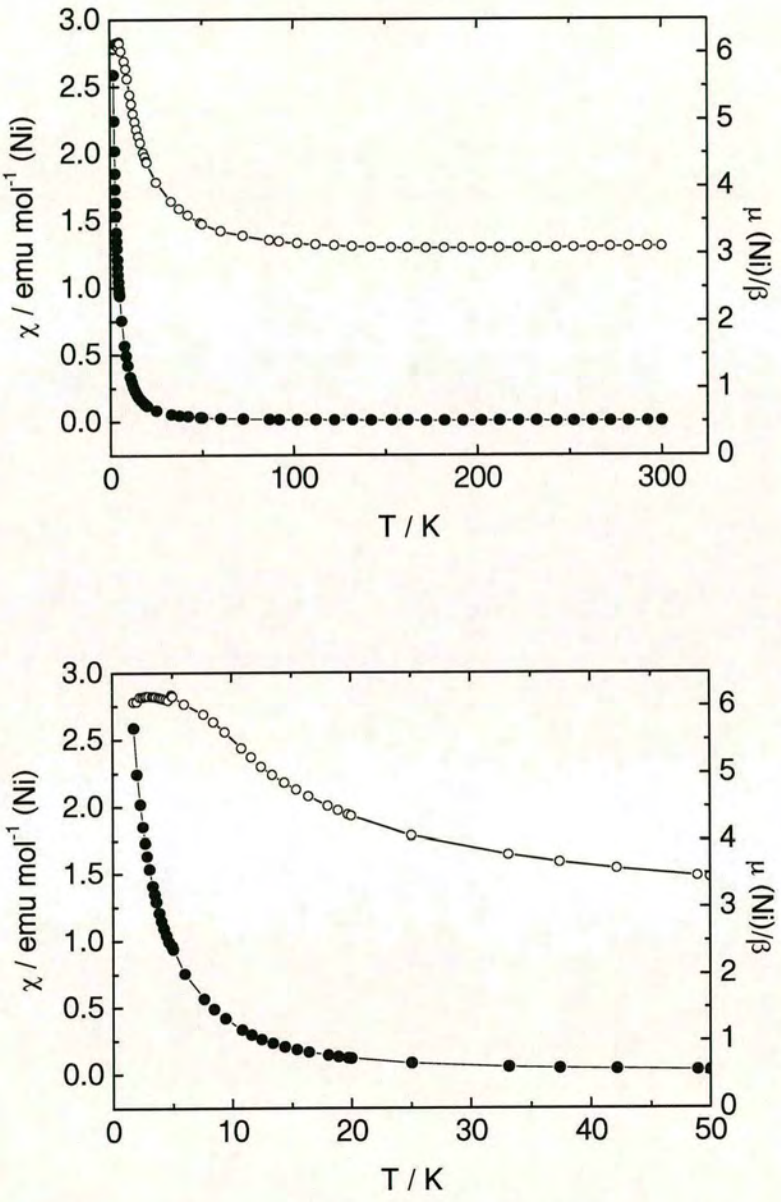

Figure 2.15: Magnetic susceptibility (closed circles) and effective moment (open circles) for $[Ni_4(\mathbf{1}\text{-}2H)_4(MeOH)_4]$ as a function of temperature, measured in a field of 0.01 T. The lower figure shows more detail of the low-temperature behaviour.

2.4.3 Solvent extraction

In order to assess the efficiency of **1** as a potential solvent extractant for nickel, the nickel complex $[Ni_2(\mathbf{1}\text{-}2H)_2]$ was subjected to an acid stripping experiment. A known volume of complex solution (5 ml, 0.00250 M) was contacted with aqueous sulfate solution (5 ml, 0.800 M) made up with varying ratios of Na_2SO_4 and H_2SO_4 solutions to a range of pHs. The two solutions were stirred for 16 hours and allowed to separate (Figure 2.16). Further details are provided in the experimental section (5.4.1).

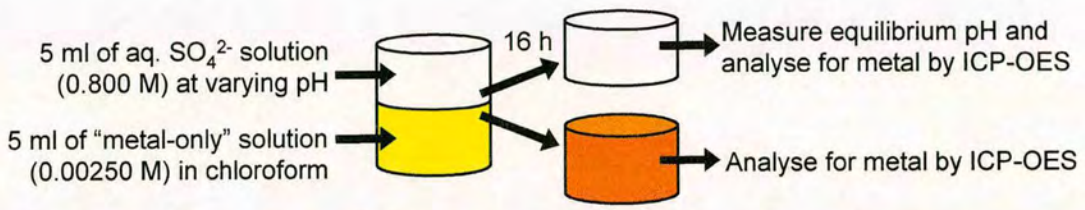

Figure 2.16: Procedure for stripping experiments.

The equilibrium pH of the aqueous layer was measured and both the organic and aqueous solutions were analysed for nickel by ICP-OES. The pH-dependence of loading/stripping is then revealed by plotting the percent loading of nickel relative to that in the stock $[Ni_2(\mathbf{1}\text{-}2H)_2]$ solution against equilibrium pH (Figure 2.17).

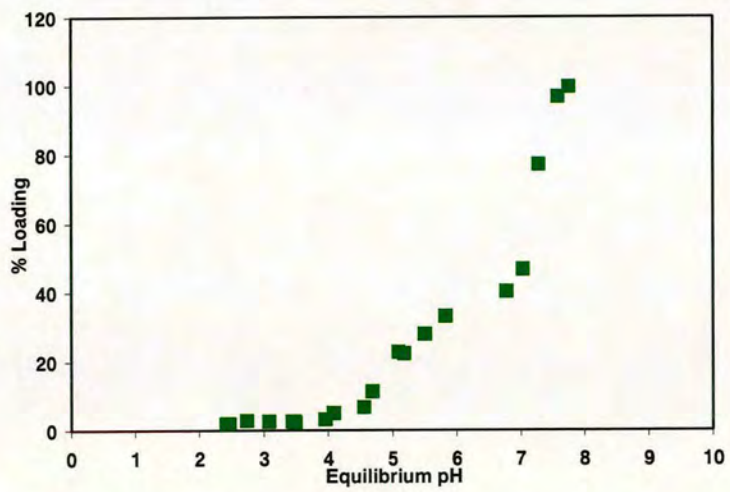

Figure 2.17: Stripping of nickel, ■, from an organic solution of $[Ni_2(\mathbf{1}\text{-}2H)_2]$ as a function of pH.

In order to confirm that no nickel was lost in the extraction process as a precipitate or another third phase, the percentage of total nickel in the system present in the aqueous phase was plotted alongside that in the organic phase (Figure 2.18). As these plots cross one another at ~50% and have the same general trend, we can account for 95% ± 5% of the nickel at any point during the extraction. Also of note is that there appears to be a slight plateau region at about 40% nickel. This suggests that there is more than one step in the stripping process.

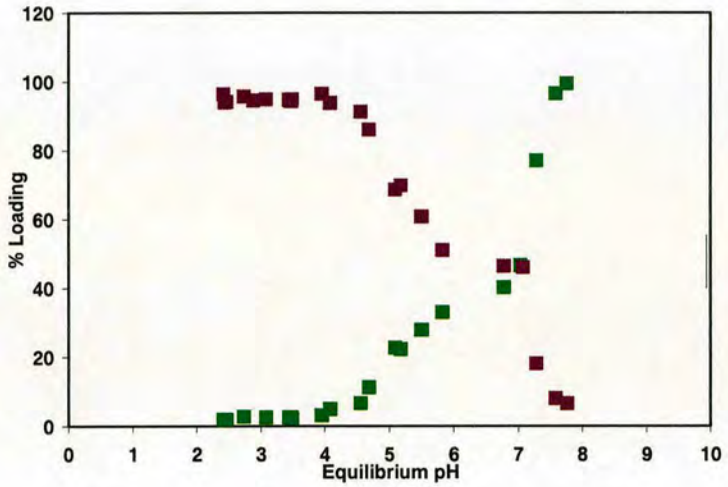

Figure 2.18: Nickel transferred to the aqueous phase, ■, and nickel remaining in the chloroform solution, ■, of $[Ni_2(1\text{-}2H)_2]$ as a function of pH.

As discussed in section 1.6.2, the commonly used indication of the strength of an extractant is its $pH_{½}$. The stripping experiment of $[Ni_2(1\text{-}2H)_2]$ has a $pH_{½}$ of 6.70. The ideal $pH_{½}$ for a nickel extractant in industry depends on the composition of the feed solution. If it contains iron(III) then in order to prevent precipitation of the iron, the feed is kept at a pH ≤ 2.5. Therefore, the $pH_{½}$ of a reagent to recover metal of value will be required to be *ca* 1.0.[83] Bulong Operations[84] in Western Australia processed nickel in the absence of iron. In order to ensure precipitation of the iron, the pH of the feed was adjusted to greater than 4, generally between 5.7 and 6.9.[85] Ligand **1** would be of minimal use in either of these conditions since at the operating pH values there would be little or no metal loading.

In conclusion, as intended in the original ligand design, **1** forms neutral complexes with nickel(II) in which the reaction stoichiometry is 1 : 1. For the yellow precipitate from the nickel complex synthesis, there is evidence from mass spectrometry, CHN and ICP-OES analysis to support the formation of a 2 : 2 complex which would be likely to have a structure as shown in Figure 2.7 with planar low-spin metal centres. This contains paramagnetic six-coordinate nickel(II) ions. Over a period of weeks, green crystals form in the presence of methanol which were found to contain a 4 : 4 ligand to nickel complex. This complex shows interesting magnetic behaviour; with predominantly ferromagnetic exchange which can be reduced at lower temperatures through antiferromagnetic coupling (either within or between Ni_4 units). Due to the high $pH_{½}$ shown for nickel(II), and the slow kinetics of complexation, it was decided investigations into nickel would be of little interest and provide less scope for study than copper.

2.5 Copper complex formation and solvent extraction by ligand 1

Reaction of **1** with copper(II) acetate gave a yellow complex which showed a peak in the mass spectrum at 773, consistent with the formation of a neutral 2 : 2 complex $[Cu_2(\mathbf{1}\text{-}2H)_2]$. The C=N peak in the IR spectrum is shifted to lower energy confirming that the ligand present had been converted to a new species and the imine nitrogen is coordinated to the copper. CHN analysis accounts for the percentage of carbon, hydrogen and nitrogen present in the complex, and the formation of an n : n complex is confirmed by analysis of the copper content by ICP-OES.

The sections which follow (2.5.1 – 2.5.3) provide information on the strength of ligand **1** as a conventional pH-swing extractant for copper, making comparison with extraction of nickel (see above) and with other cation exchange reactants. In these experiments the evidence suggests that the fully loaded system is a dinuclear complex as seen below.

$$2Cu^{2+} + 2\mathbf{1}_{(org)} \rightleftharpoons [Cu_2(\mathbf{1}\text{-}2H)_2]_{(org)} \qquad \textbf{Equ. 2.1}$$

An alternative extraction mechanism is described in section 2.5.3. This involves formation of a mononuclear complex (equation 2.2) in which L_{aux} is a neutral auxiliary ligand which occupies the fourth coordination site at Cu (II) and provides H-bonds to the two phenolate donors.

$$Cu^{2+} + \mathbf{1}_{(org)} + L_{aux\,(org)} \rightleftharpoons [Cu(\mathbf{1}\text{-}2H)L_{aux}]_{(org)} \qquad \textbf{Equ. 2.2}$$

2.5.1 Solvent extraction

When a chloroform solution of $[Cu_2(\mathbf{1}\text{-}2H)_2]$ was stripped into aqueous sulfate solutions of varying pH under the same conditions as described previously for nickel (section 2.4.3) the "S-curve" shown in Figure 2.19 was obtained.

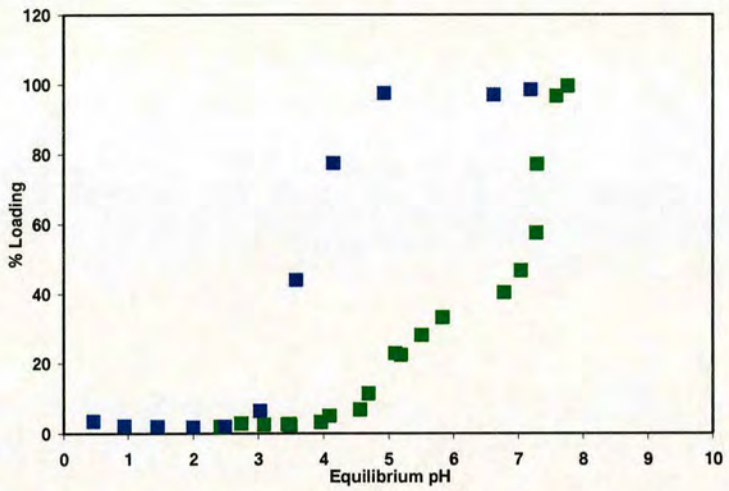

Figure 2.19: A comparison of the stripping of copper, ■, from an organic solution of $[Cu_2(\mathbf{1}\text{-}2H)_2]$ and nickel, ■, from an organic solution of [Ni2(1-2H)2] as a function of pH.

Unlike the tetranuclear nickel system, stripping appears to occur as a single step in this dinuclear complex, and the $pH_{½}$ value (3.75) is significantly lower than for the nickel system. The greater stability of the copper complex is consistent with the Irving-Williams series which gives the observed order of increasing values of formation constants for complexes of divalent 1st transition series metals (Figure 2.20). Whilst the relative stabilities of $[Cu_2(\mathbf{1}\text{-}2H)_2]$ and [Ni2(1-2H)2] are consistent with the Irving-Williams order[86] they relate to different types of complexes and copper is unlikely to be in a six-coordinate form in solution.

$$\mathbf{Ba^{2+} < Sr^{2+} < Ca^{2+} < Mg^{2+} < Mn^{2+} < Fe^{2+} < Co^{2+} < Ni^{2+} < Cu^{2+} > Zn^{2+}}$$

Figure 2.20: The Irving-Williams series for divalent metal ions.[86]

The relatively low $pH_{½}$ for stripping of copper from $[Cu_2(1\text{-}2H)_2]$ indicated that loading experiments could be carried out at pH values which will not result in precipitation of copper(II) oxy/hydroxides (Figure 2.21). The conditions used for these extractions are given in detail in section 5.4.2. They relate more closely than the stripping experiment described above to how a ligand would function in an industrial process.

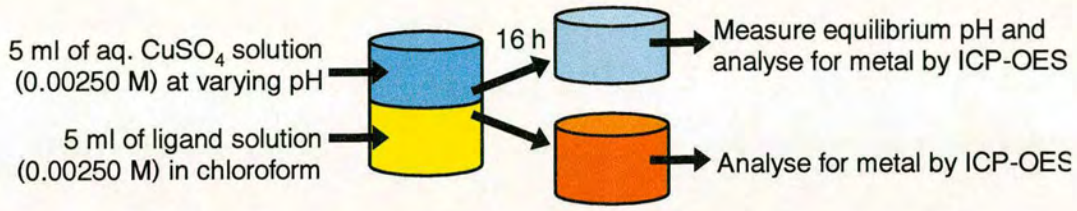

Figure 2.21: Procedure for loading experiments.

Solutions of the ligand were prepared to a known concentration (0.00250 M) in chloroform and contacted with an equal volume of aqueous $CuSO_4$ solutions at the same concentration at a range of pHs, controlled by the addition of NaOH or H_2SO_4. Again, the equilibrium pH is plotted against the percentage loading of copper, shown in Figure 2.22.

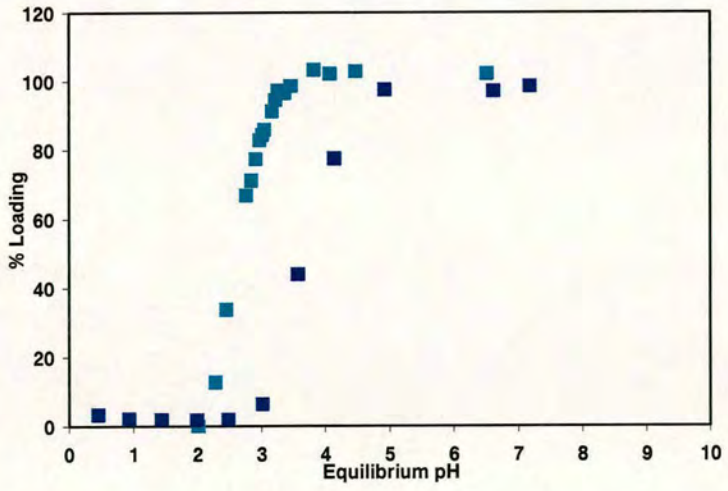

Figure 2.22: Comparison of the copper-loading, ■, and stripping, ■, dependence on pH for ligand **1**.

There is a difference in $pH_{½}$ of 1 between the curves for stripping (3.75) and loading (2.65) of copper with **1**. There are however, a number of differences in the two experimental techniques. The sulfate concentration in the stripping experiment is 0.800 M, whereas in the loading experiment it is equal to the copper concentration of 0.00250 M. Also, when performing the stripping experiment, a 0.00250 M solution of complex was used. If, as seen from mass spectrometry results, this is a 2Cu : 2L complex then the concentration of copper(II) and ligand in solution must be 0.00500 M. The loading experiment has exactly 0.00250 M of both copper(II) and ligand present in solution. To investigate whether there is a concentration dependence, a supplementary stripping experiment was carried with a 0.00125 M solution of complex, which should reduce the concentration of copper(II) and ligand in solution to 0.00250 M.. This data is shown alongside the original stripping data in Figure 2.23. It can clearly be seen that a reduction in the concentration of species in solution results in a decrease in $pH_{½}$ (to 3.0). Consequently, it can be assumed that the difference in the strip and load plots in Figure 2.22 is due to the difference in concentration.

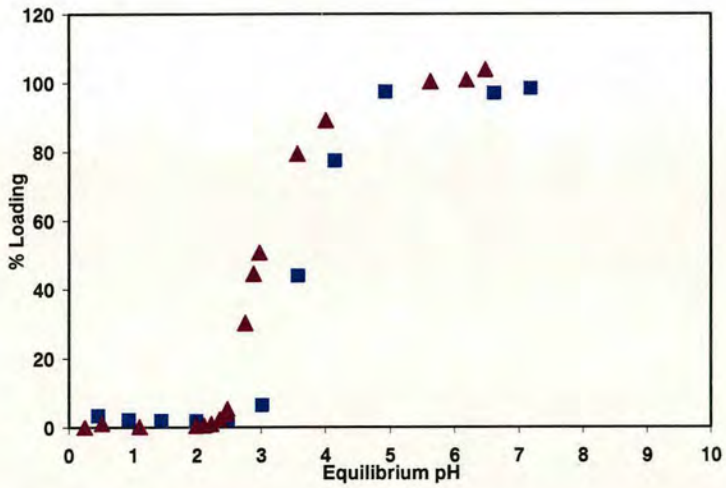

Figure 2.23: A comparison of the stripping of copper from an organic solution of $[Cu_2(\mathbf{1}\text{-}2H)_2]$ at a concentration of 0.00250 M, ■, and 0.00125 M, ▲.

2.5.2 Electron paramagnetic resonance (EPR)

We have seen from the Ni_4O_4 crystal structure, from mass spectrometry and from solvent extraction results that ligand **1** forms polynuclear complexes with both nickel and copper. Not only does copper(II) show more promising loading in solvent extraction experiments, but it also allows us further scope for study by EPR as its d^9 configuration means that it has one unpaired electron. If the unpaired electron is not antiferromagnetically coupled to another electron in a polynuclear complex, an EPR signal will be expected. Earlier work in the Tasker group[64] showed that the loading of copper by hydrazone ligands such as those discussed in section 2.3, began with the formation of a 2 : 1 complex which generated an EPR signal that grew in intensity as the concentration of copper increased towards 50% loading. This 2 : 1 structure is shown in Figure 2.24 (H). Beyond 50% loading the signal decreased in intensity, suggesting that the 2 : 2 structure formation had commenced. As the 2 : 2 structure forms, the unpaired electrons on the two copper(II) ions are antiferromagnetically coupled, resulting in loss of the EPR signal.

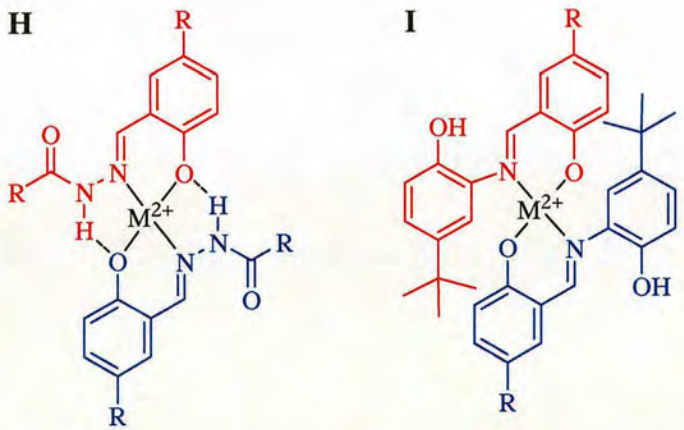

Figure 2.24: Possible 2 : 1 ligand to copper(II) complexes for a hydrazone (H) and ligand **1** (I).

It was hoped that a study of the ligand **1** copper complexes would generate similar results. Samples were taken directly from ligand **1** stripping and loading experiments for study by EPR. However, no signal was seen for either extraction over the whole range of concentrations. This indicates that there is coupling between copper centres and the complex is formed immediately, without initial 2 : 1 complexation. The

hydrazone ligand used in the previous study can easily rotate away from the copper(II) binding site, allowing two ligands to complex to one metal ion. With ligand **1**, the *t*-butyl phenol group is far more bulky and hence it would not be expected to form as favourably (Figure 2.24, (I)). The immediate formation of a multinuclear complex suggests that it is indeed the most stable, is consistent with the shape of the S-curve in Figure 2.22 and supports the low $pH_{½}$ found in the extraction experiments.

2.5.3 Mononuclear complexes containing an auxiliary ligand

As outlined in section 1.7, ligand **1** was designed to provide an NO_2^{2-} donor set which defines three vertices of a square about a copper(II) ion. It is possible for the remaining vertex to contain a neutral monodentate ligand to yield an organic soluble neutral complex as in Figure 2.25 (J). If this auxiliary ligand also contained two H-bond donors the resulting 1 : 1 : 1 assembly may be especially stable and soluble in water immiscible solvents.

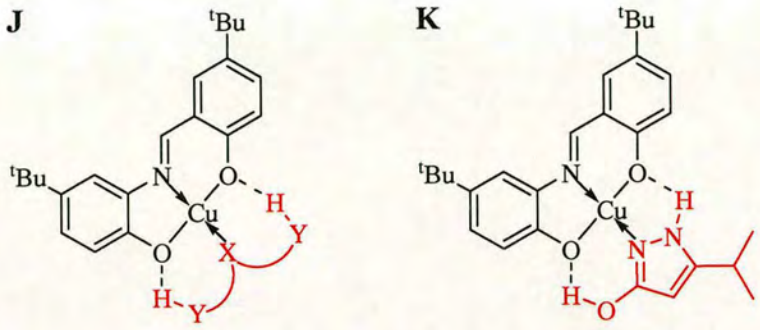

Figure 2.25: Proposed generic structure of ligand : copper : auxiliary ligand (J), and with 3-*iso*-propyl-2-pyrazol-5-one as the auxiliary (K).

The auxiliary ligand chosen was 3-*iso*-propyl-2-pyrazol-5-one. This is capable of existing in a number of tautomeric forms,[64] one of which ((iv) in Figure 2.26) has a nitrogen donor which could coordinate to the copper, while the protons on the neighbouring nitrogen and oxygen can H-bond to the phenolate oxygen atoms of ligand **1** as shown in Figure 2.25 (K).

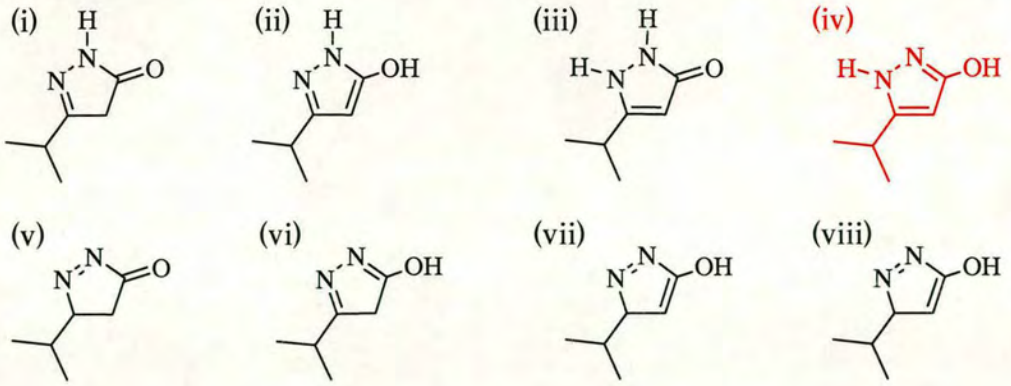

Figure 2.26: The tautomeric forms of 3-*iso*-propyl-2-pyrazol-5-one. (iv) is the form most suited to function as an auxiliary in this work. Crystal structure determination shows that (iii) predominates in the solid state.[64]

If the ternary complex is formed preferentially over the dinuclear complex, addition of the auxiliary ligand L_{aux} should result in a reduction in the $pH_{½}$ for copper-loading.

$$[Cu_2(\mathbf{1}\text{-}2H)_2] + 2L_{aux} \rightleftharpoons 2[Cu(\mathbf{1}\text{-}2H)L_{aux}] \qquad \textbf{Equ. 2.3}$$

The copper-loading experiment was carried out under identical conditions to those described in section 5.4.2 except that equimolar or excess amounts of the auxiliary ligand was added. The auxiliary ligand was insoluble in chloroform so was added to the system as a solid, forming an initial three phase extraction which, as the complex is formed, becomes two phases again.

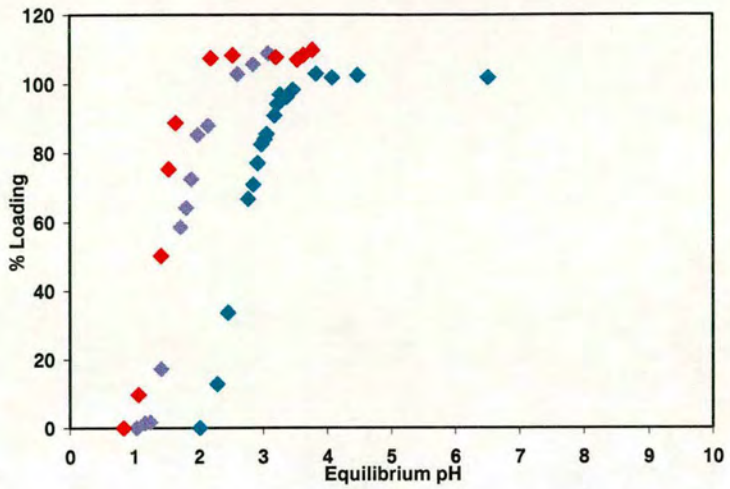

Figure 2.27: The pH dependence of loading, ■, of copper(II) by ligand **1** in the presence of equimolar, ■, and excess (0.050 M), ■, of an auxiliary ligand, 3-*iso*-propyl-2-pyrazol-5-one.

The addition of an auxiliary ligand caused a significant decrease in the $pH_{½}$ of the extraction. This improvement in complex stability adjusts the $pH_{½}$ to ~1.6. This is of great significance when compared to current working systems in industry. An extraction in the absence of ligand **1** was carried out as a control, to ensure the improvement seen was not the auxiliary loading the copper alone. The auxiliary alone loaded no copper, further confirming our assumption that the ternary complex is formed.

Formation of a 1 : 1 : 1 complex will result in a simple unpaired spin system and an EPR spectrum should be observed.

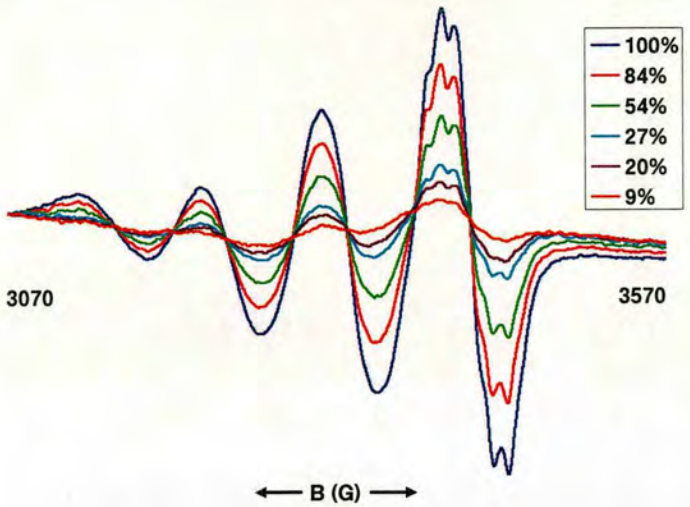

Figure 2.28: The EPR spectra of the organic phase of extractions for ligand 1 and L_{aux}. The key indicates the percentage of copper(II) in the organic phase, as measured by ICP-OES.

Figure 2.28 shows a clear EPR signal which arises from the unpaired electron on the copper centre. In a complex, the unpaired electron on a copper(II) ion is also delocalised to some extent over the ligand system. This is observed as super hyperfine splitting of the copper(II) signal by the donor atoms. Ligand **1** contains nitrogen donors which have a spin quantum number of 1, resulting in the splitting of each copper(II) peak into three. In this case, there are two distinct nitrogen splittings, from the nitrogen on ligand **1** and on the auxiliary. Comparing each of the spectra, as the concentration of copper increases, the intensity of the signal is increased.

Therefore, we have strong evidence to support our proposition for the formation of the ternary complex in a system which contains both the pyrazolone auxiliary ligand and **1**: the lower $pH_{½}$, the presence of an EPR signal and finally, the super hyperfine coupling resulting from coordination of the copper centre to two different nitrogen donors.

Copper extraction with ligand **1** has given us some promising results. The improvement in $pH_{½}$ over that for nickel is an unsurprising but welcome observation. The extraction of copper with ligand **1** has again achieved n : n stoichiometry. From mass spectrometry results, extraction experiments and EPR studies we can conclude

that there is a 1 : 1 stoichiometry of ligand **1** to metal. Addition of an auxiliary ligand into an extraction has proved to be a simple way to improve further on the $pH_{½}$ achieved with ligand **1** and EPR studies on this system support the assignment of a ternary 1 : 1 : 1 complex of copper : **1** : auxiliary ligand.

2.6 Conclusions

Ligand **1** has proved the concept that a multidentate *di*-acidic ligand can be used to generate organic soluble 1 : 1 complexes with divalent metal ions *via* pH-swing controlled equilibria. The extent to which this could lead to improved mass transport efficiency over the commercial phenolic oxime extractants which load one copper per two extractant molecules is summarised in Table 2.9.

Reagent	Molecular mass	Stoichiometry	Mass(g) of Cu transported per kg reagent	$pH_{½}$ in $CHCl_3$
P50 oxime[66]	263	2 : 1	121	1.55
1 (bis ^{t}Bu substituted)	325	1 : 1	196	2.6
1 (bis nonyl substituted)	466	1 : 1	137	-
1 + equi. 3-*iso*-propyl-2-pyrazol-5-one (L_{aux})	325 + 126	1 : 1 : 1	141	1.6

Table 2.9: Mass transport efficiencies of copper(II) extractants.

The higher the mass of copper transported, the more efficient the system. Ligand **1** shows a 62% improvement in mass transport efficiency over the commercial extractant, P50 oxime, but it is a weaker extractant as judged by its $pH_{½}$ value (2.6 *cf.* 1.6 in chloroform). P50 has a branched nonyl group in place of the *t*-butyl groups used in ligand **1**; this increases its organic solubility and might, on the basis of precedents, lower the $pH_{½}$ value when used in hydrocarbon solvents. If this alteration was made to ligand **1**, the higher molecular mass will reduce its mass transport efficiency but there would still be a small (13%) improvement over P50 oxime. Finally, the blend of ligand **1** and the auxiliary ligand again improves on the mass efficiency (17% over P50 oxime) and has a similar strength of binding (identical $pH_{½}$ in $CHCl_3$) to the commercial reagent.

With ligand **1** we have established our proof-of-concept, that we can design and synthesise, with cheap and accessible materials, a metal extractant that operates in a reasonable pH range and can multiload copper. Consequently, we were encouraged

to move to the next stage of the project and attempt to design a metal *salt* extractant based on this scaffold.

2.7 References

1 J. Szymanowski, *Critical Reviews in Analytical Chemistry*, 1995, **25**, 143.

2 J. Szymanowski, B. K. L. Mittal and B. Lindman, '*Surfactants in Solution*', Plenum Press, New York, 1989.

3 A. Chakravorty and T. S. Kannan, *Journal of Inorganic and Nuclear Chemistry*, 1967, **29**, 1691.

4 S. G. Galbraith, '*Ditopic Ligands for the Selective Solvent Extraction of Transition Metal Sulfates*', PhD thesis, University of Edinburgh, 2004.

5 S. G. Galbraith, Q. Wang, L. Li, A. J. Blake, C. Wilson, S. R. Collinson, L. F. Lindoy, P. G. Plieger, M. Schröder and P. A. Tasker, *Chemistry - A European Journal*, 2007, *submitted*.

6 J. W. Ledbetter, *The Journal of Physical Chemistry*, 1966, **70**, 2245.

7 J. W. Ledbetter, *The Journal of Physical Chemistry*, 1967, **71**, 2351.

8 J. W. Ledbetter, *The Journal of Physical Chemistry*, 1968, **72**, 4111.

9 J. W. Ledbetter, *The Journal of Physical Chemistry*, 1977, **81**, 54.

10 J. W. Ledbetter, *The Journal of Physical Chemistry*, 1982, **86**, 2449.

11 M. Uehara and J. Nakaya, *Bulletin of the Chemical Society of Japan*, 1970, **43**, 3136.

12 O. Berkesi, T. Kortvelyesi, C. Hetenyi, T. Nemetha and I. Palinko, *Physical Chemistry Chemical Physics*, 2003, **5**, 2009.

13 A. Santhi, U. L. Kala, R. J. Nedumpara, A. Kurian, M. R. P. Kurup, P. Radhakrishnan and V. P. N. Nampoori, *Applied Physics B*, 2004, **79**, 629.

14 E. S. H. El Ashry, A. El Nemra, S. A. Essawy and S. Ragab, *ARKIVOC*, 2006, **xi**, 205.

15 K. C. Emregul and O. Atakol, *Materials Chemistry and Physics*, 2003, **82**, 188.

16 K. C. Emregul and O. Atakol, *Materials Chemistry and Physics*, 2004, **83**, 373.

17 S. L. Li, Y. G. Wang, S. H. Chen, R. Yu, S. B. Lei, H. Y. Ma and D. X. Liu, *Corrosion Science*, 1999, **41**, 1769.

18 Z. Quan, S. Chen and S. Li, *Corrosion Science*, 2001, **43**, 1071.

19 J. D. Talati, M. N. Desai and N. K. Shah, *Materials Chemistry and Physics*, 2005, **93**, 54.

20 Y. Elerman, A. Elmali, O.Atakol and I. Svoboda, *Acta Crystallographica*, 1995, **C51**, 2344.

21 V. Barba, J. Vazquez, F. Lopez, R. Santilla and N. Farfan, *Journal of Organometallic Chemistry*, 2005, **690**, 2351.

22 J. Ondraöcek, A. Jegorov, Z. Kovaörov, M. Huösaka and F. Jursýkc, *Chemical Communications*, 1997, 915.

23 S. Gao, L.-H. Huo, Z.-P. Deng and H. Zhao, *Acta Crystallographica*, 2005, **E61**, m978.

24 S. M. El-Medania, O. A. M. Alib and R. M. Ramadanc, *Journal of Molecular Structure*, 2005, **738**, 171.

25 M. Minelli, F. Namuswe, D. Jeffrey, A. L. Morrow, I. A. Guzei, D. Swenson, E. Bothe and T. Weyhermuller, *Inorganic Chemistry*, 2006, **45**, 5455.

[26] T. Nakamura, E. Kuranuki, K. Niwa, M. Fujiwara and T. Matsushita, *Chemistry Letters*, 2000, 248.

[27] E. A. Abu-Gharib and J. Burgess, *Polyhedron*, 1989, **8**, 2677.

[28] R. Lal De, K. Samanta, K. Maiti and E. Keller, *Inorganica Chimica Acta*, 2001, **316**, 113.

[29] E. Labisbal, J. A. Garcia-Vazquez, J. Romero, S. Picos and A. Sousa, *Polyhedron*, 1995, **14**, 663.

[30] F. Maggio, T. Pizzino, V. Romano and A.Giovenco, *Inorganic and Nuclear Chemistry Letters*, 1973, **9**, 639.

[31] Q. Chen, J. Huang and J. Yu, *Inorganic Chemistry Communications*, 2005, **8**, 444.

[32] E. Labisbal, L. Rodriguez, A. Vizoso, M. Alonso, J. Romero, J.-A. Garcia-Vazquez, A. Sousa-Pedrares and A. Sousa, *Zeitschrift fuer Anorganische und Allgemeine Chemie*, 2005, **631**, 2107.

[33] F. Maggio, R. Bosco, R. Cefalu and R. Barbteri, *Inorganic and Nuclear Chemistry Letters*, 1968, **4**, 389.

[34] J. N. R. Ruddick and J. R. Sams, *Journal of Organometallic Chemistry*, 1973, **60**, 233.

[35] A. van den Bergen, R. J. Cozens and K. S. Murray, *Journal of the Chemical Society [Section] A: Inorganic, Physical, Theoretical*, 1970, **18**, 3060.

[36] X. Chen, F. J. Femia, J. W. Babich and J. Zubieta, *Inorganica Chimica Acta*, 2001, **316**, 33.

[37] U. Mazzi, F. Refoseo, G. Bandoli and M. Nicolini, *Transition Metal Chemistry*, 1985, **10**, 121.

[38] S. Sawusch, N. Jager, U. Schilde and E. Uhlemann, *Structural Chemistry*, 1999, **10**, 105.

[39] H. Asada, M. Ozeki, M. Fujiwara and T. Matsushita, *Chemistry Letters*, 1999, 525.

[40] T. Nakamura, K. Niwa, S. Usugi, H. Asada, M. Fujiwara and T. Matsushita, *Polyhedron*, 2001, **20**, 191.

[41] R. Bosco and R. Cefalu, *Jounal of Organometallic Chemistry*, 1971, **26**, 225.

[42] T. Majima and Y. Kawasaki, *Bulletin of the Chemical Society of Japan*, 1978, **51**, 2924.

[43] G. Dia, V. Luparello, F. Maggio, T. Pizzino, V. Roman and G. Bocchi, *Inorganic and Nuclear Chemistry Letters*, 1980, **16**, 109.

[44] L. Doretti, S. Sitran, F. Madalosso, G. Bandoli and G. Paolucci, *Journal of Inorganic Nuclear Chemistry*, 1980, **42**, 1060.

[45] A. D. Westland and M. T. H. Tarafder, *Inorganic Chemistry*, 1981, **20**, 3992.

[46] K. Morisige, *Journal of Inorganic Nuclear Chemistry*, 1978, **40**, 843.

[47] A. P. Ginsberg, R. C. Sherwood and E. Koubek, *Journal of Inorganic Nuclear Chemistry*, 1967, **29**, 353.

[48] A. van den Bergen, K. S. Murray and B. O. West, *Inorganic Physical Theory*, 1969, 2051.

[49] E. Hodnett and W. J. Dunn, *Journal of Medicinal Chemistry*, 1970, **13**, 768.

[50] R. K. Parashar, R. C. Sharma, A. Kumar and G. Mohan, *Inorganica Chimica Acta*, 1988, **151**, 201.

[51] R. D. Bereman, G. D. Shields, J. R. Dorfman and J. Bordner, *Journal of Inorganic Biochemistry*, 1983, **19**, 75.

52 D. Chatterjee, A. Mitra and S. Mukherjee, *Polyhedron*, 1999, **18**, 2659.

53 M. Greb, J. Hartung, F. Köhler, K. Spehar, R. Kluge and R. Csuk, *European Journal of Organic Chemistry*, 2004, 3799.

54 J. Hartung, S. Drees, M. Greb, P. Schmidt, I. Svoboda, H. Fuess, A. Murso and D. Stalke, *European Journal of Organic Chemistry*, 2003, 2388.

55 M. R. Maurya, H. Saklani and S. Agarwal, *Catalysis Communications*, 2004, **5**, 563.

56 S. Mukherjee, S. Samanta, B. C. Roy and A. Bhaumik, *Applied Catalysis A: General*, 2006, **301**, 79.

57 J. Qiao, L. D. Wang, L. Duan, Y. Li, D. Q. Zhang and Y. Qiu, *Inorganic Chemistry*, 2004, **43**, 5096.

58 Y. Shao, Y. Qiu, X. Hu and X. Hong, *Chemistry Letters*, 2000, 1068.

59 H. Ishii and H. Einaga, *Bulletin of the Chemical Society of Japan*, 1969, **42**, 1558.

60 Z. Cimerman, N. Galic and B. Bosner, *Analytica Chimica Acta*, 1997, **343**, 145.

61 V. Sridharan, S. Muthusubramanian and S. Sivasubramanian, *Magnetic Resonance in Chemistry*, 2003, **41**, 291.

62 V. Sridharan, S. Muthusubramanian and S. Sivasubramanian, *Indian Journal of Chemistry*, 2005, **44**, 416.

63 D. Levin, R. Aldred, R. Johnston and J. Neilan, *Journal of the Chemical Society, Perkin Transactions 1: Organic and Bio-Organic Chemistry*, 1994, **13**, 1823.

64 J. L. Wood, '*Multi-Loading Ligand Assemblies to Transport Copper*', PhD thesis, University of Edinburgh, 2005.

65 in 'Crystal Structural Database, Cambridge Crystallographic Data Centre, http://www.ccdc.cam.ac.uk', 2007.

66 R. J. Gordon, '*Unpublished results*', University of Edinburgh, 2006.

67 C. E. Anson, L. Ponikiewski and A. Rothenberger, *Inorganica Chimica Acta*, 2006, **359**, 2263.

68 B. Gustafsson, M. Hakansson, G. Westman and S. Jagner, *Journal of Organomettalic Chemistry*, 2002, **649**, 204.

69 C. Lopes, M. Hakansson and S. Jagner, *Inorganica Chimica Acta*, 1997, **254**, 361.

70 S. S. Tandon, L. K. Thompson, J. N. Bridson and M. Bubenik, *Inorganic Chemistry*, 1993, **32**, 4621.

71 P. A. Tasker, A. Parkin, D. Coventry, S. Parsons and D. Messenger, *Personal Communication*, 2005.

72 H. Yamashita, M. Koikawa and T. Tokii, *Molecular Crystals and Liquid Crystals Science and Technology, Section A: Molecular Crystals and Liquid Crystals*, 2000, **342**, 63.

73 G. Aromi, A. S. Batsanov, P. Christian, M. Helliwell, O. Roubeau, G. A. Timco and R. E. P. Winpenny, *Dalton Transactions*, 2003, **23**, 4466

74 A. J. Atkins, A. J. Blake and M. Schroder, *Chemical Communications*, 1993, 353.

75 S. Cromi, F. Launay and V. McKee, *Chemical Communications*, 2001, 1918.

76 J. Langer, H. Gorls, G. Gillies and D. Walther, *Zeitschrift fuer Anorganische und Allgemeine Chemie*, 2005, **631**, 2719.

[77] J. Reglinski, M. K. Taylor and A. R. Kennedy, *Inorganic Chemistry Communications*, 2006, **9**, 736.

[78] A. Yuchi, H. Murakami, M. Shiro, H. Wada and G. Nakagawa, *Bulletin of the Chemical Society of Japan*, 1992, **65**, 3362.

[79] S. Mukherjee, T. Weyhermüller, E. Bothe, K. Wieghardt and P. Chaudhuri, *European Journal of Inorganic Chemistry*, 2003, 863.

[80] A. Parkin, '*Crystallographic and Modelling Studies of Transition Metal Complexes*', PhD thesis, University of Edinburgh, 2002.

[81] R. L. Carlin, '*Magnetochemistry*', Springer-Verlag, 1986.

[82] G. Chaboussant, R. Basler, H.-U. Guedel, S. Ochsenbein, A. Parkin, S. Parsons, G. Rajaraman, A. Sieber, A. A. Smith, G. A. Timco and R. E. P. Winpenny, *Dalton Transactions*, 2004, 2758.

[83] P. A. Tasker, P. G. Plieger and L. C. West, *Comprehensive Coordination Chemistry II*, 2004, **9**, 759.

[84] S. Donegan, *Minerals Engineering*, 2006, **19**, 1234.

[85] N. Akkus, J. C. Campbell, J. Davidson, D. K. Henderson, H. A. Miller, A. Parkin, S. Parsons, P. G. Plieger, R. M. Swart, P. A. Tasker and L. C. West, *Dalton Transactions*, 2003, 1932.

[86] H. Irving and R. J. P. Williams, *Nature*, 1948, **162**, 746.

CHAPTER 3

3 CHAPTER 3 78

3.1 Introduction 80

3.2 Ligand synthesis and characterisation 84

3.3 Metal complex synthesis and characterisation 91

3.4 Solvent extraction 95

3.4.1 Stripping 96

3.4.2 Loading 103

3.4.3 EPR 108

3.4.4 Mononuclear complexes containing an auxiliary ligand 111

3.4.5 'Dual-Host' studies 116

3.4.6 Cooperativity of copper/anion binding 120

3.5 Conclusions 124

3.6 References 125

3.1 Introduction

Recently developed leaching processes for copper sulfides produce high tenor feed solutions which can contain 30 to 90 g l^{-1} copper (Chapter 1, section 1.8).[1] The increased concentration of copper in solution renders conventional pH-swing extractants unfavourable due to the high acid build-up at the front end of the circuit:

$$2\mathbf{L}_{(org)} + CuSO_4 \rightleftharpoons [Cu(\mathbf{L}\text{-}H)_2]_{(org)} + H_2SO_4. \quad \textbf{Equ. 3.1}$$

The commercial oxime extractants can occasionally be used if an additional circuit is present on-site, which can consume the acid produced.[2] However, when this option is not available, new ligands with the ability to function without pH adjustment must be considered. Extractants which transport metal *salts* rather than metal ions could meet this criterion. Previous work in Edinburgh has focused on the use of ditopic ligands based on functionalised "salens" ($salen^{2-}$ = *N,N'*-(salicylidene)ethylenediaminato dianion). These are *di*-imine ligands which, in their zwitterionic form, can bind a cation and anion in separate sites. They have proven to be strong extractants which operate on a 1 : 1 : 1 stoichiometry. In the solid state **L** : Cu : SO_4 complexes as in Figure 3.1 or related dimers and polymers with sulfate bridging alkylammonia groups from different molecules have been characterised.[3, 4]

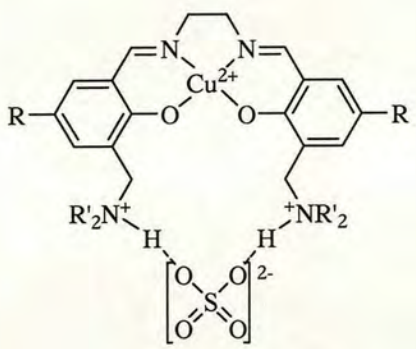

Figure 3.1: An example of a copper(II) sulfate complex of a ditopic ligand with "salen" metal-binding site.[3]

As discussed in Chapter 2, the development of multiloading metal extractants can improve metal transport efficiency. It was therefore proposed that combining this

concept with that of a metal *salt* extraction may provide a new class of ligand capable of functioning in highly efficient, novel circuits.

Having established ligand **1**'s ability to extract copper with a 1 : 1 stoichiometry, it was logical to retain this O,N,O metal binding site. Pendant amine arms could then be added to either or both of the aromatic rings which, when protonated, could bind anions. The generic structure for such a ligand is seen in Figure 3.2.

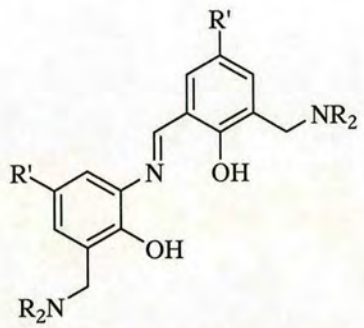

Figure 3.2: Proposed structure of novel metal salt extractant.

If two of these ligands came together to coordinate two divalent copper ions then the protonated pendant arms could bind two divalent or four monovalent anions as seen below in Equation 3.2 and in Figure 3.3. The ligand is therefore present in its zwitterionic form.

$$2Cu^{2+} + 2X^{2-} + 2\mathbf{L}_{(org)} \rightleftharpoons [Cu_2\mathbf{L}_2X_2]_{(org)} \qquad \textbf{Equ. 3.2}$$

The overall stoichiometry is then 2 : 2 : 2 for an assembly with divalent anions in a neutral complex with the formula $[Cu_2\mathbf{L}_2X_2]$. If extracting from sulfate medium, X = SO_4, whereas in the presence of chloride, X = 2Cl.

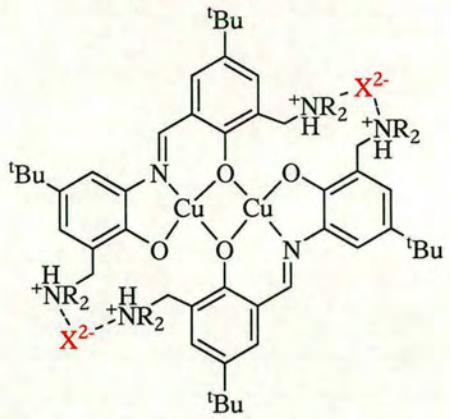

Figure 3.3: Proposed metal salt complex structure, where X=SO_4 or 2Cl.

Synthesising simpler ligands with one pendant arm may result in alternative complexes with different stoichiometries (Figure 3.4). In the presence of a monovalent anion, one ligand can coordinate a divalent metal atom and one anion (Equation 3.3), with the possibility that the latter could be present in the inner coordination sphere of the metal.

$$Cu^{2+} + X^{-} + \mathbf{L}_{(org)} \rightleftharpoons [Cu(\mathbf{L}\text{-}H)X]_{(org)} + HX \qquad \textbf{Equ. 3.3}$$

However, in order to coordinate a divalent anion and form a charge neutral complex, two metal-ligand assemblies must come together in order to balance the charges, as shown in Equation 3.4.

$$2Cu^{2+} + X^{2-} + 2\mathbf{L}_{(org)} \rightleftharpoons [Cu_2(\mathbf{L}\text{-}H)_2X]_{(org)} + H_2X \qquad \textbf{Equ. 3.4}$$

These extractants would not remove all attendant anions from solution, as seen in Equations 3.3 and 3.4, but may extract enough to reduce the equilibrium pH of the extraction significantly.

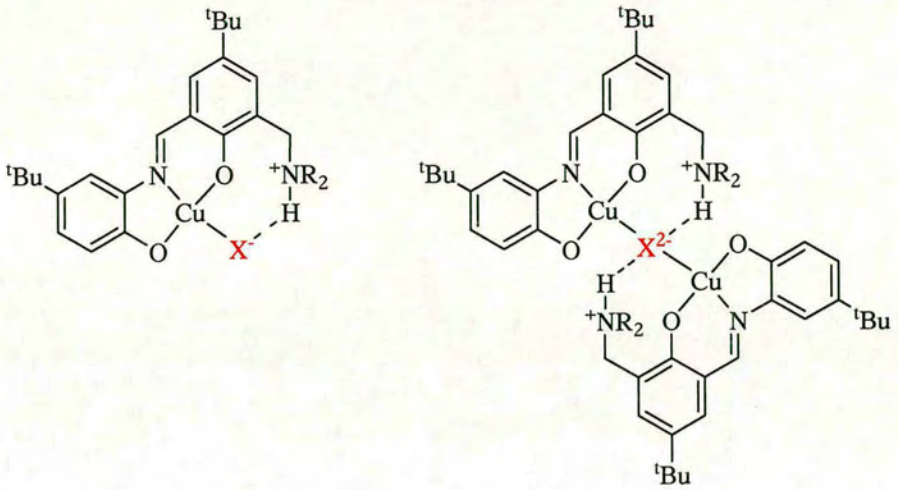

Figure 3.4: One arm ligand modes of binding.

The following sections document the synthesis and characterisation of a series of ligands related to the structure in Figure 3.2. One of these, **5**, which showed promise as an extractant for copper sulfate, was studied in depth in a range of experiments.

3.2 Ligand synthesis and characterisation

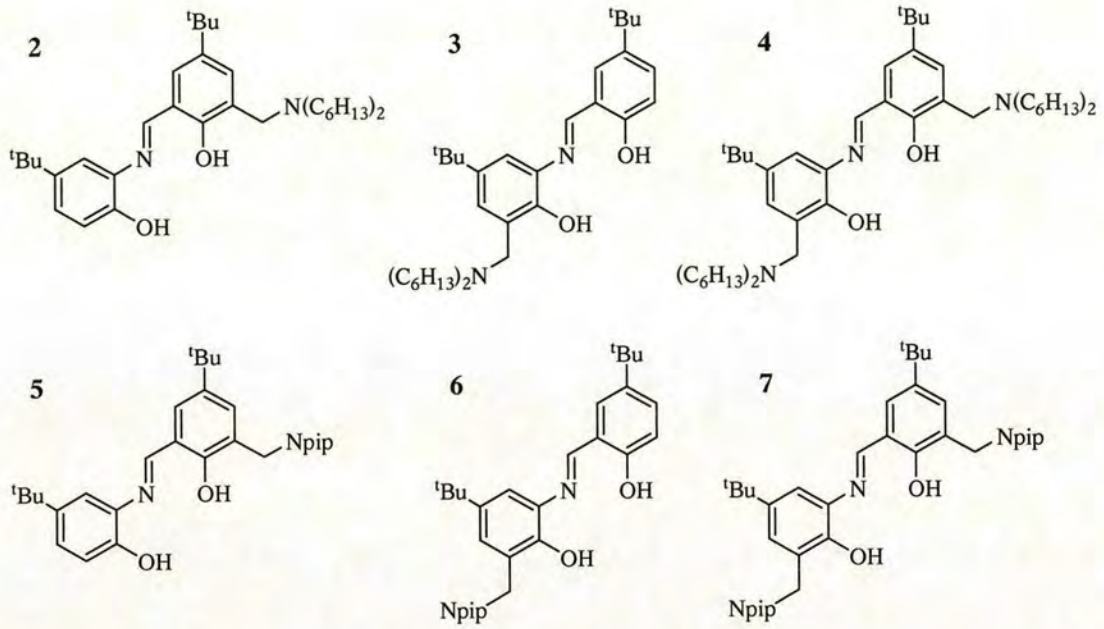

Figure 3.5: Ligands discussed in Chapter 3.

Ligands **2-7** were prepared by Schiff base condensations of the amine and aldehyde starting materials, as for ligand **1**. Each ligand has either one or two pendant amine arms *ortho* to the phenolic hydroxyl. Two different Mannich bases were prepared to be incorporated into the ligands as pendant amine arms. The syntheses of ligands **2-4** involved reaction with *N*-ethoxymethyldi-*n*-hexylamine. This amine was chosen because the bis(*n*-hexyl)aminomethyl group has been found in other work to impart high solubility to ligands and complexes in chloroform.[3] The later ligands (**5-7**) incorporate an *N*-piperidinomethyl group into their structure. This group has proved useful in earlier work for growing crystals suitable for X-ray crystallography.[3] Both bases were prepared *via* an adaptation of the method used by Fenton and co-workers,[5] from dihexylamine/piperidine and paraformaldehyde in ethanol with potassium carbonate as a desiccant. The mechanism for this preparation is shown in Scheme 3.1. Purification was achieved *via* vacuum distillation/recrystallisation.

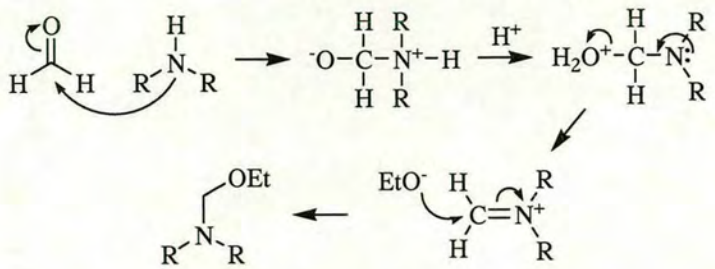

Scheme 3.1: Mechanism of preparation of Mannich bases (R = C_6H_{13} or NR_2 = piperidine).

In order to substitute in the remaining position *ortho* to the phenol in 5-*t*-butyl-salicylaldehyde with the chosen base, a Mannich reaction under non-aqueous aprotic conditions was carried out. The proposed mechanism is shown in Scheme 3.2.

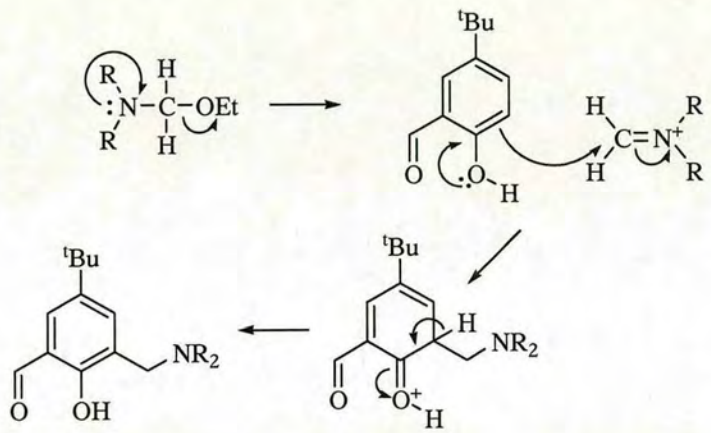

Scheme 3.2: Proposed mechanism of Mannich step.

For ligands **2** and **5**, the Schiff base condensations of the substituted salicylaldehydes with 2-amino-4-*t*-butylphenol were undertaken at room temperature in methanol, as for ligand **1**. For ligands **3**, **4**, **6** and **7**, before the Schiff base condensation could be carried out, 2-amino-4-*t*-butylphenol first required the addition of a pendant amine group *via* a Mannich reaction. In order to effect clean addition of the Mannich base, the amine was protected prior to the Mannich step. This ensured addition of the pendant arm in the *ortho*-position relative to the phenol hydroxyl group.

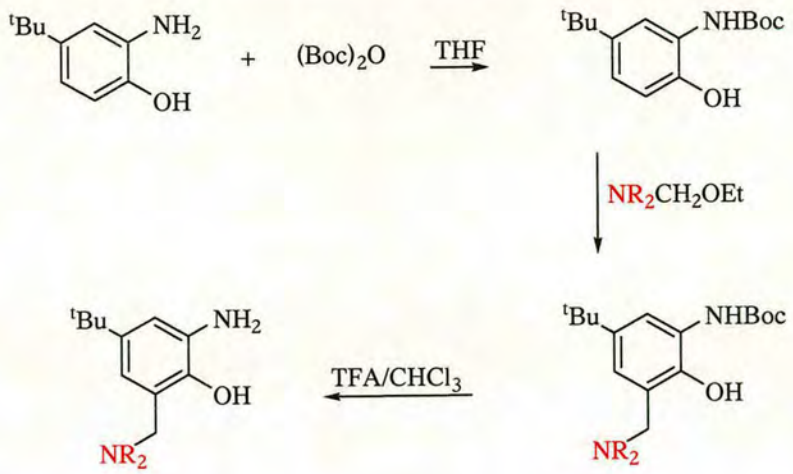

Scheme 3.3: Synthesis of 2-amino-4-*t*-butyl-6-dihexylaminomethyl-phenol (R = C_6H_{13}) and 2-amino-4-*t*-butyl-6-piperidinyl-phenol (NR_2 = piperidine).

Boc anhydride (di-*t*-butyldicarbonate) was chosen as the method of protection and the synthesis carried out by an adaptation of a method used previously (Scheme 3.3).[6] Substitution at the *ortho*-position involved a Mannich reaction before removal of the Boc group was effected with 1 : 1 trifluoroacetic acid (TFA) in chloroform for the dihexylaminomethyl substituted amine. For the piperidine equivalent, an excess of TFA in dichloromethane was used. Residual TFA was removed by washing with base. The Schiff base condensation could then be carried out with the desired amine as before. All ligands were recrystallised from methanol.

During the purification and characterisation of precursors, recrystallisation of the protected amine containing the pendant piperidino group formed colourless blocks of X-ray crystallographic quality. The structure confirms the clean protection and Mannich steps prior to deprotection. It also shows the presence of the piperidino group *ortho* to the hydroxyl position, as expected. There is one hydrogen bond present in the molecule, between the H on O11 and N21 in the piperidine ring.

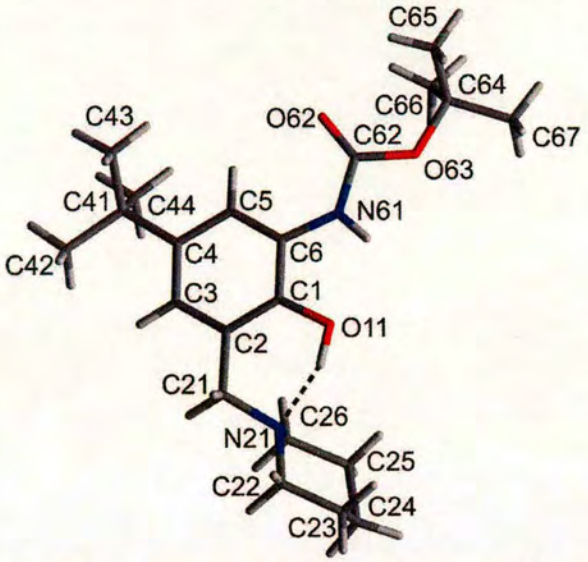

Figure 3.6: Structure of the piperidine-substituted, protected amine showing the atom labelling scheme used in tables of bond lengths and angles (available in detail on the appendix CD) and the intramolecular H-bonding contact between the H on O11 and N21 (1.73(3) Å).

Each ligand was characterised by ^{1}H and ^{13}C NMR spectroscopy, CHN analysis, IR and FAB mass spectrometry. As for ligand **1**, ^{1}H NMR spectroscopy was particularly useful in indicating purity and confirming completion of the Schiff base reactions. Scheme 3.4 shows the range of ligands prepared and the synthetic routes used.

Ligand	X	X'
2	$CH_2N(C_6H_{13})_2$	H
3	H	$CH_2N(C_6H_{13})_2$
4	$CH_2N(C_6H_{13})_2$	$CH_2N(C_6H_{13})_2$
5	$CH_2N(C_5H_{10})$	H
6	H	$CH_2N(C_5H_{10})$
7	$CH_2N(C_5H_{10})$	$CH_2N(C_5H_{10})$

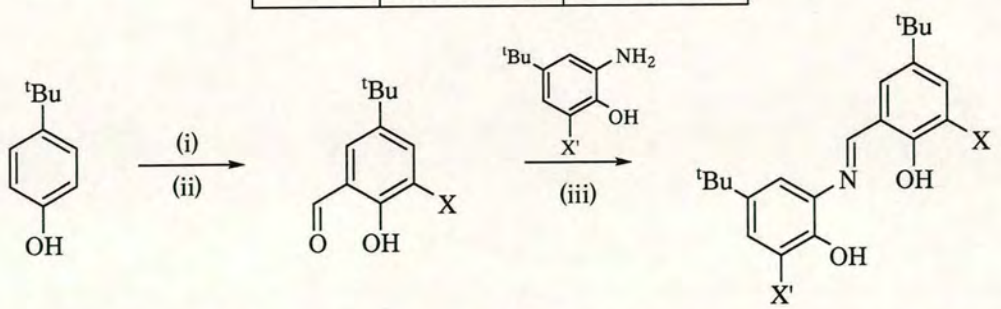

Scheme 3.4: Synthesis of Ligands **2-7** (i) $Mg(OMe)_2$, paraformaldehyde, toluene; (ii) Mannich reaction (ligands **2**,**4**,**5**,**7**); (iii) Schiff base, methanol.

Initially, ligands **2-4** with pendant dihexylaminomethyl groups were intended for use in extraction experiments. However, upon investigation, it was discovered that **5**, with the pendant piperidinomethyl group had adequate solubility in chloroform at the desired concentrations. It was therefore decided that the bulk of the experiments would be performed with ligand **5**, due to its relative ease of synthesis and in the hope that crystals of complexes could be obtained to undertake X-ray structure determination.

Recrystallisation from methanol yielded yellow blocks of ligand **5** suitable for X-ray crystallography (Figure 3.7). The ligand has the same E-conformation as **1** and has the same type of intramolecular H-bond between the H on O9 and N13, with a distance of 1.70(2) Å between H and N13. There are no solvent molecules in the unit cell and the ligand forms an intermolecular H-bond between the H on O16 and the piperidine nitrogen of an adjacent ligand (1.87(2) Å). Again, there is a twisting from planarity, with an angle of 35.37° between the planes of the benzene rings. The piperidine ring lies almost perpendicular to the aldehyde half of the ligand, with an angle of 71.72° between the planes defined by the aromatic and piperidine rings. The angles in the five and six-membered rings (Table 3.1) which would be formed upon metal complexation are very similar to those in **1**, suggesting that **5** will also be capable of acting as a tridentate ligand, defining three vertices of an octahedron or square.

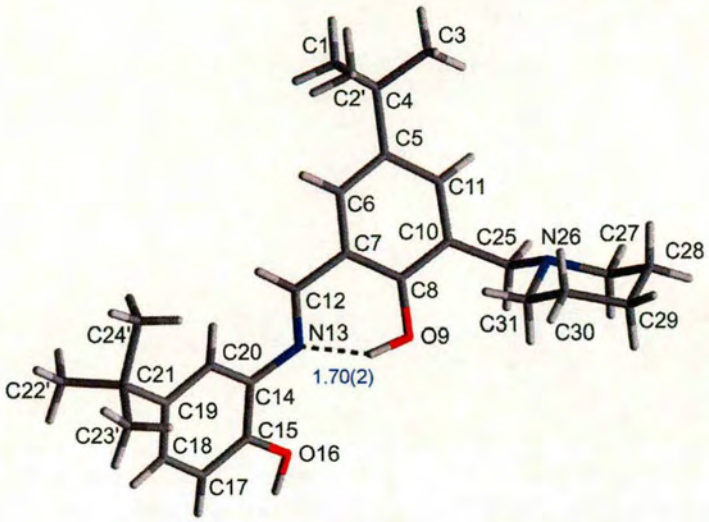

Figure 3.7: Structure of ligand **5** showing atom labelling scheme used in tables of bond lengths and angles (available in detail on the appendix CD) and the intramolecular H-bonding contact between the H on O9 and N13 (1.70(2) Å).

	6-membered ring			5-membered ring	
Angle	**O-C-C**	**C-C-C**	**C-C-N**	**O-C-C**	**C-C-N**
Lig 1	121.4(2)	120.50(18)	120.8(2)	118.6(2)	117.1(2)
Lig 5	121.49(12)	121.04(14)	121.46(14)	118.59(12)	117.88(13)

Table 3.1: Comparison of angles in chelating portions of putative ligands **1** and **5**.

The angle between O1, N2 and O2 is 93.86(4)°, is marginally larger than that in ligand **1** (90.42(8)°) but still suitably preorganised for formation of square planar complexes (Figure 3.8). Putting a metal, M on the midpoint between the two O donors, would generate M-O and M-N bond lengths of 1.93 Å and 1.81 Å respectively, similar but slightly shorter than those normally observed in octahedral copper(II) and nickel(II) salicylaldimine complexes.[7]

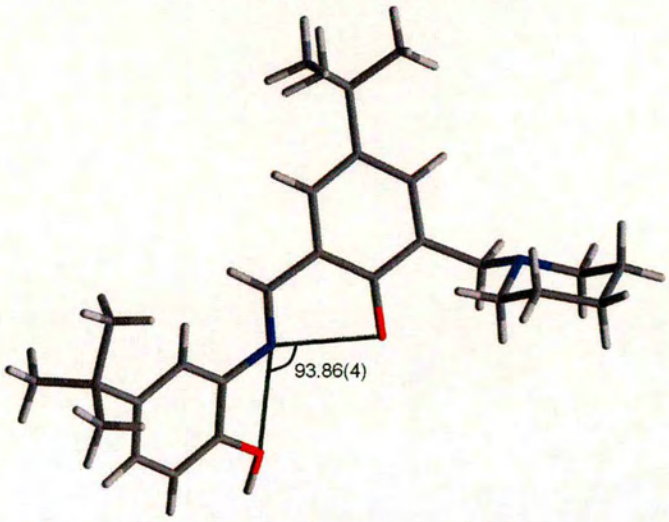

Figure 3.8: Potential coordination polyhedron reflex angle in ligand **5**.

3.3 Metal complex synthesis and characterisation

At the outset, for extraction experiments it was assumed that the dihexylaminomethyl ligands **2-4** and their metal complexes would show high solubility in chloroform. However, during initial testing, it was discovered that the mono piperidinomethyl substituted ligand **5** had the required solubility and extracted copper(II) sulfate, despite having just one pendant arm.

Metal-only complexes were formed by mixing stoichiometric amounts of metal acetate (Ni or Cu) and ligand in methanol, and analysed by FAB mass spectrometry (Table 3.2). Ligand **5** formed 2 : 2 ligand to metal complexes $[M_2(\mathbf{5}\text{-}2H)_2]$ with both copper and nickel. The second piperidinomethyl group on ligand **7** results in low organic solubility. Consequently, metal complexes of $[Ni_2(\mathbf{7}\text{-}2H)_2]$ and $[Cu(\mathbf{7}\text{-}2H)]$ formed as precipitates in methanol and hence ligand **7** was not used in subsequent solvent extraction experiments. We were unable to isolate crystals of complexes with ligands **5** and **7** suitable for X-ray structure determination.

Ligand	Metal	m/z	M : L Ratio
2	Ni	1157	2 : 2
5	Cu	969	2 : 2
5	Ni	957	2 : 2
7	Cu	582	1 : 1
7	Ni	1151	2 : 2

Table 3.2: Metal complexes for ligands **2, 5** and **7** with nickel and copper.

Ligand **2**, the mono dihexylaminomethyl substituted ligand, formed the 2 : 2 brown complex $[Ni_2(\mathbf{2}\text{-}2H)_2]$. However, when the attempted recrystallisation of this complex was left to evaporate for several months, small red plates formed. The structure shows that the recrystallised complex contains a new ligand, resulting from the loss of one C_6H_{13} from each ligand **2**. This new ligand, **8** is shown in Figure 3.9. Loss of the C_6 chain is unprecedented and the mechanism is unknown. However, the degradation of **2** over time does indicate that this class of compound would not be

suitable for use in the metal extraction industry where ligands are subjected to extreme conditions and required to be recycled for use many times.[8]

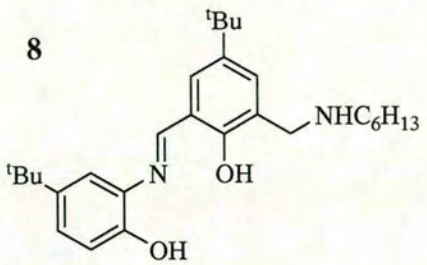

Figure 3.9: Ligand **8**, resulting from recrystallisation of the ligand **2** nickel complex.

The asymmetric unit contains two ligand molecules and two nickel atoms. Each nickel is in a pseudo-square planar geometry with the three donor atom set from one ligand, the fourth donor is the pendant nitrogen from the second ligand. The complex formula is $[Ni_2(\mathbf{8}\text{-}2H)_2]$. The pendant C_6H_{13} arms are located above and below the plane of the nickels and there is one molecule of ethanol present per complex.

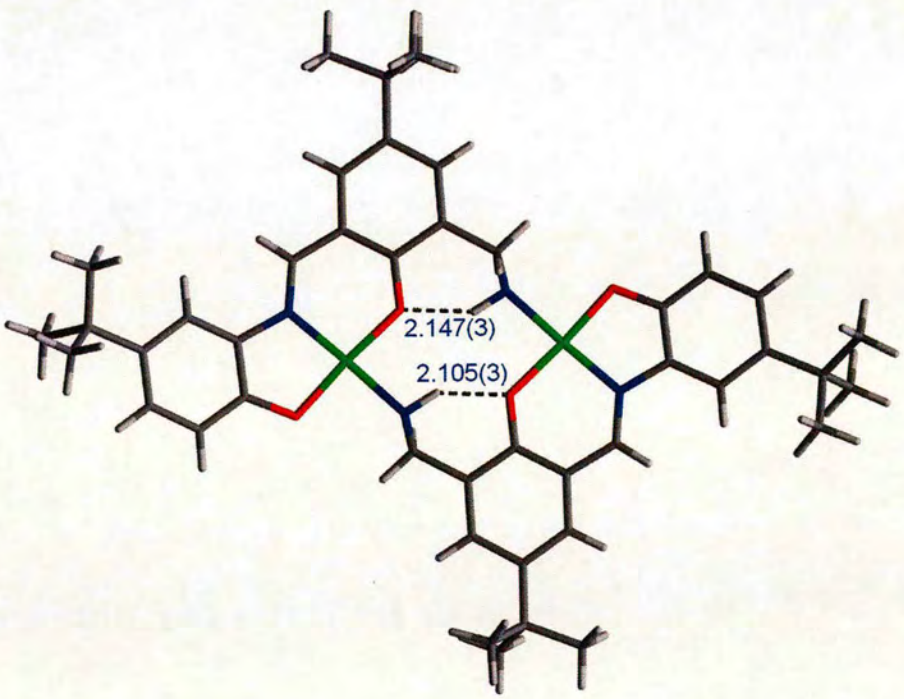

Figure 3.10: $[Ni_2(\mathbf{8}\text{-}2H)_2]$ complex, with pendant C_6H_{13} chains removed for clarity. Intramolecular hydrogen bonds are shown.

There is an intramolecular H-bond in each ligand from the H on the pendant amine to the deprotonated phenol on the same aromatic ring; these distances are 2.105(3) and 2.147(3) Å (Figure 3.10). The ligand bound to Ni1 has an angle of just 4.77° between the planes of the two aromatic rings while the other is 15.09°. These angles are significantly reduced from either of the free ligand structures of ligands **1** or **5** due to the square planar nature of the metal centres, forcing planarity to be increased within the ligand structure. The NiN_2O_2 planes are approximately parallel. The Ni1 plane has maximum deviation from the least squares plane of -0.0206 Å for O11 and 0.0162 Å for N462, with an average deviation from the least squares plane of 0.0162 Å. Similarly, for the Ni2 plane, the maximum deviations are -0.0808 Å for N262 and 0.0733 Å for O31. The average deviation from the least squares plane of Ni2 is 0.0641 Å. The nitrogens mentioned (N462 and N262) are from the two pendant hexylamino groups, which cause the step between the two planes seen in Figure 3.11. There is an angle of 4.81° between the Ni1 and Ni2 planes.

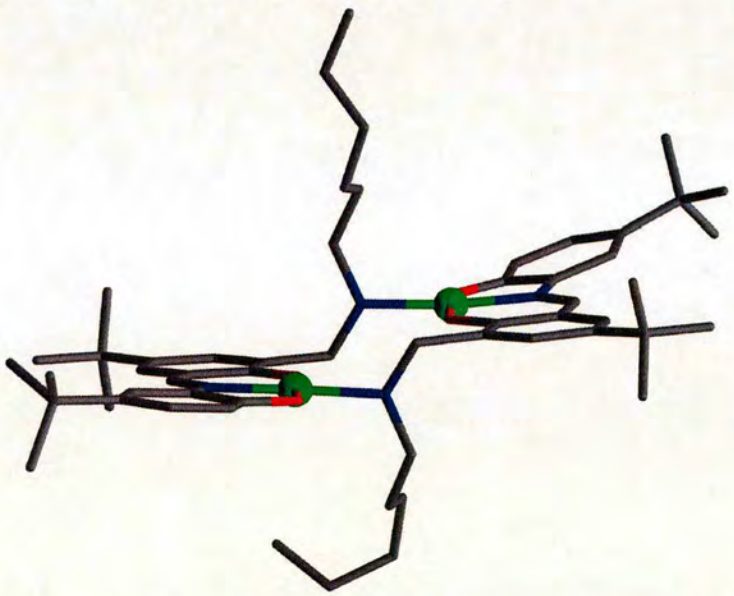

Figure 3.11: $[Ni_2(8\text{-}2H)_2]$ complex showing the two NiN_2O_2 planes, the pendant C_6H_{13} arms above and below the nickel planes and the difference in planarity of the two ligands.

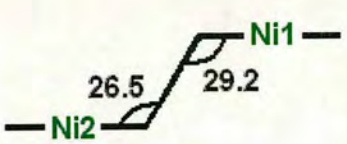

Figure 3.12: The angles of CH_2N bond displacement from the nickel planes (°).

The CH_2N bond displacement from the plane of Ni1 is at an angle of 29.2° and is 26.5° from the plane of Ni2, as depicted in Figure 3.12. Ni1 is 1.191 Å from the plane of Ni2 while Ni2 is 1.419 Å from the Ni1 plane.

A regular square planar metal has four identical donors, each with the same bond length and with four 90° angles between the donors. The deviations from square planarity are shown in Table 3.3. From the free ligand structure of ligand **5**, the expected Ni-O bond lengths were 1.93 Å, whereas those found in the nickel complex are, on average, significantly shorter at 1.825 Å. The Ni-N bond length from the tridentate unit is slightly longer than the 1.81 Å expected value, at an average length of 1.858 Å. Comparing these values to previous work in the Tasker group on related structures such as the nickel analogue of the salen complex shown in Figure 3.1, both Ni-O and Ni-N bonds are significantly shorter, suggesting that the metal is more strongly bound in the ligand **8** structure. Also of note is that the Ni-O and Ni-N distances in the tridentate unit are significantly shorter than the Ni-N bond from the pendant amine arm. The pendant arm Ni-N bond is a more typical length of those expected for nickel complexes of this type.[7]

Angle at Ni defined by:	Ni1	Ni2
O_{amine}, O_{ald}	176.20(15)	174.96(16)
O_{amine}, N_{imine}	87.93(17)	87.96(17)
O_{ald}, N_{imine}	95.52(18)	95.77(17)
O_{amine}, $N_{pendant}$	89.95(16)	90.20(17)
O_{ald}, $N_{pendant}$	86.61(16)	86.43(17)
N_{imine}, $N_{pendant}$	177.74(18)	173.88(19)

Length of bond between:	Ni1	Ni2
Ni-O_{amine}	1.816(3)	1.840(3)
Ni-O_{ald}	1.826(3)	1.818(3)
Ni-N_{imine}	1.854(4)	1.862(4)
Ni-$N_{pendant}$	1.926(4)	1.930(4)

Table 3.3: Bond angles (Å) and lengths (°) in $[Ni_2(\mathbf{8}\text{-}2H)_2]$ complex.

3.4 Solvent extraction

Ligand **5** differs from ligand **1** only in having a pendant piperidinomethyl group *ortho* to the phenolic hydroxyl of the ring derived from the aldehyde precursor. Both the free ligand and its copper complexes show high solubility in chloroform allowing us to carry out a series of extraction experiments. However, **5** can in theory also extract the attendant anion along with the metal as shown in Equations 3.4 and 3.5. This allows for studies to compare the behaviour of different anions.

$$[Cu_2(\mathbf{5}\text{-}H)_2X_2]_{(org)} + 2HX \rightleftharpoons 2Cu^{2+} + \mathbf{25}_{(org)} + 4X^- \quad \textbf{Equ. 3.5}$$

$$[Cu_2(\mathbf{5}\text{-}H)_2Y]_{(org)} + H_2Y \rightleftharpoons 2Cu^{2+} + \mathbf{25}_{(org)} + 2X^- \quad \textbf{Equ. 3.6}$$

Loading experiments where the ligand is prepared to a known concentration in chloroform and contacted with an aqueous copper solution were also performed (Equation 3.6). These allow a more direct comparison to industrial processes.

$$2Cu^{2+} + 4X^- + \mathbf{25}_{(org)} \rightleftharpoons [Cu_2(\mathbf{5}\text{-}H)_2X_2]_{(org)} + 2HX \quad \textbf{Equ. 3.7}$$

Again, since copper is the metal of interest, EPR can be used to analyse metal loading and as with **1** in section 2.5.3, the addition of an auxiliary ligand (L_{aux}) can be used to alter the extraction equilibrium as shown in Equation 3.7.

$$Cu^{2+} + \mathbf{5}_{(org)} + L_{aux\,(org)} \rightleftharpoons [Cu(\mathbf{5}\text{-}2H)L_{aux}]_{(org)} + 2H^+ \quad \textbf{Equ. 3.8}$$

In order to establish whether the tethering of the pendant amine group in the position *ortho* to the phenol has important consequences on anion uptake, a control experiment was designed in which **1** was used in combination with an amine (L) capable of replicating the properties of the pendant amine (Equation 3.8).

$$Cu^{2+} + 2X^- + \mathbf{1}_{(org)} + L_{(org)} \rightleftharpoons [Cu(\mathbf{1}\text{-}2H)]_{(org)} + [HLX]_{(org)} + HX \quad \textbf{Equ. 3.9}$$

3.4.1 Stripping

Stripping experiments were carried out by contacting the copper complex [Cu_2(5-2H)$_2$] with sulfate or chloride solutions at a range of pHs, using the procedure depicted in Figure 3.13. Further details are provided in the experimental section (5.4.1).

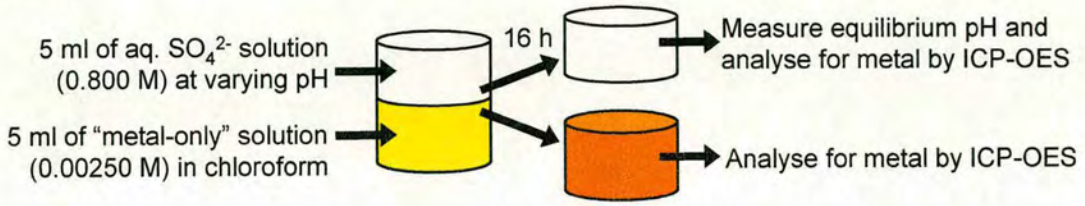

Figure 3.13: Procedure for stripping experiments.

Since ligand **5** contains a pendant amine arm, it is expected that any anions present during the experiment will be complexed. If anion complexation does occur, the stability of the whole ligand/metal/anion assembly could be anion dependent. Therefore, the following experiments were carried out in the presence of either sulfate or chloride. The analysis includes both metal and anion content and a $pH_{½}$ can be established for each. In Figure 3.14 the pH-dependence of copper-loading on the nature of the anion in the feed appears to be negligible. The plots show a $pH_{½}$ of 1.50 for copper-stripping in the presence of 0.800 M chloride or sulfate. This lack of anion dependence is surprising, as one would assume there to be some difference in stability between the sulfate and chloride complexes.

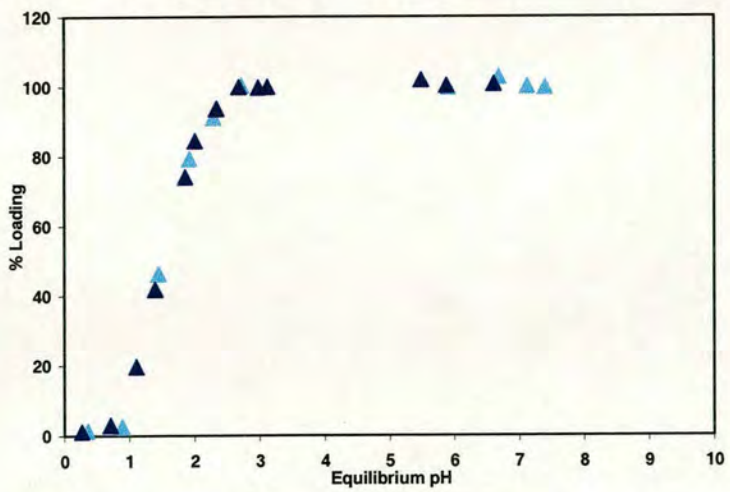

Figure 3.14: Copper stripping from [Cu_2(5-2H)$_2$] with acidic sulfate (▲) and chloride (▲) showing copper-loading.

In order to further investigate the relative binding strengths of the anion, the sulfate and chloride loadings can be plotted (Figures 3.18 and 3.19). When plotting loading curves, 100% loading of copper is taken to be when there is an equimolar amount of ligand and metal. Upon complex formation including an anion, the charge on the anion must be considered. So, to form a chloride complex, each ligand can carry one singly negatively charged atom, giving a stoichiometry of $n\mathbf{L}^{-} : nCu^{2+} : nCl^{-}$. Since sulfate has a charge of 2-, the complex must involve two ligand molecules for every sulfate anion, $2n\mathbf{L}^{-} : 2nCu^{2+} : nSO_4^{2-}$. These stoichiometries were assumed when calculating percentage loadings and are possible structures are shown in Figure 3.15.

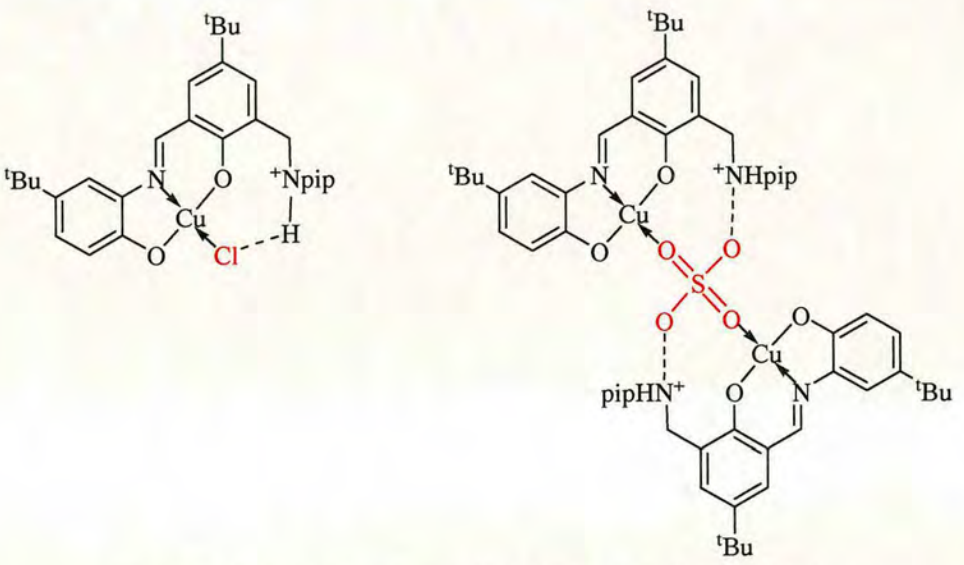

Figure 3.15: Possible structures of [Cu(5-H)Cl] and $[Cu_2(5\text{-}H)_2SO_4]$.

For an ideal metal salt extractant, the pH loading profile is as in Figure 3.16. Anion loading is favoured by *lowering* the pH as protonation of the pendant amines is needed to bind the anion and generate a neutral, organic soluble complex. In contrast, cation loading is favoured by *raising* pH because deprotonation of the phenolic oxygens is required to bind the metal. There should be a plateau region where the pH for simultaneous loading of the metal and anion matches the pH of the feed solution. When sulfate is the anion under consideration, the loading increases above 100% at low pH as HSO_4^{-} dominates over SO_4^{2-} at pH < 2,[3] resulting in the double inflection seen in Figure 3.16.

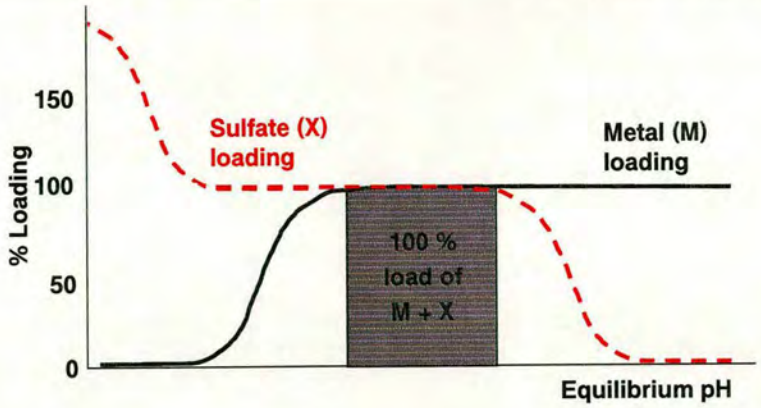

Figure 3.16: Ideal metal and anion binding profile for a metal sulfate extractant.

Previous work in the Tasker group involving "salen"-type complexes such as that seen in Figure 3.17 produced copper sulfate-loading curves very similar to this ideal plot.[3] Complexation of the metal in the N_2O_2 donor site preorganises the ligand to allow sulfate binding in the anion binding site between the two pendant amine arms. At very low pH, the anion loading exceeds 100% as each of the protonated amine arms can coordinate to one hydrogen sulfate (HSO_4^-) anion.

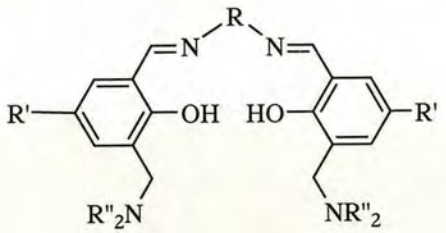

Figure 3.17: "Salen" ligand used in previous metal salt extractant studies.[3] Ideal extraction plots were obtained when R = $(CH_2)_2$, R' = ^{t}Bu and R'' = $(C_6H_{13})_2$.

The data presented in Figure 3.18 shows copper and chloride loadings in the organic phase when preformed $[Cu_2(\mathbf{5}\text{-}2H)_2]$ solutions are contacted with aqueous solutions of HCl/NaCl (0.8 M) at different pH. The system displayed ideal behaviour. Between pH 3 and 6 the ligand is fully loaded with copper and chloride as [Cu(**5**-H)Cl]. In principle the chloride could be fully stripped at pH > 8.0 and copper at a pH < 1.0. As **5** has only one protonatable amine, the double inflection of the anion plot is no

longer expected. The $pH_{½}$ for copper and chloride loadings are 1.52 and 7.16 respectively.

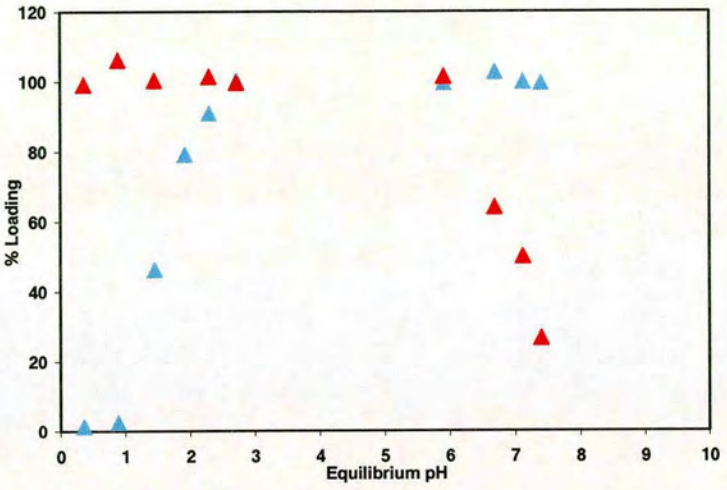

Figure 3.18: Cu (▲) and Cl (▲) loadings of **5** as [Cu(**5**-H)Cl] when a solution of [Cu_2(**5**-2H)$_2$] is contacted with varying pH values of HCl/NaCl solutions.

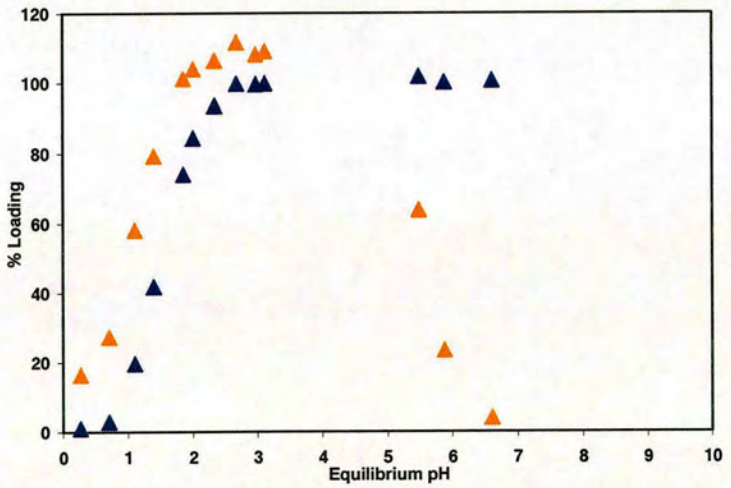

Figure 3.19: Cu (▲) and SO_4 (▲) loadings of **5** as [Cu_2(**5**-H)$_2SO_4$] when a solution of [Cu_2(**5**-2H)$_2$] is contacted with varying pH values of H_2SO_4/Na_2SO_4 solutions.

When [Cu_2(**5**-2H)$_2$] is contacted with H_2SO_4/Na_2SO_4 (0.800 M) solutions the anion-loading curve is quite different (Figure 3.19). It is clear that sulfate is bound more weakly ($pH_{½}$, 5.60) than chloride ($pH_{½}$, 7.16). The more efficient extraction of

chloride into a non-polar solvent is consistent with the Hofmeister series (Figure 3.20), which places anions in an order, according to how strongly hydrated they are. The series was originally derived in 1888[9] when Franz Hofmeister was conducting experiments to rank the availability of various ions to precipitate a mixture of hen egg white proteins. It has been suggested[10, 11] that the term Hofmeister bias be used when predicting distribution coefficients for anions in 2-phase systems, the bias representing the relative solvation free energies of anions in water and a water immiscible solvent. Whilst chloride has a lower solvation energy in water than sulfate it is probable that it also has a more favourable solvation energy in chloroform than sulfate and consequently there will be a large Hofmeister bias.

strongly hydrated anions **weakly hydrated anions**

$Citrate^{3-} > SO_4^{2-} = tartrate^{2-} > HPO_4^{2-} > CrO_4^{2-} > OAc^- > HCO_3^- > Cl^- > NO_3^- > ClO_4^-$

Figure 3.20: The original Hofmeister series.[9]

The sulfate plot shows anomalous behaviour. At high pH there is high copper-loading and loss of sulfate as expected. However, at low pH, there is loss of sulfate from the organic phase as the copper-loading drops off. This implies that there must be some cooperative binding between copper and sulfate such that upon loss of copper, the complex is no longer stable and the sulfate is lost simultaneously.

At pH 2-3 sulfate-loadings are greater than 100%. At these low pH's, not only will the ligand be protonated but some sulfate anions will be too, forming hydrogen sulfate. This carries only one negative charge and therefore one could be coordinated to each ligand-bound copper, forming a neutral $1L^- : 1Cu^{2+} : 1HSO_4^-$ complex (Figure 3.21). If a mixture of this species and the $2L^- : 2Cu^{2+} : 1SO_4^{2-}$ complex were present simultaneously, greater than 100% loading would be seen.

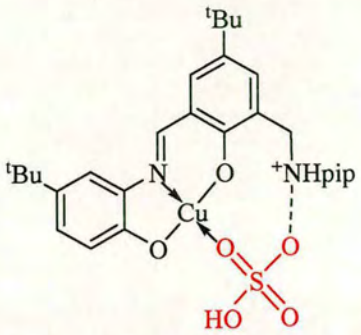

Figure 3.21: Proposed low pH structure.

Also of note is the lower $pH_{½}$ of the copper-loading compared to that seen previously with ligand **1**. The two plots are compared in Figure 3.22. The $pH_{½}$ for copper-loading by ligand **5**, 1.52, is over two pH units lower than that of ligand **1**, 3.75.

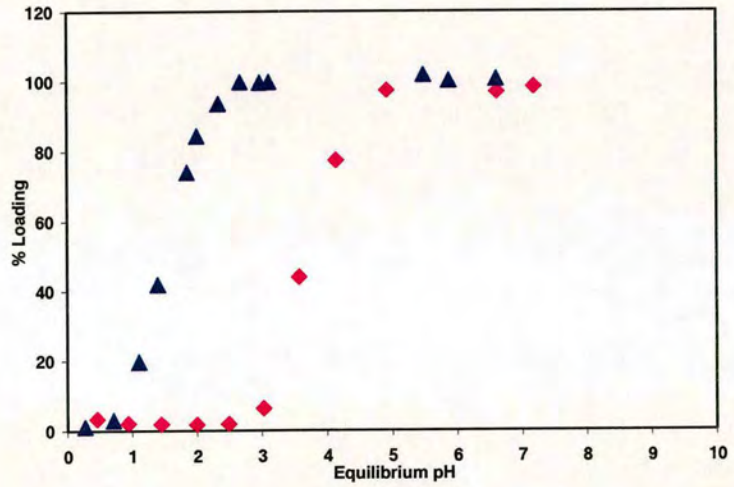

Figure 3.22: The pH-dependence of stripping of copper from chloroform solutions of $[Cu_2(\mathbf{5}\text{-}2H)_2]$ (▲) and $[Cu_2(\mathbf{1}\text{-}2H)_2]$ (♦).

For the stripping of the ligand **1** complex $[Cu_2(\mathbf{1}\text{-}2H)_2]$, every 2 moles of acid strip one mole of complex as in Equation 3.9, resulting in a relatively facile strip and high $pH_{½}$.

$$[Cu_2(\mathbf{1}\text{-}2H)_2]_{(org)} + 2H_2SO_4 \rightleftharpoons \mathbf{21}_{(org)} + 2CuSO_4 \qquad \textbf{Equ. 3.10}$$

However, for the stripping of the copper sulfate complex of ligand **5**, since there is now a pendant arm which can be protonated, the equilibrium is different. Before the phenols can be reprotonated causing loss of copper, the pendant amine arm will be protonated and pick up a sulfate or hydrogen sulfate anion, resulting in the consumption of acid. Therefore, four moles of acid can be consumed by the system before the pH of the equilibrium is altered (Equation 3.10). Hence, the loss of copper is seen at a lower pH than for the ligand **1** strip.

1 mole of acid: $[Cu_2(\mathbf{5}\text{-}2H)_2]_{(org)} + H_2SO_4 \rightleftharpoons [Cu_2(\mathbf{5}\text{-}H)_2SO_4]_{(org)}$

2 moles: $[Cu_2(\mathbf{5}\text{-}H)_2SO_4]_{(org)} + H_2SO_4 \rightleftharpoons [Cu_2(\mathbf{5}\text{-}H)_2(HSO_4)_2]_{(org)}$

3 moles: $[Cu_2(\mathbf{5}\text{-}H)_2(HSO_4)_2]_{(org)} + H_2SO_4 \rightleftharpoons [(\mathbf{5}+H)_2SO_4]_{(org)} + 2CuSO_4$

4 moles: $[(\mathbf{5}+H)_2SO_4]_{(org)} + H_2SO_4 \rightleftharpoons [(\mathbf{5}+H)_2(HSO_4)_2]_{(org)} + 2CuSO_4$

Overall:

$$[Cu_2(\mathbf{5}\text{-}2H)_2]_{(org)} + 4H_2SO_4 \rightleftharpoons [(\mathbf{5}+H)_2(HSO_4)_2]_{(org)} + 2CuSO_4 \qquad \textbf{Equ. 3.11}$$

The low $pH_{½}$ for copper loading/stripping (1.52) by ligand **5** has great practical consequences. The current commercial extractants, such as P50 (Chapter 1, section 1.6), have a $pH_{½}$ of around 1.55 in chloroform, which meets the requirements of the circuits outlined in section 1.5. Consequently, we were encouraged to carry out further investigations into **5** as a development candidate for a future industrial extractant.

3.4.2 Loading

A loading experiment using copper sulfate and ligand **5** was carried out as detailed in section 5.4.2 and shown in Figure 3.24 (bottom). The loading plot is shown overlaid with the stripping plot in Figure 3.23. The $pH_{½}$ is very similar for both plots, although that for the loading process appears to be slightly higher and hence less favourable. As for ligand **1**, there is also a steeper gradient for the loading plot. The variance in these plots may be due to a difference in the two experimental techniques as explained below.

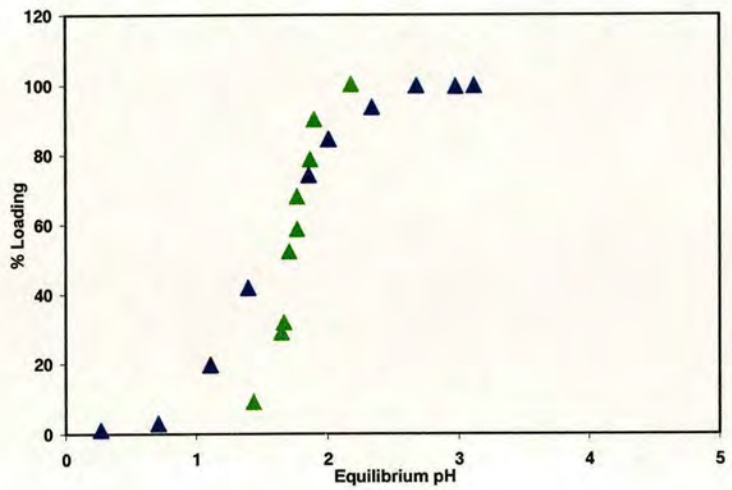

Figure 3.23: The pH-dependence of copper-loading (▲) by ligand **5** and stripping from $[Cu_2(\mathbf{5}\text{-}2H)_2]$ in sulfate media (▲).

When the protocols for the stripping and loading experiments were designed, they were not intended for comparative study. Stripping experiments were designed to study the anion uptake of metal *salt* extractants, whilst loading experiments were intended to focus only on metal uptake. Consequently, the anion concentrations used in the two experiments are not consistent (Figure 3.24). There is a constant excess of sulfate (or chloride) present (0.800 M) in the stripping experiment compared to an equimolar amount (0.00250 M) in the loading. It is fair to assume that when formation of the complex in the water-immiscible phase involves anion coordination, the complex will form more readily in the presence of an excess of anion in the

aqueous phase. As a result the copper-loading is favoured in the strip experiment and a lower $pH_{½}$ is observed (1.52 for the strip vs. 1.70 for the load).

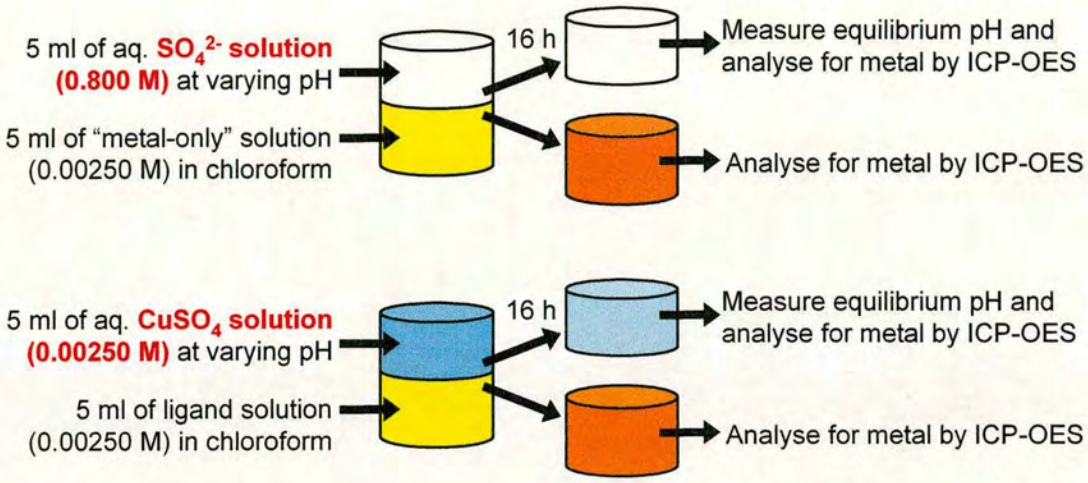

Figure 3.24: Conditions used for stripping of $[Cu_2(\mathbf{5}\text{-}2H)_2]$ (above) and loading of **5** (below), highlighting the difference in sulfate concentration in the aqueous phase.

In order to remedy this inconsistency, a loading experiment was carried out using the same excess sulfate in the aqueous phase as was used in the stripping experiment but maintaining a molar equivalent of copper to ligand concentration as in the previous loading experiments. The results are shown in Figure 3.25.

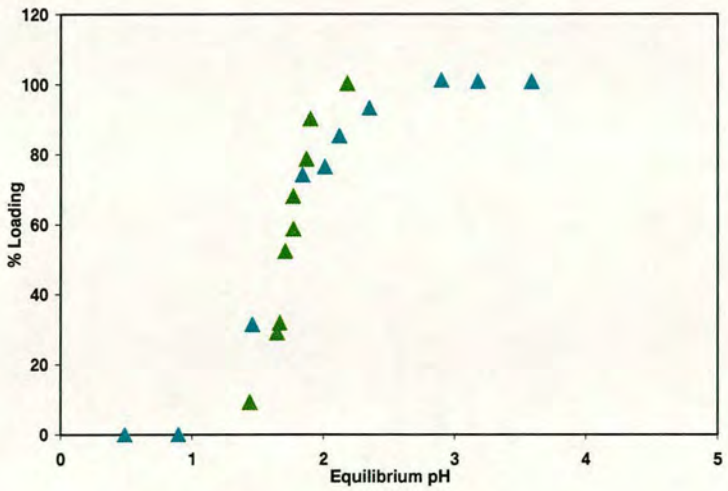

Figure 3.25: Comparison of the copper-loading by ligand **5** with an equimolar (0.00250 M, ▲) and excess (0.800 M, ▲) amount of sulfate in the aqueous phase.

The loading and stripping curves obtained in the presence of excess sulfate are very similar. The steeper gradient, characteristic of all previous loading experiments, is no longer apparent. This loss of sharpness is attributed to the excess sulfate in the system. Sulfate can act as a pH buffer, since it has its own equilibrium process between sulfate and hydrogen sulfate anions.

$$SO_4^{2-} + H^+ \rightleftharpoons HSO_4^-$$

This results in a loss of proton activity in the aqueous phase which causes a spread in the extraction points and hence a less steep curve. The $pH_{½}$ for loading is also lower (1.60) with excess sulfate than an equimolar amount. It is therefore concluded that anion concentration is an important factor in the extraction of copper with a metal salt extractant.

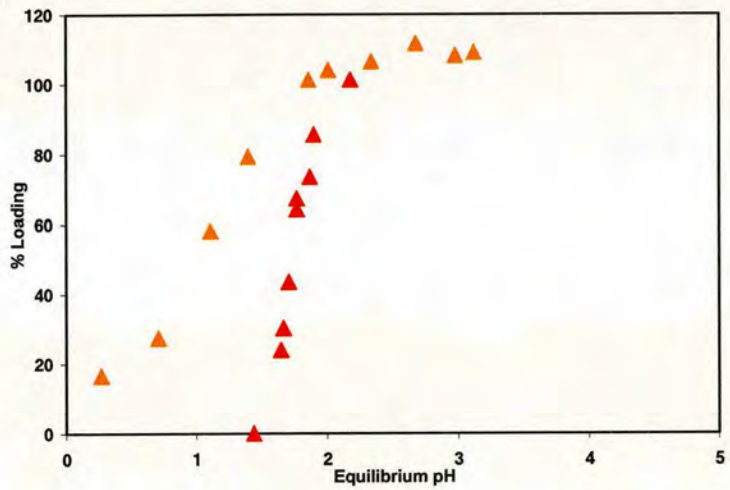

Figure 3.26: The pH-dependence of sulfate-loading (▲, equimolar sulfate) and stripping (▲, excess sulfate) by ligand **5**.

A difference in total anion concentration in the aqueous phase also influences the sulfate-loading plots for each extraction method (Figure 3.26). When there is an equimolar amount of sulfate present as in the loading experiment, the metal and anion loading curves overlap one another. However, once there is an excess of sulfate available in the system, the sulfate-loading exceeds that of the copper. As

discussed in section 3.4.1, this is probably due to the presence of hydrogen sulfate, in this case being loaded by the free ligand.

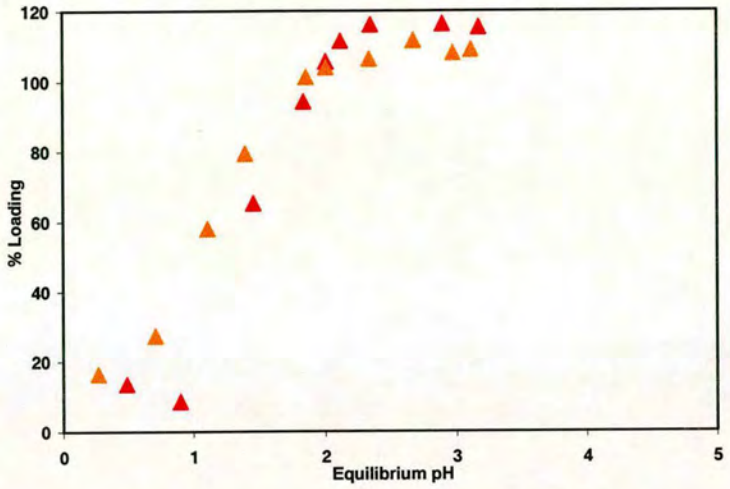

Figure 3.27: The pH-dependence of sulfate-loading (▲) and stripping (▲) by ligand **5** in the presence of excess sulfate in the aqueous layer.

Performing the loading experiment in the presence of excess sulfate results in a sulfate plot similar to the stripping plot obtained previously, as seen in Figure 3.27. Finally, the copper and sulfate-loading plots for the excess sulfate experiment are shown in Figure 3.28, which closely resemble those for the stripping experiment.

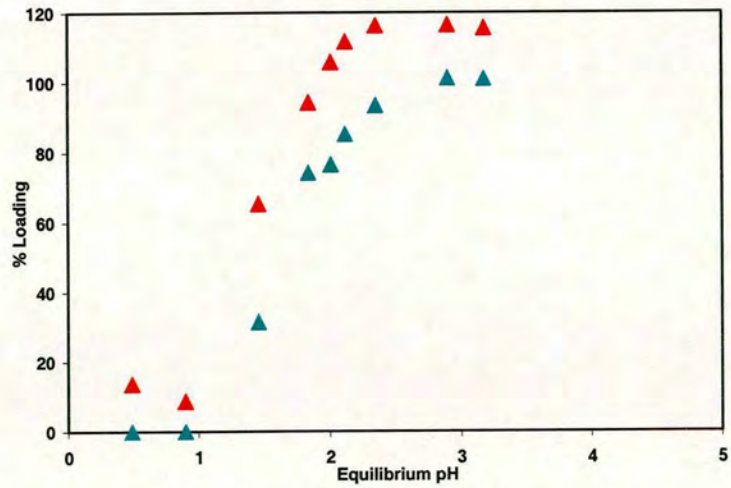

Figure 3.28: The pH-dependence of copper (▲) and sulfate (▲) loading by ligand **5** in the presence of excess sulfate in the aqueous layer.

Ligand **5** is a very promising copper sulfate extractant. Since the shape of the sulfate-loading plots resemble the copper-loading curves, the complex formed during extraction must involve copper and sulfate in such a way that upon loss of copper, the sulfate is simultaneously lost to the aqueous layer. This is indicative of a cooperatively bound complex. Increasing the concentration of sulfate in the system can also further improve the effectiveness of the ligand whilst also emphasising the importance of sulfate in complex formation and resulting in a $pH_{½}$ of 1.52 and 1.60 for the stripping and loading experiments respectively in the presence of excess sulfate. It is important to note that not only is loading of sulfate dependent on copper-binding, but also the reverse; copper binding is favoured in the presence of sulfate.

3.4.3 EPR

As with ligand **1**, it was hoped that the study of copper complex formation by ligand **5** by EPR would help define the speciation. The organic solutions from the sulfate stripping of $[Cu_2(\mathbf{5}\text{-}2H)_2]$ were taken directly for analysis by EPR. At low pH when there is little copper present in the organic phase, no signal is seen. As the pH is increased and hence the copper concentration is increased, a characteristic copper signal can be seen. This signal increases in intensity to about 50% loading as seen in Figure 3.29. As the concentration is increased beyond 50% loading, there is a gradual loss of EPR signal until, at 100% loading, the signal is completely lost (Figure 3.30). It appears that the system behaves similarly to the hydrazone ligands studied by Wood *et al.* (Figure 3.31).[12] At pH-values (pH $\leq$ 2) showing < 50% loading it was assumed that mononuclear complexes are predominating whereas at higher pH, with > 50% loading, dinuclear complexes form which are EPR silent.

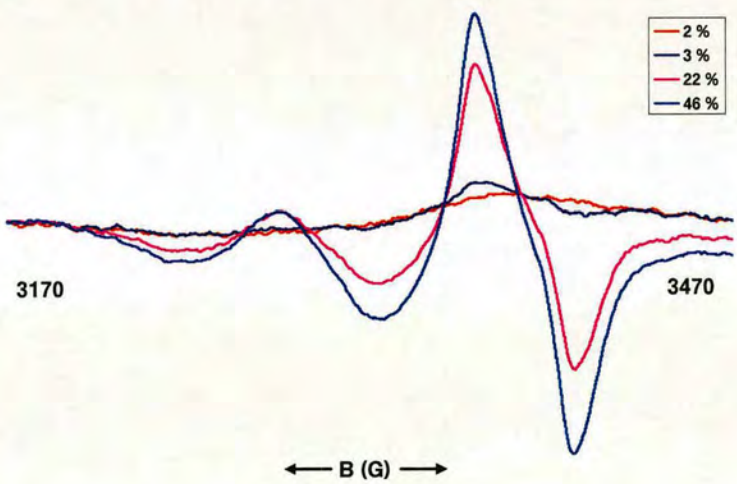

Figure 3.29: EPR spectra of the organic phase of extractions for ligand **5** which showed copper-loading of 0-50%. The key indicates the percentage of copper(II) extracted, as measured by ICP-OES.

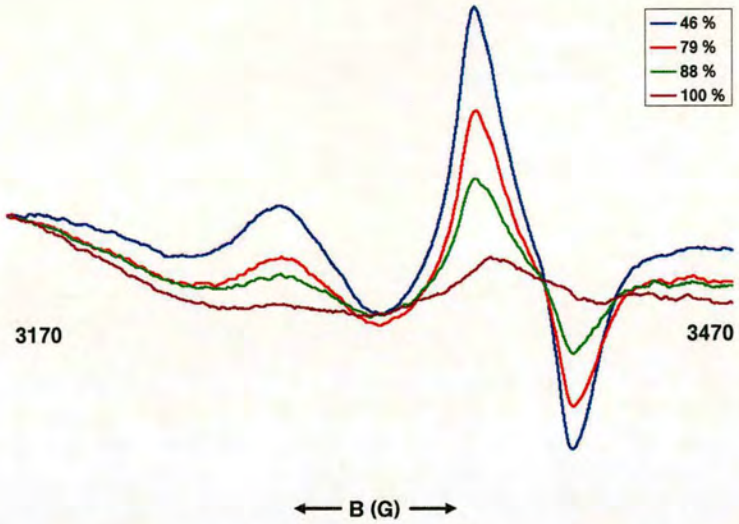

Figure 3.30: EPR spectra of the organic phase of extractions for ligand **5** which showed copper-loading of 50-100%. The key indicates the percentage of copper(II) extracted, as measured by ICP-OES.

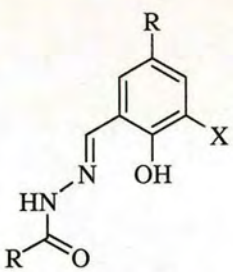

Figure 3.31: Structure of the hydrazone ligands studied using EPR by Wood *et al.*.[12]

As discussed in section 3.4.1, the presence of hydrogen sulfate could allow for the formation of $1\mathbf{L}^{-} : 1Cu^{2+} : 1HSO_4^{-}$ complexes. This is consistent with the EPR data at pH $\leq$ 2, when the majority of the sulfate in the aqueous solution will be present as hydrogen sulfate, resulting in predominance of a mononuclear complex which is responsible for the signal. As the pH increases above 2, the hydrogen sulfate is deprotonated and the predominant complex may become that with $2\mathbf{L}^{-} : 2Cu^{2+} : 1SO_4^{2-}$, and coupling of the unpaired electrons through a bridging sulfate may result in loss of signal. Possible structures for these complexes can be seen in Figure 3.32.

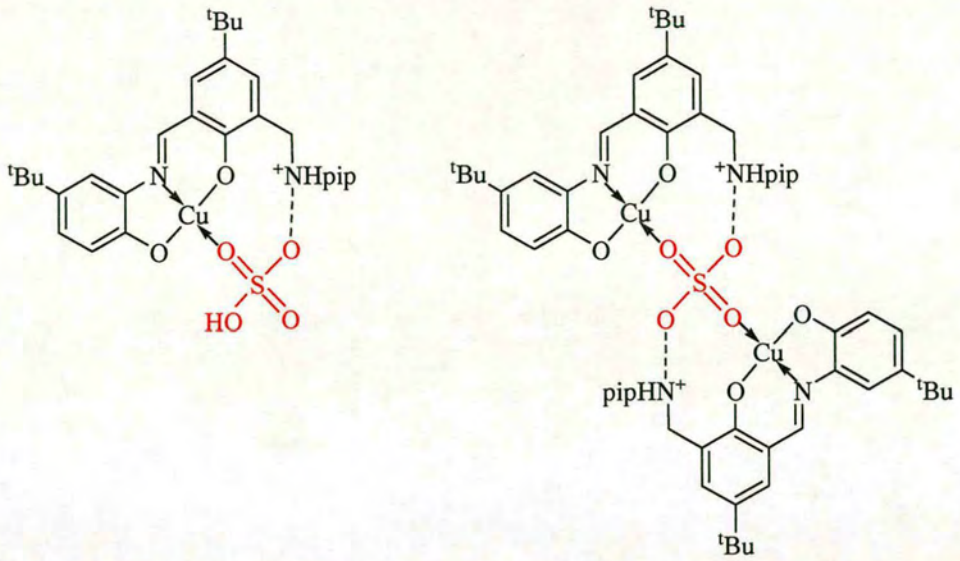

Figure 3.32: Proposed structure of 1 : 1 : 1 and 2 : 2 : 1 complexes with ligand **5**, copper and (hydrogen) sulfate.

In the previous section, the cooperativity of binding between copper and sulfate was discussed. In the structures above, it is clear that the stability of each complex is dependent on both the metal and its attendant anion being bound simultaneously.

3.4.4 Mononuclear complexes containing an auxiliary ligand

The introduction of an auxiliary pyrazolone ligand into the extraction experiment with ligand **1** resulted in the formation of a neutral 1 : 1 : 1 ternary complex of ligand, copper and auxiliary (see Section 2.5.3). This study was repeated with ligand **5** using the same auxiliary, 3-*iso*-propyl-2-pyrazol-5-one. It was assumed that the presence of the pendant piperidino group on ligand **5** would not disrupt the hydrogen bonding network in the inner coordination sphere and either copper-only or copper sulfate complexes as in Figure 3.33 would be formed. There are two possible orientations the auxiliary may take on forming the complex and the sulfate may be bound as shown, or alternatively as a ligand in the axial site on the copper.

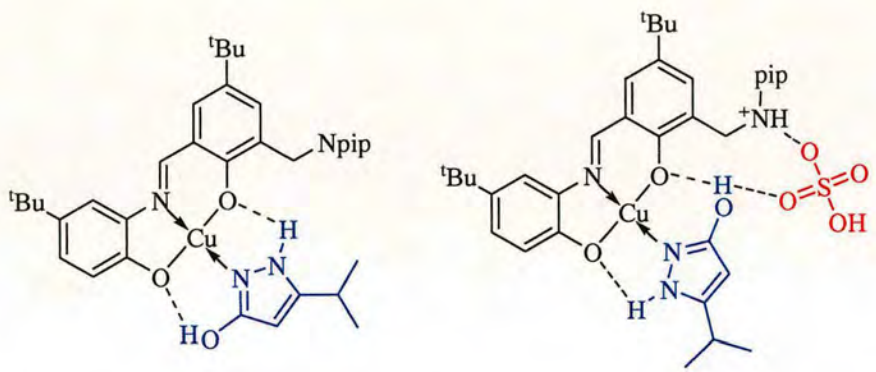

Figure 3.33: Proposed structures of complexes of auxiliary (3-*iso*-propyl-2-pyrazol-5-one) with ligand **5**, showing the two possible orientations of the auxiliary ligand and how sulfate may also be coordinated *via* hydrogen bonding.

In Chapter 2 it was shown that a significant decrease in $pH_{½}$ for copper-loading by ligand **1** occurred upon addition of the auxiliary ligand. This was not the case in extractions with ligand **5** (see below). Experiments were carried out to see how both copper and sulfate loading in the presence of the auxiliary depended on the concentration of auxiliary and the concentration of sulfate in the aqueous phase, resulting in four separate experiments.

The initial loading experiments, with an equimolar amount of sulfate and copper in the system, were carried out in the presence of either an equimolar or an excess

amount of auxiliary ligand. These results were then compared with those from the normal loading experiment with no auxiliary ligand (section 3.4.2).

Addition of an equimolar amount of auxiliary resulted in a significant increase in $pH_{½}$ for copper-loading, from 1.70 to 2.74 (Figure 3.34). The sulfate-loading is also affected; before addition of the auxiliary there was an equal loading percentage of copper and sulfate. Now, the maximum sulfate-loading is about 60%, much less than the maximum 100% loading reached for the copper. If the auxiliary ligand competes for the inner coordination sphere binding site on the ligand-bound copper, the increase in $pH_{½}$ for both copper and sulfate would be expected, due to the synergistic nature of copper- and sulfate-loading. Since no copper is loaded until above pH 2, when the presence of hydrogen sulfate is negligible, it is expected that the sulfate is present as its divalent anion, requiring the formation of $2\mathbf{L} : 2Cu : 1SO_4$ complexes.

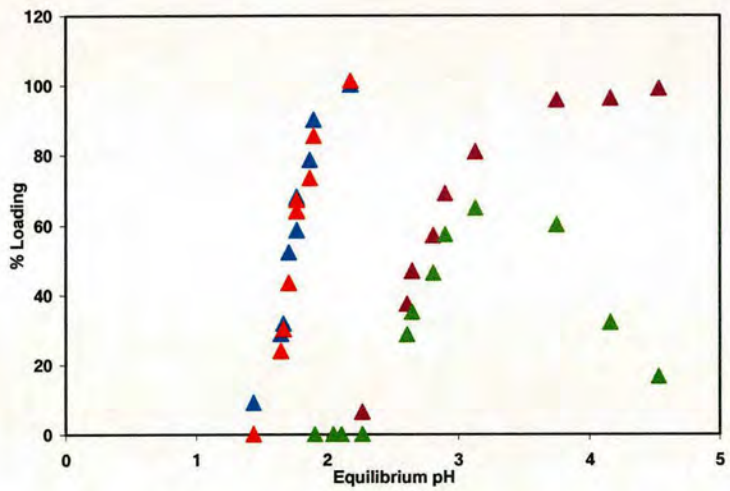

Figure 3.34: Copper and sulfate-loadings (▲and▲) by ligand **5** (0.00250 M in 5 ml $CHCl_3$) from an aqueous solution of $CuSO_4$ (0.00250 M, 5 ml) as a function of pH compared with those (▲and▲) when equimolar (0.00250 M) auxiliary, L_{aux} is present.

When the concentration of auxiliary ligand is greatly increased, the $pH_{½}$ of both copper- and sulfate-loading decreased (Figure 3.35). The copper-loading now has a $pH_{½}$ of 1.90, suggesting that a more stable complex is formed. It is possible that the high concentration of auxiliary allows more than one auxiliary ligand to coordinate to each copper centre, resulting in a different complex which can resist acid stripping

to a lower pH. If the pendant arm is not involved in this coordination, it may be able to bind sulfate and hence an increase in sulfate-loading is seen. Since copper-loading begins at a low pH, it is also possible that some loaded sulfate may be present as hydrogen sulfate, allowing for higher sulfate-loading. Consequently, mononuclear copper species would be expected which should be observed in EPR studies. The species in solution at pH less than 2.5 are EPR silent, whereas above this pH a strong signal is observed, including super hyperfine coupling attributed to nitrogen coupling. The species present at high pH could therefore be similar to that seen in Figure 3.33 (left), when the sulfate is no longer present in the organic phase.

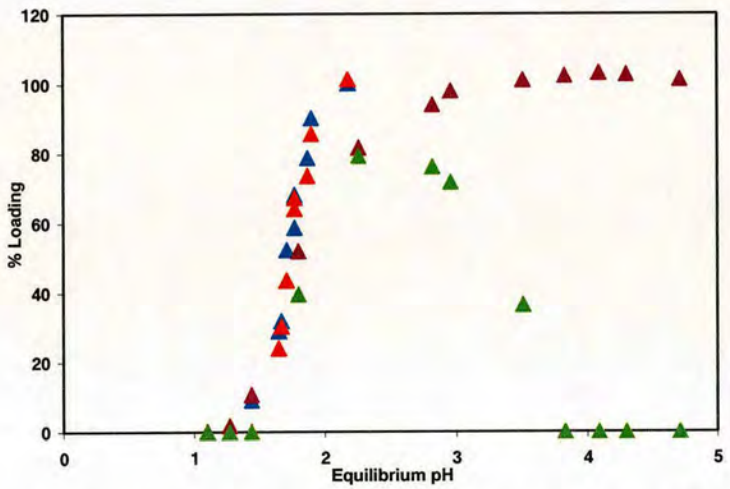

Figure 3.35: Copper and sulfate-loadings (▲and▲) by ligand **5** (0.00205 M in 5 ml $CHCl_3$) from an aqueous solution of $CuSO_4$ (0.00250 M, 5 ml) as a function of pH compared with those (▲and▲) when excess (0.0500 M) auxiliary, L_{aux} is present.

The two experiments above were repeated in the presence of excess sulfate in the aqueous phase and compared to the plots obtained when no auxiliary was present and the $pH_{½}$ for copper-loading was 1.52. When an equimolar amount of auxiliary was added, the $pH_{½}$ was increased to 1.60 (Figure 3.36). The presence of an excess of sulfate relative to the auxiliary seems to allow the $[Cu_2(\mathbf{5}\text{-H})_2SO_4]$ or $[Cu(\mathbf{5}\text{-H})HSO_4]$ complexes to predominate over any auxiliary-containing assembly. This is supported by the presence of an excess of sulfate-loading relative to the copper up to pH 2, as seen when no auxiliary is present. The slight reduction in sulfate loading above pH 2

compared to when there is no auxiliary added suggests that the auxiliary may again be competing for the sulfate binding site.

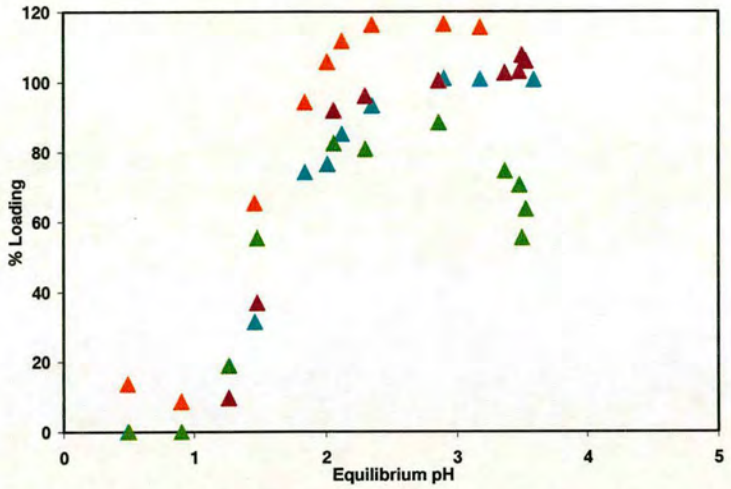

Figure 3.36: Copper and sulfate-loadings (▲and▲) by ligand **5** (0.00250 M in 5 ml $CHCl_3$) from an aqueous solution of $CuSO_4$ (0.0025 M, 5 ml), with an excess of sulfate (0.800 M) in the aqueous layer as a function of pH compared with those (▲and▲) when equimolar (0.00250 M) auxiliary, L_{aux} is present.

When there is an excess of both auxiliary and sulfate (Figure 3.37), the detrimental competition between auxiliary and sulfate appears to be present again, with a loss of steepness in the copper-loading and still further depression of the sulfate-loading. The $pH_{½}$ for copper-loading is now 2.05.

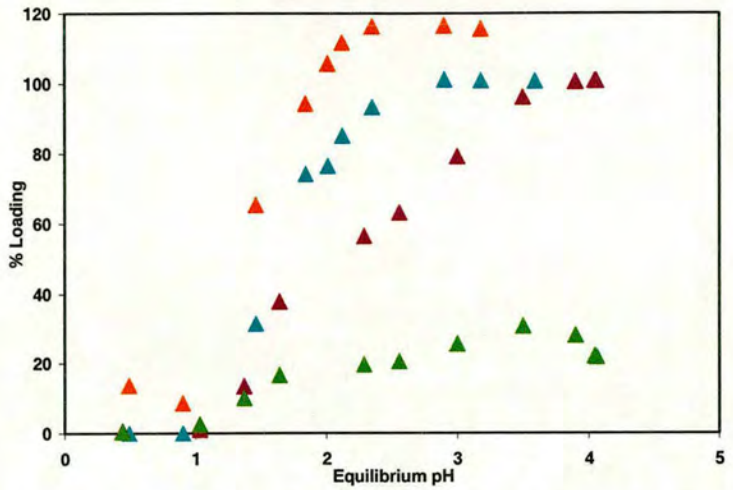

Figure 3.37: Copper and sulfate-loadings (▲and▲) by ligand **5** (0.00250 M in 5 ml $CHCl_3$) from an aqueous solution of $CuSO_4$ (0.0025 M, 5 ml), with an excess of sulfate (0.800 M) in the aqueous layer as a function of pH compared with those (▲and▲) when excess (0.0500 M) auxiliary, L_{aux} is present.

In contrast to the copper extraction by **1**, the loading of copper and sulfate by **5** is adversely affected by the addition of the auxiliary ligand. Its addition results in a higher $pH_{½}$ of copper-loading. When the auxiliary and sulfate are present at equimolar concentrations, they compete for ligand **5**'s copper binding site and result in higher $pH_{½}$ for copper-loading. If either is in excess then a decrease in $pH_{½}$ is seen, although never reaching as low a $pH_{½}$ as that observed with ligand **5** alone. In all cases, the sulfate-loading does not reach maximum loading of 100% in the presence of auxiliary, supporting the assumption that the auxiliary is coordinating to the copper and interfering with the sulfate binding site.

3.4.5 'Dual-Host' studies

Ligand **5** was designed to extract a metal and its attendant anion. The results presented in sections 3.4.1-3.4.3 indicate the formation of a cooperatively bound assembly, $[Cu_2(\mathbf{5}\text{-}H)_2SO_4]$, upon extraction. This was a favourable property of ligand **5** which had not previously been envisaged. An alternative approach to the recovery of metal salts is to add a second ligand capable of forming anion-complexes into an extraction system containing a conventional cation-exchange metal extractant. Such an approach has been referred to as the "dual-host" approach in Chapter 1 (section 1.8).[10, 13] There are then two separate extraction equilibria; one for the metal cation and another for the anion. If the two can operate as well as or better than a more complicated ligand then from an industrial standpoint, it will be preferred on the basis of ease of synthesis and costs. To investigate this, ligand **1** was used as the metal extractant and the tertiary amine 1-*t*-butyl-4-*N*-piperidinylmethylbenzene, **11**, in Figure 3.38 was used as the anion extractant because it can be assumed that this contains a nitrogen atom with a very similar environment and basicity to that in the pendant arm of **5**.

11

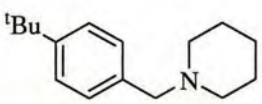

Figure 3.38: *t*-Butyl-4-N-piperidinylmethylbenzene), **11**, a potential anion-exchange reagent for the recovery of anions from low pH aqueous feeds.

The equilibrium for anion loading would then be:

$$\mathbf{11}_{(org)} + H^+ + X^- \rightleftharpoons [(\mathbf{11}H)X]_{(org)}.$$

An equimolar amount of the amine and ligand **1** were used in a loading experiment in exactly the same way as ligand **1** and **5** have been used previously, with an equimolar amount of sulfate present in the aqueous layer, relative to the copper concentration. The copper-loading curve obtained can be seen in Figure 3.39, compared to those for ligands **1** and **5** alone.

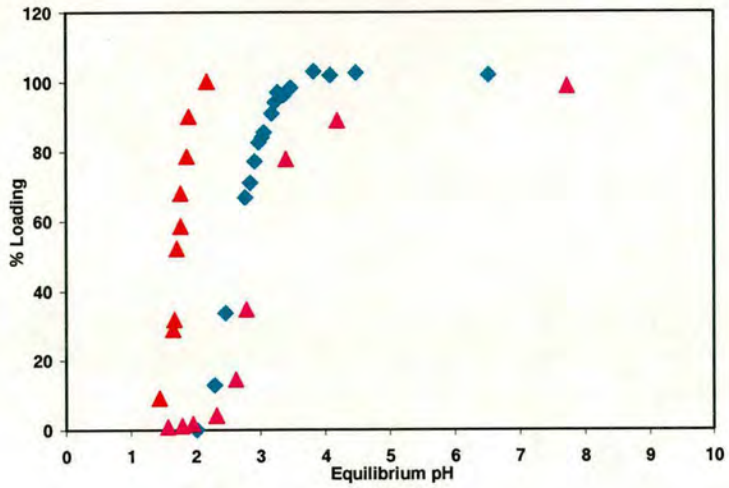

Figure 3.39: Comparison of copper-loading by chloroform solutions (0.00250 M, 5.0 ml) of ligand **5** (▲), ligand **1** (♦) and ligand **1** + the piperidino amine, **11** (▲).

The copper-loading is slightly less efficient than with ligand **1** or **5** alone, with a $pH_{½}$ of 3.10. The higher $pH_{½}$ for copper loading by **1** and **11** suggests that the protonated form of **11** may compete with copper for **1**.

Sulfate measurements were also made. There was very little sulfate-loading (a maximum of 3%) of the chloroform phase when **1** and an equimolar concentration of **11** were contacted with an aqueous solution of copper(II) sulfate. However, it was suspected that the protonated amine ligand may be water soluble and therefore unable to load sulfate into the organic layer. Distribution coefficient experiments which confirmed this assumption were therefore carried out as described in appendix 7.4.

In order to overcome this water solubility problem, a more organic-soluble amine, **12** with dihexylamino groups in place of the piperidine was synthesised (Figure 3.40). This amine was used in the same way as the piperidino analogue, **11** in a copper sulfate-loading experiment. The results are shown in Figure 3.41.

12

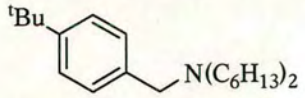

Figure 3.40: The second amine ligand 1-*t*-butyl-4-dihexylaminomethylbenzene, **12**, designed for use as an anion extractant.

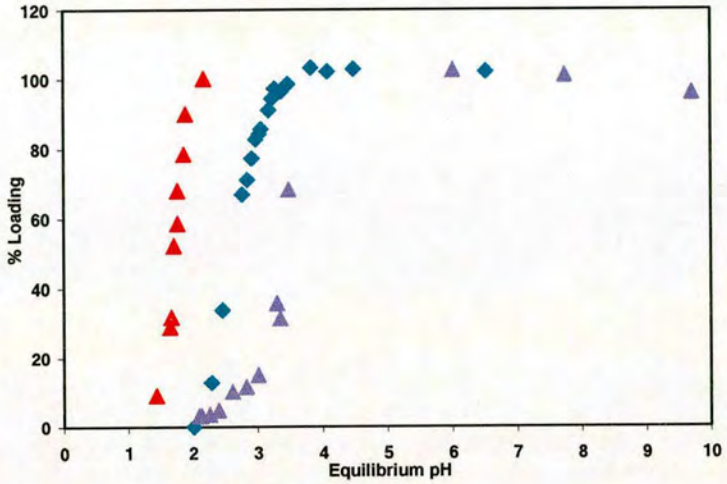

Figure 3.41: Comparison of copper-loading by chloroform solutions (0.00250 M, 5.0 ml) of ligand **5** (▲), ligand **1** (♦) and ligand **1** + the dihexylamino amine, **12** (▲).

Again, the copper-loading is less efficient than that with either ligand **1** or **5** alone. It also has a higher $pH_{½}$ (3.40) for copper loading than the piperidino ligand. It appears that the protonated form of **12** interacts more strongly with **1** than the protonated form of **11**. This could be due to **12**'s organic solubility, resulting in a higher concentration of **12** present in the organic layer than for **11**. Proposed equilibria are shown below, where R_3NH^+ is the protonated form of the dihexylamino ligand, **12**.

$$2R_3NH^+ + \mathbf{21} \rightleftharpoons 2[R_3NH\cdots\cdots\mathbf{1}]^+$$

$$+ 2Cu^{2+} \Big\Downarrow$$

$$2Cu^{2+} + \mathbf{21} \rightleftharpoons 2[Cu(\mathbf{1}\text{-}2H)] + 2R_3NH^+$$

The sulfate-loading with this ligand reached a maximum of 60% at the lowest pH which dropped gradually until it reached zero at pH 3.5 (Figure 3.42). In order to ensure this loading was entirely due to the amine, the experiment was repeated without ligand **1**. The sulfate-loading is identical in the pH range 2.0-3.5. It is interesting to note that at the point where sulfate is no longer present in the organic layer (pH ~ 3.4) and hence the amine is no longer protonated, there is a sharp increase in copper-loading. This further supports the assumption that the protonated form of **12** competes with copper for ligand **1**.

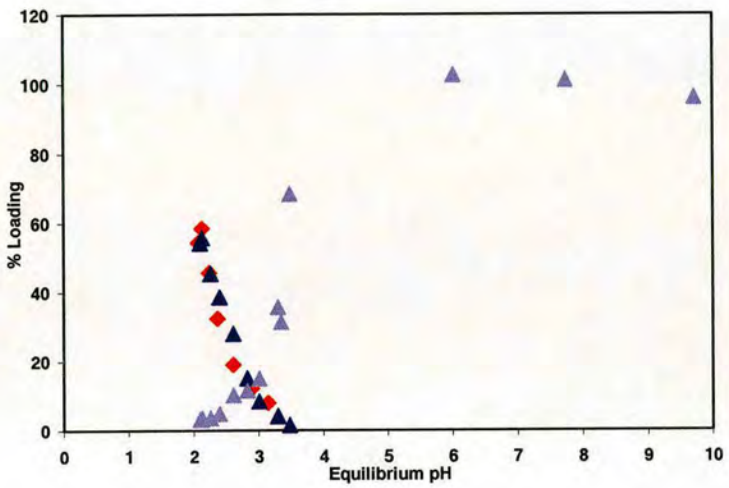

Figure 3.42: The pH dependence of copper (▲) and sulfate (▲) loadings by Ligand **1** with the dihexylamino ligand **12** and the sulfate-loading of **12** alone (♦).

The preorganised ligand **5** extracts both copper and sulfate better than the sum of its parts (**1** and **11/12**), i.e. the ditopic ligand approach in this case is more effective than the "dual-host" approach. It has not been possible to interpret with confidence the origin of the difference in terms of the structures of complexes and adducts formed in solution. However, the results obtained do confirm the impressive property of ligand **5,** that it can extract both copper and sulfate cooperatively, in pH ranges of practical consequence in extractive metallurgy.

3.4.6 Cooperativity of copper/anion binding

In order to investigate further the cooperativity of copper and anion binding by ligand **5**, loading experiments were extended to aqueous solutions containing copper(II) and an excess of chloride or nitrate. The extractions were carried out under the same conditions as for copper sulfate in the presence of excess sulfate (see section 3.4.2). The three extraction plots are shown in Figure 3.43. The chloride and nitrate plots are identical, with copper-loading curves overlapping each other and a $pH_{½}$ of 1.70. The sulfate plot has a slightly less steep gradient which begins to load copper at a lower pH, and reaches 100% loading at a higher pH. This results in a $pH_{½}$ of 1.60.

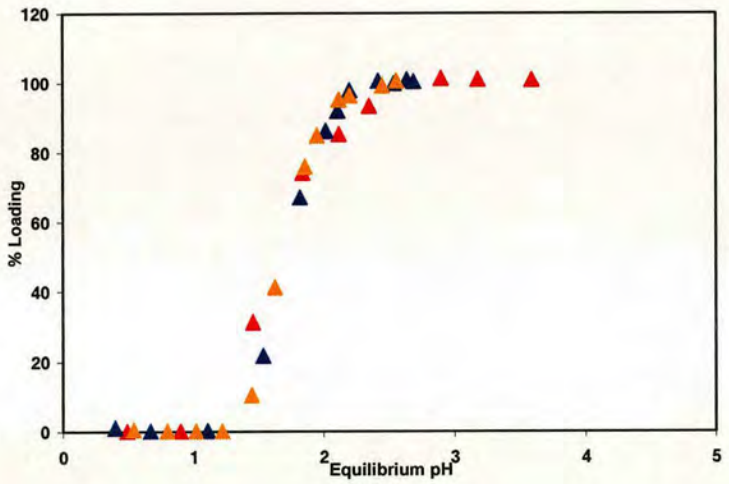

Figure 3.43: Comparison of copper-loading by ligand **5** in chloroform (0.00250 M, 5.0 ml), with an excess (0.800 M) of sulfate, (▲) nitrate (▲) and chloride (▲) in the aqueous layer.

An alternative experiment was carried out with ligand **5** and six different copper salts to investigate further any possible dependence of copper-loading on the nature of the anion. A 5.0 ml solution of ligand (0.00250 M) was contacted with an excess of aqueous copper salt solution such that the copper concentration was 0.0050 M. The solutions were stirred overnight, and a 1.0 ml sample of each organic phase was analysed for copper content. The results are shown in Figure 3.44.

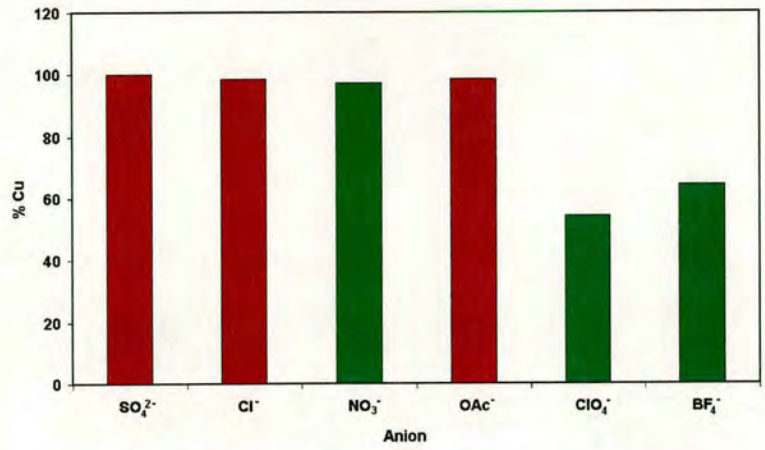

Figure 3.44: Percentage copper-loading by ligand **5** with various copper salts. The colours indicate the colour of the organic solution after the experiment.

The extent to which the nature of the anion influences the efficiency of loading of copper is a feature of considerable interest. The data in Figure 3.44 suggest that ligand : copper : anion assemblies in chloroform are significantly less stable when the anion is BF_4^- or ClO_4^-. A number of different properties of the anion could contribute to this.

The Hofmeister bias[10, 11] (Figure 3.45) plays an important part, affecting how stable each anion will be in the non-polar organic solvent. The most extractable anion based on the Hofmeister bias is perchlorate and consequently the extractability of the anion appears to be of little importance in determining the stability of the ligand : copper : anion assembly, because the copper loading for this perchlorate system is significantly lower than for sulfate, which on the Hofmeister scale is the least extractable anion.

strongly hydrated anions **weakly hydrated anions**

$Citrate^{3-} > SO_4^{2-} = tartrate^{2-} > HPO_4^{2-} > CrO_4^{2-} > OAc^- > HCO_3^- > Cl^- > NO_3^- > ClO_4^-$

Figure 3.45: The original Hofmeister series.[9]

The stability of complexes is also dependent on how strongly coordinating an anion is. It is widely accepted[14] that both BF_4^- and ClO_4^- are weakly coordinating anions. It

is for this reason that metal salts of these anions are often used when complexation to other weakly coordinating ligands is desired.[15, 16] In order to assess the stability of different anions on complexation to copper, the first formation constants for complex formation could be compared.[17] However, it is difficult to find data obtained under the same conditions for direct comparison.

The final influencing factor is whether the anion is capable of forming the cooperatively bound ligand : copper : anion species proposed in this thesis. One way in which this might be achieved is to have the anion binding to both copper and the pendant piperidinium group in the ligand. Both nitrate and chloride could form a 1 : 1 : 1 complex as in Figure 3.46 (i and ii), although NO_3 may link to NH^+ more efficiently.

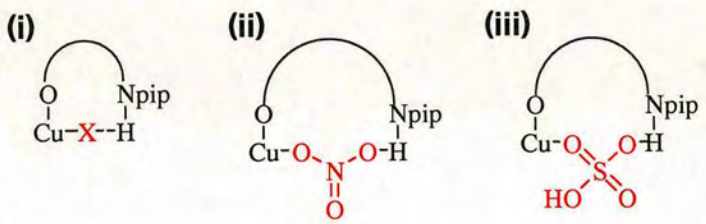

Figure 3.46: Possible anion binding motifs for 1 : 1 : 1 complexes.

Sulfate can form these complexes in its protonated form, hydrogen sulfate (Figure 3.46, iii). It can however, also form 2 : 2 : 1 complexes as a bridging anion between two ligand-bound coppers, as seen in Figure 3.47.

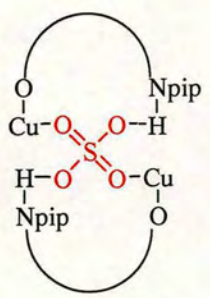

Figure 3.47: 2 : 2 : 1 complex formed in presence of sulfate anion.

It is not possible to conclude from these results which factor is the most influential in the stability of copper extraction. However, the weakest-coordinating anions, perchlorate and tetrafluoroborate, do not form complexes as stable as with each of the other anions, suggesting that formation of complexes which bind the attendant anion within the inner coordination sphere of the metal is key to successful copper extraction.

3.5 Conclusions

Ligand **5** has produced a range of surprising and potentially useful results. It can function as a successful copper sulfate extractant, with good solubility in chloroform, excellent $pH_{½}$ values and cooperative copper/sulfate binding. As a potential extractant for use in industry, the key features of ligand **5** of interest are:

- the ease and low cost of synthesis;
- the relatively low $pH_{½}$ for copper-loading (1.60);
- the cooperativity of copper and sulfate binding and, hence;
- the ability to extract copper(II) sulfate more effectively than its dual host equivalent.

In order to explore further whether ligand **5** could function in an industrial process, other studies must be done to establish its suitability for development as a commercial extractant. The ligand must be able to withstand many strip/load cycles, be resistant to hydrolysis at low pH and have high solubility in the required solvents. High selectivity of both metal cation and attendant anion transport are also essential. These issues will be addressed in Chapter 4.

3.6 References

1 K. C. Sole, *Solvent Extraction and Ion Exchange*, 2002, **20**, 601.

2 D. Dreisinger, *Hydrometallurgy*, 2006, **83**, 10.

3 S. G. Galbraith, '*Ditopic Ligands for the Selective Solvent Extraction of Transition Metal Sulfates*', PhD thesis, University of Edinburgh, 2004.

4 S. G. Galbraith, Q. Wang, L. Li, A. J. Blake, C. Wilson, S. R. Collinson, L. F. Lindoy, P. G. Plieger, M. Schröder and P. A. Tasker, *Chemistry - A European Journal*, 2007, *submitted*.

5 H. Adams, N. A. Bailey, D. E. Fenton and G. Papageorgiou, *Journal of the Chemical Society, Dalton Transactions*, 1995, 1883.

6 C. Buon, L. Vhacun-Lefevre, R. Rabot, P. Bouyssou and G. Coudert, *Tetrahedron Letters*, 2000, **56**, 605.

7 A. Parkin, '*Crystallographic and Modelling Studies of Transition Metal Complexes*', PhD thesis, University of Edinburgh, 2002.

8 J. Szymanowski, '*Hydroxyoximes and Copper Hydrometallurgy*', CRC Press, London, 1993.

9 F. Hofmeister, *Archiv for Experimentelle Pathologie und Pharmakologie*, 1888, **24**, 247.

10 K. Kavallieratos and B. A. Moyer, *Chemical Communications*, 2001, 1620.

11 T. G. Levitskaia, M. Marquez, J. L. Sessler, J. A. Shriver, T. Vercouter and B. A. Moyer, *Chemical communications*, 2003, 2248.

12 J. L. Wood, '*Multi-Loading Ligand Assemblies to Transport Copper*', PhD thesis, University of Edinburgh, 2005.

13 K. Kavallieratos, R. A. Sachleben, G. J. Van Berkel and B. A. Moyer, *Chemical Communications*, 2000, 187.

14 I. Krossing and I. Raabe, *Angewandte Chemie International Edition*, 2004, **43**, 2066

15 W. Beck and K. Sunkel, *Chemical Reviews*, 1988, **88**, 1405.

16 S. H. Strauss, *Chemical Reviews*, 1993, **93**, 927.

17 R. M. Smith and A. E. Martell, '*Critical Stability Constants, Volume 4: Inorganic Complexes*', Plenum Press, New York, 1981.

CHAPTER 4

4 CHAPTER 4 126

4.1 Introduction 128

4.2 Synthesis and characterisation of ligands 130

4.3 Solvent extraction 132

4.3.1 Stripping 132

4.3.2 Loading 133

4.3.3 EPR of extracted species 136

4.4 Stability 138

4.4.1 Strip/load cycles 138

4.4.2 Ligand stability to hydrolysis 140

4.5 Selectivity 143

4.5.1 Copper(II) and iron(III) 143

4.5.2 Sulfate and chloride 143

4.6 Conclusions 145

4.7 References 147

4.1 Introduction

Having established the proof-of-concept that ligands of the type discussed in Chapter 3 give efficient extraction of copper dications or copper(II) salts, it was proposed to synthesise and test extractants for a number of the criteria for commercial use. These criteria (see Figure 4.1) were discussed in Section 1.9 of Chapter 1. In view of their novel and potential use for metal processing using new flowsheets, work focused on reagents similar to **5** which would transport copper(II) sulfate. The requirements chosen for study in this chapter are solubility, stability and selectivity, because without satisfactory performance in these areas there would be little point in undertaking a development programme to optimise performance under the other headings.

Safety	**Selectivity**	**Separation**
Solubility	**Speed**	**Stability**
Strength	**Synthesis**	**System**

Figure 4.1: Criteria important in the design of new extractants. For a more detailed description, see Section 1.9 of Chapter 1.

An increase in organic solubility of a ligand in non-polar and water immiscible media can usually be achieved by increasing the bulk of alkyl substituents attached to the molecule. Consequently, an analogue of ligand **5** with multiply branched nonyl groups in place of the 5-*t*-butyl substituents (ligand **10**) was synthesised and tested to ensure the extraction of copper was not detrimentally affected by this change. EPR was again used as a useful tool for probing the speciation in solution.

In order to probe the chemical stability of ligands **5** and **10**, load/strip cycles were carried out under conditions which a commercial extractant would be expected to withstand in operation. The copper content of solutions was measured after each cycle.

The metal-selectivity of extractants such as **10** is important, since feed solutions containing copper often contain an equal, if not higher concentration of iron(III) and traces of several other metals.[1] The ability of an extractant to load only one metal in the presence of others is a key feature required of an industrial extractant. Selectivity is key to an efficient *separation* operation. If co-extraction of two or more metals occurs, different types of downstream problems can arise:

(i) If the stripping of the organic phase to generate an electrolyte for metal production results in an impurity metal being present, this may electrodeposit with the copper, generating a product of low commercial value. If the impurity metal is not electrodeposited, then each cycle of stripping will lead to an increased concentration in the electrolyte which increases viscosity, reducing current efficiency. Taking a bleed of the electrolyte to remove the impurity metal and return the copper to the front end of the circuit or to the electrolyte greatly reduces the efficiency.

(ii) If the stripping does not remove the impurity metal from the organic phase then its concentration will build up on each loading cycle and the reagent will become "poisoned" and will be unable to load any of the copper. Again taking a bleed from the organic phase will be required and forcing conditions will be needed to purge the impurity metal. This will have unfavourable effects on efficiency and materials balances.

Selective transport of sulfate in the presence of chloride is another important feature. Electrowinning from copper chlorides is less favoured as Cl_2 is generated, which causes engineering problems and is a safety hazard. The high proton activity associated with hydrochloric acid creates engineering difficulties and a poorer quality of copper is generated at the anode.[2, 3] The transport of SO_4^{2-} instead of Cl^- in a solvent extraction circuit reduces these problems as the electrowinning of metal sulfates is well defined and sulfuric acid is less corrosive.

4.2 Synthesis and characterisation of ligands

In order to increase the solubility of ligand **5**-type extractants in non-polar water immiscible solvents, the tertiary butyl groups can be replaced with branched alkyl chains. In industry, the common alkyl groups used to ensure high solubility are 2-ethyl hexyl, multibranched nonyl and multibranched dodecyl.[4] In the Tasker group, *t*-butyl is used primarily for ease of synthesis, *t*-octyl is often used because it is branched while also being a single isomer and for high organic solubility the branched nonyl group, C_9H_{19} is frequently used.

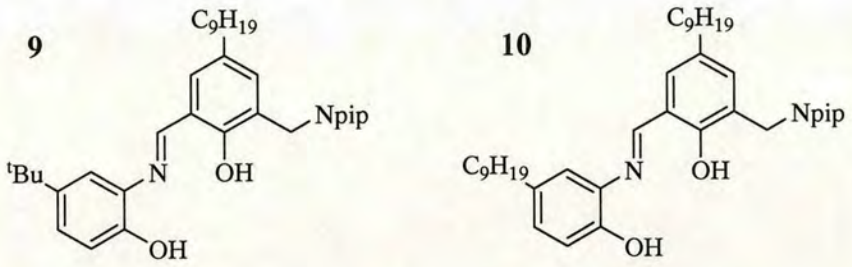

Figure 4.2: Ligands synthesised and discussed in Chapter 4.

The synthesis of ligands **9** and **10** is analogous to that for **5**. The 5-nonyl salicylaldehyde undergoes a Mannich reaction with *N*-piperidinomethylamine, as carried out previously on the *t*-butyl analogue (Chapter 3, section 3.2). For the formation of ligand **9**, this substituted salicylaldehyde then undergoes a Schiff base condensation with 2-amino-4-*t*-butylphenol. In order to synthesise ligand **10**, 4-nonyl-2-aminophenol must first be produced. 4-Nonylphenol was first converted to 4-nonyl-2-nitrophenol *via* nitration using iron(III) nitrate. The nitro group was reduced under an atmosphere of hydrogen (1 atm) using palladium charcoal catalyst to obtain 4-nonyl-2-aminophenol in excellent yield and the Schiff base reaction (Scheme 4.1) results in the formation of ligand **10**.

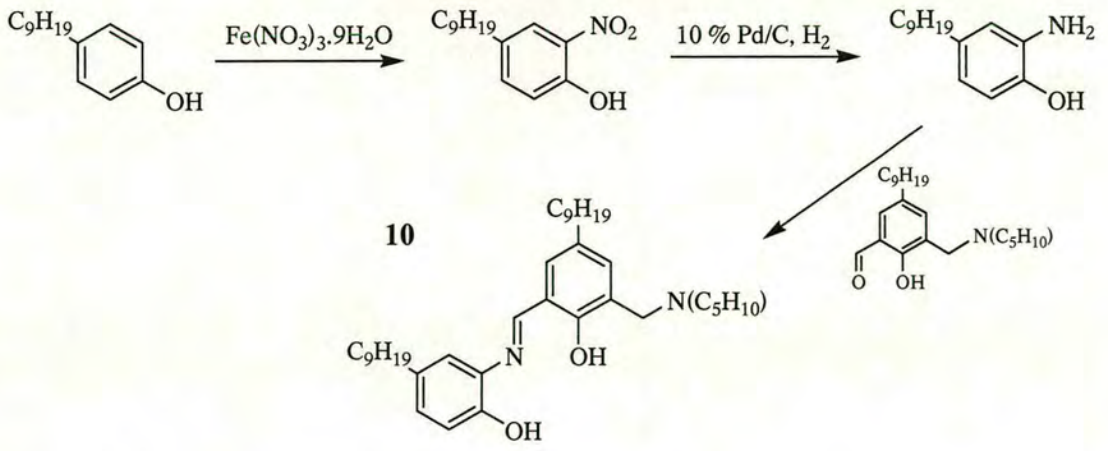

Scheme 4.1: Synthesis of ligand **10**.

Since the material exists as a mixture of branched isomers of the nonyl group, characterisation by NMR spectroscopy is difficult. The CH_2 and CH_3 region of the ^1H NMR spectrum is broad and complex. However, the ligands can be assigned using the aromatic region in conjunction with the presence of the imine peak at δ ~ 9.0 and absence of any residual aldehyde peak at δ ~ 10.0. Due to the presence of mixed isomers, ^{13}C NMR spectroscopy is also too complex for use as an analytical tool. IR also confirms absence of aldehyde and appearance of the imine. The greasy nature of the nonyl group results in the ligand being present as an oil and hence, recrystallisation is not possible.

The copper complex of **10** was prepared by mixing stoichiometric amounts of ligand and copper acetate in methanol. Analysis by mass spectrometry confirmed the presence of the 2 : 2 ligand to metal complex, $[Cu_2(\mathbf{10}\text{-}2H)_2]$ with a peak at 1249.

4.3 Solvent extraction

Ligand **5** was shown in Chapter 3 to be an effective extractant for copper(II) sulfate. Having synthesised the more hydrophobic analogue ligand **10**, it was necessary to carry out solvent extraction experiments to establish whether the new ligand's behaviour as an extractant for copper(II) sulfate was similar.

4.3.1 Stripping

Stripping of the copper-only complex of **10** [Cu_2(**10**-H)$_2$] with sulfuric acid was carried out in the same manner as previously discussed Chapter 3 (section 3.4.1). Full experimental details are given in Chapter 5, section 5.4.1. Copper and sulfate loadings as a function of pH are presented in Figure 4.3 and 100% loading is, as for ligand **5**, assumed to be when the species present in solution is 2 ligands, 2 coppers and 1 sulfate (2 : 2 : 1 stoichiometry).

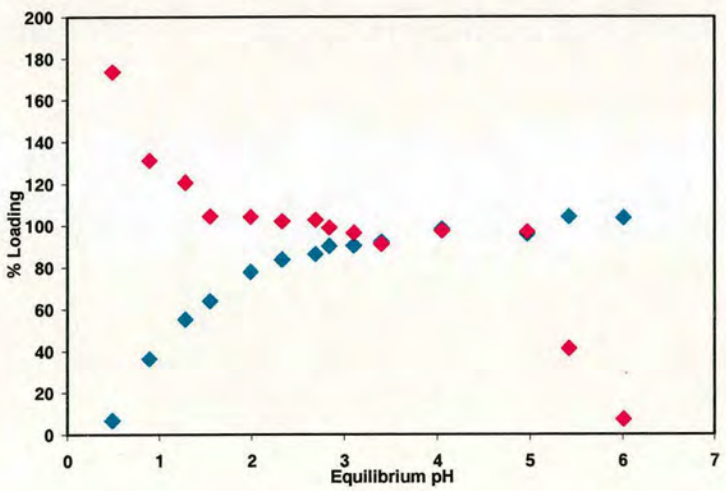

Figure 4.3: Cu (♦) and SO_4 (♦) loadings of **10** as [Cu_2(**10**-H)$_2SO_4$] when a solution of [Cu_2(**10**-2H)$_2$] is contacted with varying pH values of H_2SO_4/Na_2SO_4 solutions.

The $pH_{½}$ of copper loading, 1.20, is slightly lower than that of ligand **5**, 1.52. It appears that the increased hydrophobicity increases the stability of ligand : copper (and ligand : copper : sulfate) assemblies in chloroform solutions in contact with low pH aqueous solutions. A key difference is the form of the sulfate-loading curve. In all ligand **5** experiments, the sulfate loading dropped to zero at low pH, following the

copper loading curve (see section 3.4). Here, the sulfate-loading approaches 200% at very low pH when no copper is loaded. This is consistent with the free ligand being doubly protonated to give a hydrogen sulfate salt [(**10**+2H)$(HSO_4)_2$] or with hydrolysed components giving hydrogen sulfate salts as in Figure 4.4. This is in marked contrast to the behaviour of **5** where the sulfate loading falls to zero at low pH.

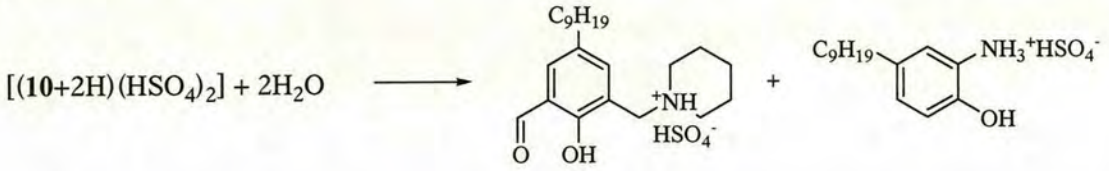

Figure 4.4: Formation of hydrogen sulfate salts of the aniline and piperidinomethylaldehyde components of **10**.

The $pH_{½}$ of sulfate loading is very similar, 5.50, to that for ligand **5**, 5.60, which is not surprising since the sulfate-binding site is identical. There is a significant plateau of sulfate-loading at around 100% loading from pH 1.5-5, before dropping to zero at about pH 6. As this coincides with copper loading of greater than 90%, this is close to an ideal pH-profile for a copper(II) sulfate extractant. On dropping the pH after 100% loading has been achieved the sulfate loading remains constant until pH less than 1.5 when it rises steeply.

4.3.2 Loading

The extractive behaviour of ligand **10** was investigated further using a loading experiment as discussed in Chapter 3, section 3.4.2 and described in detail in Chapter 5, section 5.4.2. Solutions of **10** were prepared to a known concentration (0.00250 M) in chloroform and contacted with an equal volume of aqueous $CuSO_4$ solutions at the same concentration at a range of pHs, and the equilibrium pH is plotted against the percentage loading of copper. Plotting the copper loading curve alongside that obtained in the stripping experiment shows that the two plots are almost identical (Figure 4.5). There is only a 0.1 difference in $pH_{½}$, with the strip being slightly lower.

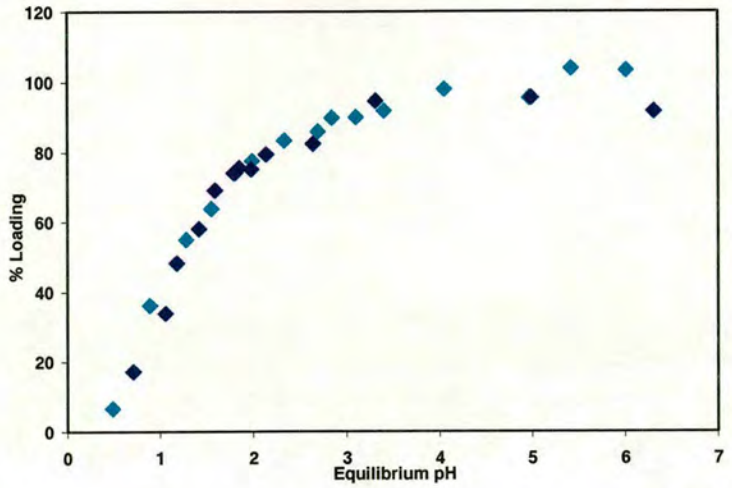

Figure 4.5: The pH-dependence of copper-loading (♦) by a 0.00250 M solution of ligand **10** and stripping from a 0.00250 M chloroform solution of $[Cu_2(\mathbf{10}\text{-}2H)_2]$ with 0.800 M aqueous sulfate solution (♦).

Sulfate loading by the ligand in the absence of copper and the loading in the presence of copper with an equimolar quantity and with an excess of sulfate are shown in Figure 4.6. As might be expected the sulfate loading at pH > 3 is less efficient when carried out with equimolar concentrations of copper and sulfate than with an excess of sulfate and the plateau of 100% loading in the pH region 1.5-5.0 is no longer observed.

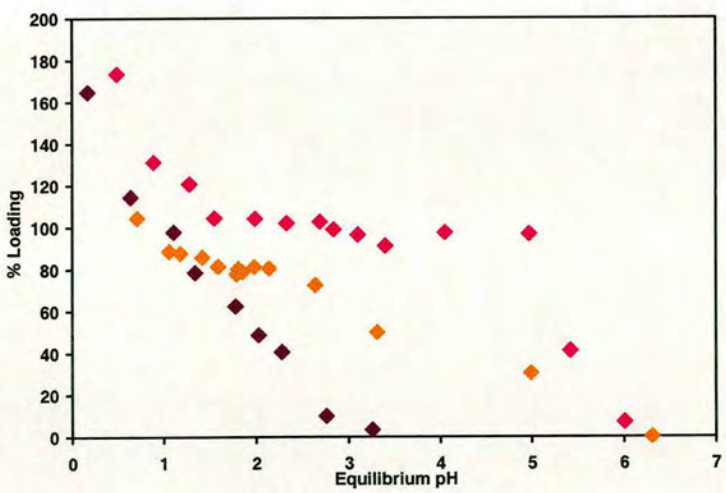

Figure 4.6: The pH-dependence of sulfate-loading (♦) by a 0.00250 M chloroform solution of **10** in the presence of an equimolar concentration of copper and stripping from a 0.00250 M chloroform solution of $[Cu_2(\mathbf{10}\text{-}2H)_2]$ with a 0.800 M aqueous sulfate solution (♦) compared to sulfate loading by a 0.00250 M solution of **10** from a 0.800 M aqueous sulfate solution in the absence of copper (♦).

The free ligand shows no sulfate uptake until the pH is less than 3.0 and then rises to greater than 100%, indicating that the system is capable of double protonation and transport of two hydrogen sulfate ions into the organic phase. The difference between the behaviour of the system in the presence and absence of copper strongly suggests that sulfate binding in the copper complex is cooperative, which is compatible with structures such as that proposed in Figure 4.7.

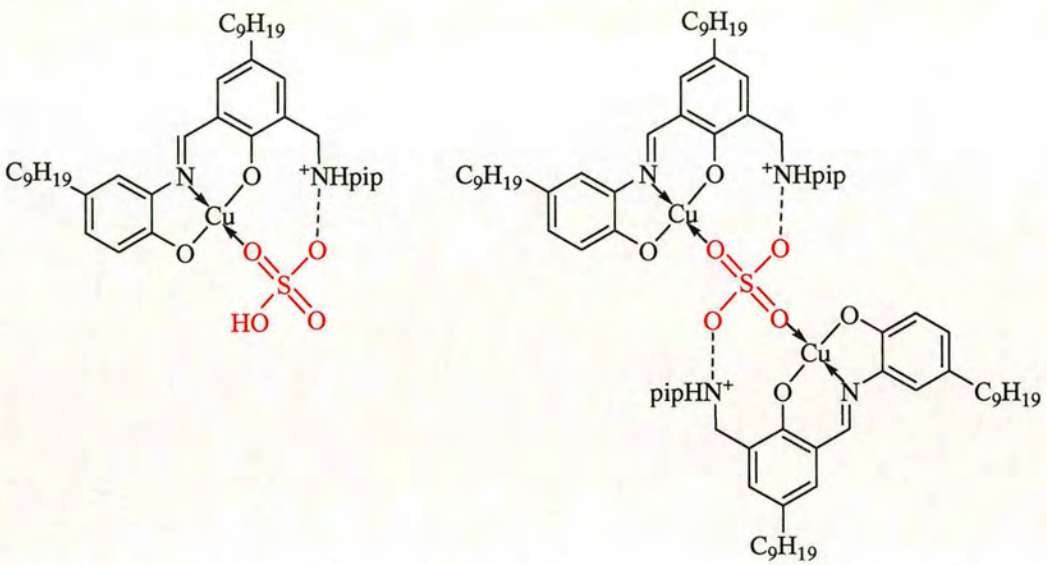

Figure 4.7: Proposed 1 : 1 : 1 structure of low pH and 2 : 2 : 1 structure of high pH extracted species with ligand **10**.

Ligand **10** has proven to be a successful copper sulfate extractant. It has a lower $pH_{½}$ than ligand **5**, and the stripping experiment showed an ideal plateau between pH 1.5-5 when both copper and sulfate are loaded at greater than 90%. Despite the difference in shape of the sulfate plots to those seen previously, the loading of sulfate remains dependent on the presence of ligand-bound copper.

4.3.3 EPR of extracted species

As it was assumed that complexes of ligand **10** in solution would behave similarly to those obtained with **5**, chloroform solutions of $[Cu_2(\mathbf{10}\text{-}2H)_2]$ after contact with sulfate solutions at a range of pH were taken for direct EPR analysis. The spectra obtained show the same pattern as before. From zero to around fifty percent copper-loading (pH = 0.0-1.5), there is a gradual increase in signal intensity, to a maximum at 55% loading (Figure 4.8). As the percentage loading of copper increases towards 100% and the pH is further increased, the signal intensity decreases (Figure 4.9).

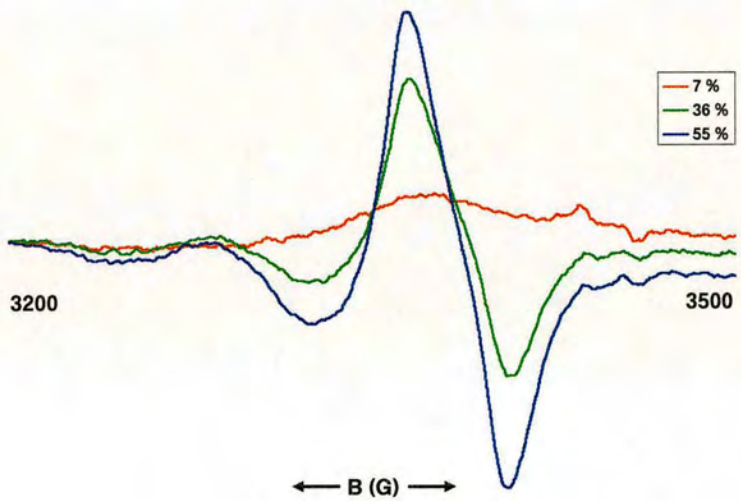

Figure 4.8: EPR spectra of the chloroform solutions of **10** as $[Cu_2(\mathbf{10}\text{-}H)_2SO_4]$ when a solution of $[Cu_2(\mathbf{10}\text{-}2H)_2]$ is contacted with varying pH sulfate solutions.
The key indicates the percentage of copper(II) remaining in the organic phase after contact with acidic sulfate solutions, as measured by ICP-OES.

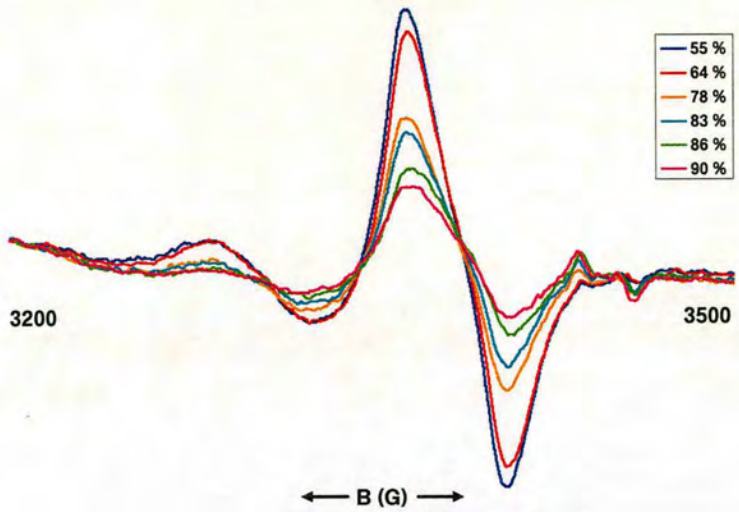

Figure 4.9: EPR spectra of the chloroform solutions of **10** as $[Cu_2(\mathbf{10}\text{-}H)_2SO_4]$ when a solution of $[Cu_2(\mathbf{10}\text{-}2H)_2]$ is contacted with varying pH sulfate solutions.

The key indicates the percentage of copper(II) remaining in the organic phase after contact with acidic sulfate solutions, as measured by ICP-OES.

These spectra support the assumption that at low pH and lower copper-loading, a mononuclear 1 : 1 : 1 complex involving hydrogen sulfate is formed (Figure 4.7, left). As the pH increases, the predominance of sulfate increases, and the complex can form dinuclear 2 : 2 : 1 species, such as that shown in Figure 4.7 (right). This species allows for coupling between the two copper centres through the sulfate anion and therefore, as its concentration increases relative to the mononuclear species, the signal is lost. This is in good agreement with the stripping plot, as at around 55% copper loading the sulfate loading starts to plateau at 100%, which is associated with this dinuclear complex.

4.4 Stability

4.4.1 Strip/load cycles

To evaluate the chemical stability of the ligands under conditions similar to those which would be used in a plant, a series of load and strip experiments were carried out. The ligand was made to a known concentration (0.00250 M) in chloroform and contacted with an excess of an aqueous (1.0 M) copper(II) sulfate solution to achieve maximum copper loading. The organic and aqueous layers were stirred at room temperature for 1 hour, before setting aside to separate. A small sample (1.0 ml) of the chloroform was removed for analysis for copper content using ICP-OES. The organic layer was then contacted with an aqueous sulfuric acid solution typical of electrolyte concentration (150 g l^{-1}), stirred for 1 hour, separated and a sample (1.0 ml) of the organic layer analysed for copper content. Two of these cycles were carried out for ligand **5** and three cycles were carried out for ligand **10**, with one extra loading experiment to finish.

With ligand **5**, 100% of the theoretical loading was observed for the initial load. However, after the first sulfuric acid contact, the ligand fails to reload any copper in subsequent loading steps (Figure 4.10). This result is indicative of ligand hydrolysis under the conditions used for stripping, the imine bond is protonated and the products of hydrolysis are the starting materials used to synthesis the ligand (Scheme 4.2). The solubility of these component parts is key at this stage, as if they are suitably organic soluble then, when the pH is increased again upon contact with copper sulfate solution, they could recombine and reform the ligand. It is probable that one or both of the precursors for ligand **5** are water-soluble under acid conditions, or recombination is not possible on the timescale of the experiment because no copper-loading was observed.

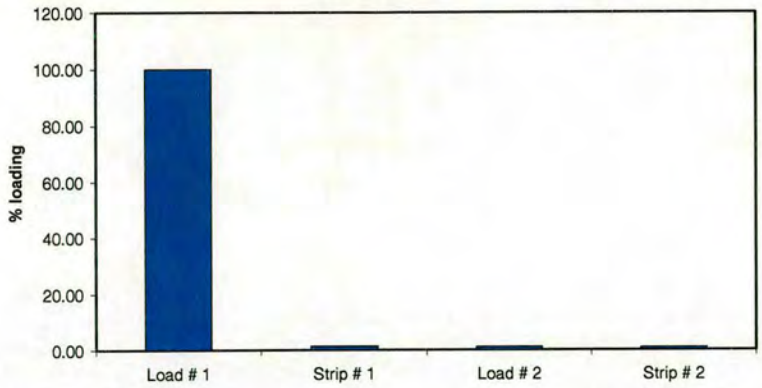

Figure 4.10: The percentage of copper in the organic phase during load/strip cycles performed on ligand **5**.

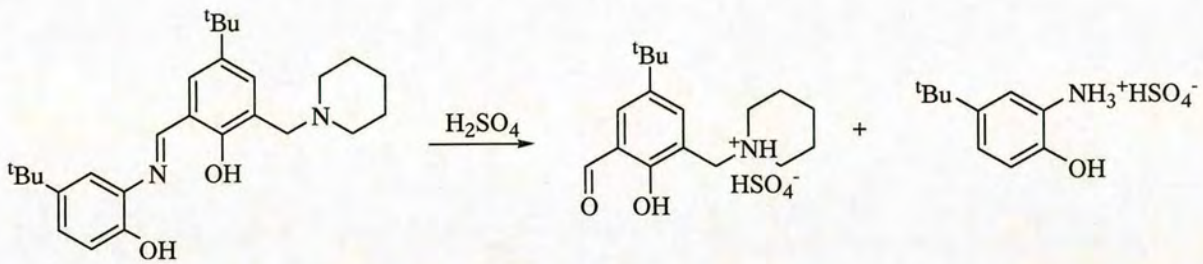

Scheme 4.2: Hydrolysis of ligand **5** under acidic conditions.

Repeating the load/strip cycles with ligand **10** gives strikingly different results, which are shown in Figure 4.11. Even after the first stripping cycle, 10% of the copper still remains in the organic layer. The second cycle then loads to just under 60%, which strips to about 5%. By the third load, only 40% of the initial ligand in solution loads copper, although the strip again only goes as low as 5% and the final loading step picks up 35%. Consequently, it can be assumed that the hydrophobic nonyl groups have a large influence on the organic solubility and probably the stability to hydrolysis under acid conditions of ligand **10**.

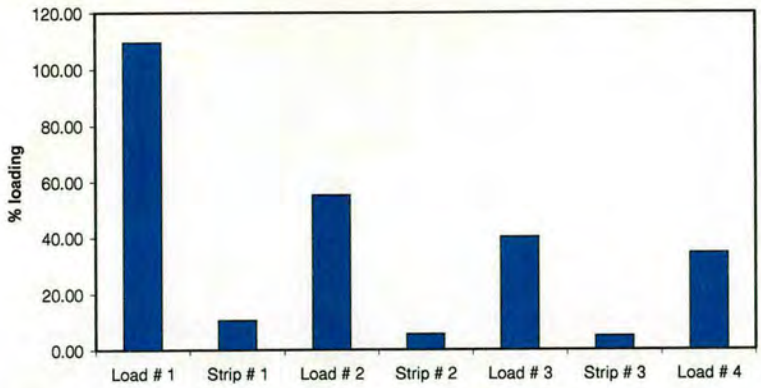

Figure 4.11: The percentage of copper in the organic phase during load/strip cycles performed on ligand **10**.

There clearly remains an issue of ligand hydrolysis despite this improvement in solubility, resulting in the gradual decrease in copper loading after each load/strip cycle. In order to probe this further, hydrolytic stability experiments can be carried out using sulfate-loading and NMR spectroscopy to quantify ligand breakdown. These studies are discussed in Section 4.4.2.

4.4.2 Ligand stability to hydrolysis

To investigate the stability of the free ligands at low pH, a solution of ligand (0.00250 M) in chloroform was contacted with a range of aqueous solutions with different pH but constant sulfate concentration (0.800 M) at room temperature for 16 hours. The organic layer was analysed for sulfate content and a 2.0 ml portion was dried *in vacuo* and dissolved in 1.0 ml deuterated chloroform for NMR analysis. The ratio of the integrals of the ligand's imine peak and the precursor aldehyde peak indicates the percentage of ligand intact. Figure 4.12 shows the sulfate loadings for ligand **5** resulting from this experiment. At low pH there is very little sulfate present, but on increasing pH the loading increases to a maximum of ~ 80% (100% represents 1 mol of sulfate per 2 mols of ligand). This appears to suggest that the ligand is not 100% intact at pH ranges in which sulfate can be extracted.

The pH dependence of sulfate loading is compared with results for ligand **10** in Figure 4.12. The marked differences at low pH where **10** shows high sulfate-loading can be attributed to the increased solubility of the ligand and/or its integral parts, as discussed previously (page 133).

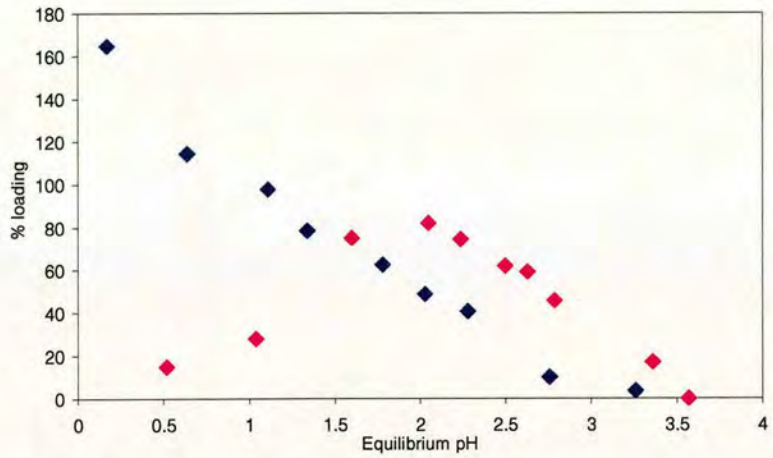

Figure 4.12: The pH-dependence of sulfate-loading by **5** (♦) and by **10** (♦) in the absence of copper.

NMR analysis of the organic phase containing ligand **5** shows the imine peak to be present at pH > 2.5, below which no imine signal is observed. The aldehyde peak begins to appear at pH < 3.5 and its integral increases in size relative to the imine peak, until the imine peak is no longer visible and only aldehyde signal is seen. Since there is never complete loss of the aldehyde signal, it may be assumed that it retains some organic solubility although this does not give a quantitative analysis of what percentage of the aldehyde is in the organic and/or aqueous phase.

The NMR data are in good agreement with the sulfate data (Figure 4.12), as the low sulfate loading in the organic layer at low pH indicates that the ligand is not 100% present, and the products of hydrolysis are either not able to pick up sulfate, or are water soluble and therefore in the aqueous layer. The ligand's inability to load copper after the strip cycle of the load/strip experiment can therefore be attributed to acid hydrolysis at the very low pH of the sulfuric acid solution. To improve hydrolytic stability, an alkyl substituent could be incorporated onto the carbon atom

of the imine, as has proved successful for "salen-type" ligands in previous work in the Tasker group.[5]

Ligand **10** appears to be much more stable to acid hydrolysis. There is evidence in the NMR spectrum for the imine peak as low as pH 0.2 when the ratio of imine to aldehyde peak is 1 : 1. This indicates that even at low pH, 50% of the initial ligand remains intact. It cannot be confirmed whether the sulfate loading in the organic layer is due to this intact ligand or whether the products of hydrolysis are loading the sulfate. This is also in good agreement with the results of the load/strip cycles discussed in section 4.4 where each cycle results in some loss of copper loading, assumingly due to ligand breakdown. There is, however, never complete loss of copper loading and hence it can be concluded that this is due to a proportion of the ligand remaining intact.

4.5 Selectivity

4.5.1 Copper(II) and iron(III)

As discussed in the introduction, selectivity is an important feature required of commercial extractants. Selectivity over iron is particularly important in copper recovery. For ligand **10** copper(II)/iron(III) selectivity was investigated by carrying out a loading experiment with an equal concentration of both copper and iron (0.00250 M) in the aqueous feed solution. The results can be seen in Figure 4.13. There is clearly no selectivity for copper. At low pH values (< 1.2) approximately equal concentrations of copper and iron are loaded. Iron is increasingly favoured as the pH is increased to ~ 2.7, after which the precipitation of iron(III)oxy/hydroxides from solution allows for an increase in copper loading. This lack of selectivity is clearly unsuitable for the recovery of copper from iron-containing feeds.

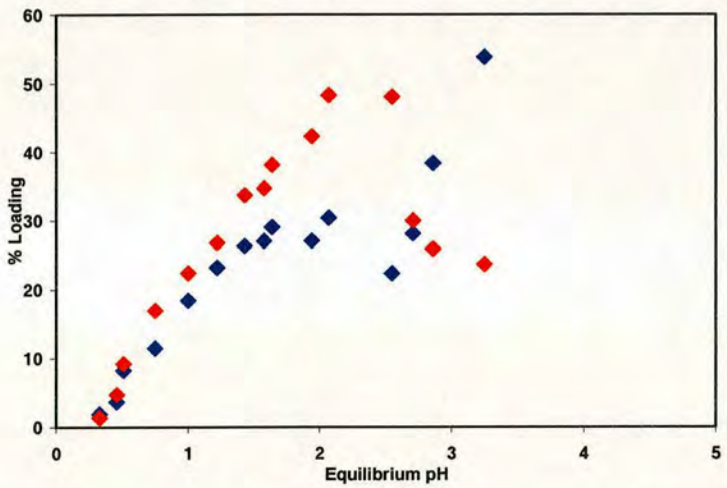

Figure 4.13: The pH-dependence of copper (♦) and iron-loading (♦) by a 0.00250 M chloroform solution of ligand **10** when both are present in equal concentrations (0.00250 M) in the aqueous layer as their sulfate salts.

4.5.2 Sulfate and chloride

In order to investigate whether ligand **10** will show a preference for loading chloride over sulfate in the presence of copper(II) salts, a chloroform solution (0.00250 M) of $[Cu_2(\mathbf{10}\text{-}2H)_2]$ was contacted with a series of different pH aqueous solutions containing equal concentrations (0.800 M) of chloride and sulfate anions at various pH values. The solutions were stirred for 16 hours then allowed to separate and the

organic layer analysed for copper and sulfate. The plots obtained are shown in Figure 4.14. The copper-loading plot is very similar to those reported previously, with a $pH_{½}$ of ~1.3. There is a dramatic drop in sulfate loading in the presence of chloride. It can therefore be assumed that the ligand preferentially loads chloride over sulfate. Chloride has a lower solvation energy in water than sulfate and most probably a more favourable solvation energy in chloroform, resulting in a large Hofmeister bias,[6, 7] as discussed in Chapter 3, section 3.4.1. This allows chloride to be extracted into chloroform more readily by ligand **10**. Chloride is also a better ligand for copper(II), as discussed in Chapter 3, section 3.4.6.

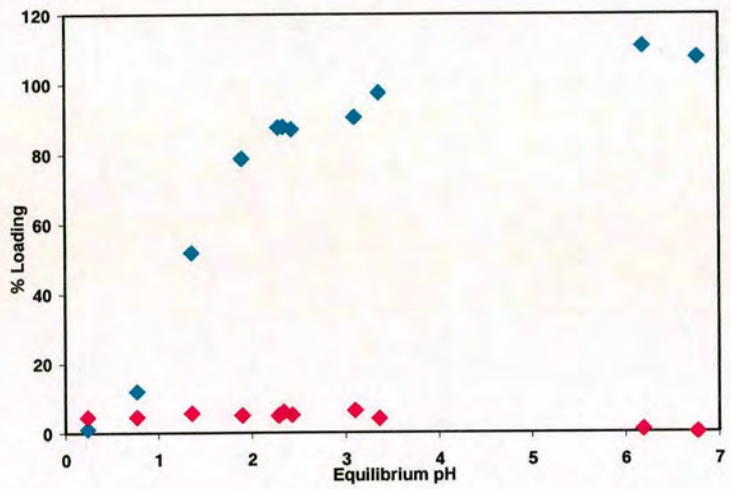

Figure 4.14: The pH-dependence of copper (♦) and sulfate-loading (♦) by chloroform solutions (0.00250 M) of ligand **10** when sulfate and chloride anions are present in equal concentrations (0.800 M) in aqueous solution.

4.6 Conclusions

The introduction of very hydrophobic nonyl substituents into the framework of ligand **5** improves its hydrolytic stability in chloroform but not sufficiently for it to be useable in commercial processes. It is probable, based on previous experiences[8] that the stability to hydrolysis will be substantially greater in high boiling hydrocarbon solvents of the types used in industry. It is also possible that stability could be enhanced by incorporating an alkyl substituent on the imine carbon atom, based on studies of "salen-type" ligands made by Galbraith *et al.*[5] Developmental work to increase the hydrolytic stability will only be useful if ligands can be identified which show better selectivity in metal recovery (see below).

Ligand **10** shows an almost ideal pH-profile for copper and sulfate loading but does not have the desirable feature which was apparent in **5** that *both* copper and sulfate can be stripped when the pH is lowered. The most problematic features of the new extractant, **10** are associated with its loading selectivity. At low pH it loads iron(III) very effectively. Given the donor set this is not very surprising since there is a predominance of oxygen donors, which are considered to be relatively hard bases, and iron is a hard acid, resulting in very favourable coordination.

On the basis of the preliminary experiments above, **10** will transport chloride from an aqueous feeds in preference to sulfate. This will have a very adverse effect on the processing of feeds which contain any significant levels of chloride impurity, for the reasons outlined in section 4.1. It is possible that the selectivity for chloride over sulfate could be put to advantage in circuits which operate in chloride media, such as the CUPREX process[9] which uses oxidative leaching of sulfidic ores with ferric chloride to produce pregnant leach solutions (containing mainly $CuCl_2$, $FeCl_2$, $FeCl_3$) as seen in Figure 4.15. A key feature for practicable use in such a circuit will be selectivity of transport of $CuCl_2$ over $FeCl_3$ or $FeCl_2$.

Leach	$4FeCl_3 + Cu_2S$	⟶	$4FeCl_2 + 2CuCl_2 + S\downarrow$
High Cl^- activity	$2CuCl_2 + 4\mathbf{L}_{(org)}$	⟶	$2Cu\mathbf{L}_2Cl_{2\,(org)}$
Low Cl^- activity	$2Cu\mathbf{L}_2Cl_{2\,(org)}$	⟶	$2CuCl_2 + 4\mathbf{L}_{(org)}$
Electrowin	$2CuCl_2$	⟶	$2Cu + 2Cl_2$
Overall	$\mathbf{Cu_2S_{(s)}}$	⟶	$\mathbf{2Cu^0_{(s)} + S_{(s)}}$

Figure 4.15: A simplified flowsheet and materials balance for the recovery of copper from sulfidic ores by oxidative chloride leaching, solvent extraction and electrowinning. [4]

4.7 References

1 J. Szymanowski, '*Hydroxyoximes and Copper Hydrometallurgy*', CRC Press, London, 1993.

2 A. Borowiak-Resterna, G. Kyuchoukov and J. Szymanowski, *International Solvent Extraction Conference*, Cape Town, South Africa, 2002.

3 J. Szymanowski and G. Kyuchoukov, *Canadian Metallurgical Quarterly*, 2002, **41**, 399.

4 P. A. Tasker, P. G. Plieger and L. C. West, *Comprehensive Coordination Chemistry II*, 2004, **9**, 759.

5 S. G. Galbraith, '*Ditopic Ligands for the Selective Solvent Extraction of Transition Metal Sulfates*', PhD thesis, University of Edinburgh, 2004.

6 K. Kavallieratos and B. A. Moyer, *Chemical Communications*, 2001, 1620.

7 T. G. Levitskaia, M. Marquez, J. L. Sessler, J. A. Shriver, T. Vercouter and B. A. Moyer, *Chemical communications*, 2003, 2248.

8 J. Campbell, *Cytec Industries Ltd*, 2007, personal communication.

9 R. F. Dalton, G. Diaz, R. Price and A. D. Zunkel, *The Journal of The Minerals, Metals & Materials Society*, 1991, **43**, 51.

CHAPTER 5

5 CHAPTER 5 148

5.1 Instrumentation 150

5.2 Ligand Synthesis 152

5.3 Metal complex synthesis 177

5.4 Liquid : liquid extraction experiments 180

5.4.1 Stripping 180

5.4.2 Loading 181

5.4.3 Load/Strip Cycles 182

5.4.4 Selectivity of copper(II)/ iron(III) 182

5.4.5 Selectivity of sulfate/chloride 182

5.5 X-ray Crystallography 183

5.6 EPR 183

5.1 Instrumentation

^{1}H nuclear magnetic resonance (NMR) spectra were recorded at ambient temperature (unless otherwise stated) on Bruker AC250 (250 MHz) and Bruker DPX360 (360 MHz) Fourier transform instruments. The data is presented as follows: chemical shift (in ppm on the δ scale relative to $\delta_{TMS} = 0$), multiplicity (s = singlet, d = doublet, t = triplet, q = quartet, m = multiplet, sept = septet, br = broad), coupling constant and interpretation. ^{13}C NMR spectra were recorded at ambient temperatures on Bruker AC250 (62.9 MHz) and DPX360 (90.7 MHz) Fourier transform instruments and were referenced to the solvent carbon peak. The data is presented as follows: chemical shift (in ppm on the δ scale) and assignment; and were confirmed by DEPT90 and DEPT135 experiments.

Infra-red spectra were recorded on a Perkin Elmer Paragon 100 FT-IR machine using 5 mm sodium chloride plates as Nujol mulls. The wavelengths of maximum absorbance (υ_{max}) are quoted in cm^{-1}.

Fast atom bombardment (FAB) mass spectra were obtained using a Kratos MS50TC mass spectrometer at The University of Edinburgh using a 3-nitrobenzyl alcohol (NOBA) or thioglycerol matrix. Elemental analysis was carried out on a Carlo Erba CHNS analyser at The University of St Andrews. CHN analyses of products obtained as oils and liquids have not been reported.

Inductively coupled plasma optical emission spectroscopy (ICP-OES) analysis was performed on a Perkin Elmer Optima 5300 DV. Data was processed using the software programme, WinLab32 for ICP-OES, version 3.0.0.0103, 2004.

The measurement of pH was carried out using an Orion 410A pH meter using a Thermo TR/CW711/TB pH electrode. Chloride analysis was carried out using an Orion 9617BNWP Thermo Electron Corporation ionplus Sure-Flow Chloride electrode

X-band EPR data were recorded on an X-band Bruker ER 200-D SRC spectrometer connected to a datalink 486DX desktop PC running EPR acquisition system version 2.42. A quartz flat cell was used.

Tlc was performed on Merck $60F_{245}$ (0.25 mm) glass silica plates and visualised by ultraviolet (UV) light. Flash column chromatography was carried out on Merck Kieselgel (Merck 9385) under positive pressure by means of a hand pump.

All commercially available materials were used as received. General laboratory solvents were of analytical reagent grade, laboratory reagent grade or HPLC grade. Solvents used for analytical purposes were of spectroscopic grade. Water used to make aqueous solutions was of high purity, purified using a Milli-Q® water purification system.

5.2 Ligand Synthesis

2-Hydroxy-5-*t*-butylbenzaldehyde

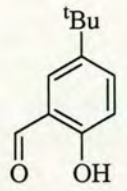

Magnesium turnings (19.5 g, 0.80 mol), methanol (370 ml), toluene (160 ml) and magnesium methoxide (a few drops of 8% w/w solution in methanol) were heated at reflux for 2 hours until the magnesium had dissolved and H_2 evolution had ceased. 4-*t*-Butylphenol (200 g, 1.30 mol) was added and the reaction refluxed for a further hour. Toluene (330 ml) was added and the mixture distilled (1 mm Hg, 120 °C) to remove the methanol-toluene azeotrope. A slurry of paraformaldehyde (120 g, 4.00 mol) in toluene (200 ml) was added slowly over 2 hours with continuous distillation. Once the addition was complete distillation was continued for a further 2 hours to remove solvent. After cooling the solution to 25 °C, cold H_2SO_4 (20%, 800 ml) was added slowly and the mixture stirred at 50 °C for 2 hours. The aqueous layer was separated and extracted with toluene (2 x 400 ml). The combined organic extracts were washed with H_2SO_4 (10%, 2 x 130 ml) and water (100 ml), dried over magnesium sulfate, reduced *in vacuo* and distilled (1 mm Hg, 120 °C). The yellow oil obtained was purified by column chromatography on silica gel, eluting with 5% ethyl acetate in hexane. The solution was dried *in vacuo* to yield a yellow oil (150 g, 65%); ν_{max}/cm^{-1} (neat) 3200 (OH), 1698 (C=O), 1515 (Ar C=C), 1395 (^tBu CH_3); ^1H NMR (250 MHz, $CDCl_3$) δ 10.69 (s, 1H, O*H*), 9.71 (s, 1H, C*H*O), 7.41 (d, 1H, *J* 2.5 Hz, Ar*H*), 7.34 (d, 1H, *J* 2.5 Hz, Ar*H*), 6.76 (d, 1H, *J* 8.6 Hz, Ar*H*), 1.12 (s, 9H, $(CH_3)_3C$); ^{13}C NMR (250 MHz, $CDCl_3$) δ 196.7 (*C*HO), 159.4 (Ar*C*), 142.6 (Ar*C*), 134.6 (Ar*C*), 129.6 (Ar*C*), 119.9 (Ar*C*), 117.1 (Ar*C*), 33.9 ($C(CH_3)_3$), 31.1 ($C(CH_3)_3$); FAB MS, *m/z* 179 (MH^+).

Ligand 1

4-*t*-Butyl-2-{[(*E*)-5-*t*-butyl-2-hydroxy-phenylimino]methyl}-phenol

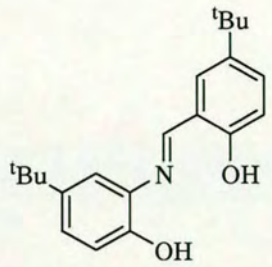

A solution of 2-amino-4-*t*-butylphenol (2.00 g, 12.1 mmol) and 2-hydoxy-5-*t*-butylbenzaldehyde (2.20 g, 12.1 mmol) in methanol (50 ml) was stirred for 4 hours. The resulting yellow solid was collected by filtration and a second crop obtained by reducing the mother liquor to *ca.* 10 ml. The product is obtained by filtration as an orange solid. Recrystallisation from methanol yielded orange crystals suitable for crystallography (1.90 g, 49%); ν_{max}/cm^{-1} (nujol) 3153 (OH), 1624 (N=C), 1376 (^tBu CH_3); (Anal. Calc. for $C_{21}H_{27}NO_2$ (crystals ground and dried): C, 77.5; H, 8.4; N, 4.3. Found: C, 77.2; H, 8.7; N, 4.3%); ^1H NMR (250 MHz, $CDCl_3$) δ 8.90 (s, 1H, ArC*H*N), 7.69-7.64 (m, 2H, 2 x Ar*H*), 7.45 (dd, 1H, *J* 8.5, 2.3 Hz, Ar*H*), 7.34 (d, 1H, *J* 2.3 Hz, Ar*H*), 7.20 (d, 1H, *J* 8.5 Hz, Ar*H*), 7.16 (d, 1H, *J* 8.5 Hz, Ar*H*), 1.27 (s, 18H, 2 x C(CH_3)$_3$); ^{13}C NMR (250 MHz, $CDCl_3$) δ 163.9 (Ar*C*HN), 158.2 (Ar*C*), 147.3 (Ar*C*), 143.9 (Ar*C*), 142.2 (Ar*C*), 135.1 (Ar*C*), 131.0 (Ar*C*), 128.9 (Ar*C*), 125.4 (Ar*C*), 118.5 (Ar*C*), 116.7 (Ar*C*), 115.1 (2 x Ar*C*), 34.3 (*C*(CH_3)$_3$), 33.9 (*C*(CH_3)$_3$), 31.4 (C(*C*H_3)$_3$), 31.3 (C(*C*H_3)$_3$); FAB MS, *m/z* 326 (MH^+).

_N_-Ethoxymethyldihexylamine

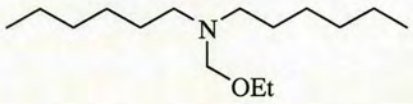

To a stirred suspension of paraformaldehyde (12.0 g, 400 mmol) and potassium carbonate (85.5 g, 620 mmol) in ethanol (1.5 l) at 0 °C was added dihexylamine (60.0 g, 320 mmol). The suspension was allowed to warm to room temperature and stirred for 3 days. The suspension was filtered and the filtrate concentrated *in vacuo*. Distillation (0.5 mm Hg, 138 °C) gave the product as a colourless oil (62.0 g, 79%); ^{1}H NMR (250 MHz, $CDCl_3$) δ 4.08 (s, 2H, $CH_2OCH_2CH_3$), 3.37 (q, 2H, *J* 7.0 Hz, $CH_2OCH_2CH_3$), 2.52 (t, 4H, *J* 7.4 Hz, 2 x $NCH_2(CH_2)_4CH_3$), 1.40-1.30 (m, 4H, 2 x $NCH_2CH_2(CH_2)_3CH_3$), 1.27-1.14 (m, 12H, 2 x $NCH_2CH_2(CH_2)_3CH_3$), 1.11 (t, 3H, *J* 7.0 Hz, $CH_2OCH_2CH_3$), 0.81 (t, 6H, *J* 6.6 Hz, 2 x $N(CH_2)_5CH_3$); ^{13}C NMR (250 MHz, $CDCl_3$) δ 85.2 (NCH_2O), 63.1 (OCH_2CH_3), 51.9 (2 x NCH_2CH_2), 31.7 (2 x NCH_2CH_2), 28.1 (2 x $N(CH_2)_2CH_2(CH_2)_2CH_3$), 27.0 (2 x $N(CH_2)_3CH_2CH_2CH_3$), 22.6 (2 x $N(CH_2)_4CH_2CH_3$), 15.2 (OCH_2CH_3), 14.0 (2 x $N(CH_2)_5CH_3$); FAB MS, *m/z* 244 (MH^+).

2-Hydroxy-3-dihexylaminomethyl-5-t-butyl-benzaldehyde

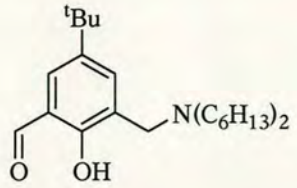

A solution of 2-hydroxy-5-*t*-butylbenzaldehyde (20.0 g, 112 mmol) and *N*-ethoxymethyldihexylamine (27.3 g, 112 mmol) in acetonitrile (400 ml) was stirred at reflux under a flow of nitrogen for 6 days. The product was obtained as an orange oil after removal of the acetonitrile *in vacuo*. The orange oil obtained was purified by column chromatography on silica gel, eluting with 10% ethyl acetate in hexane. The solution was concentrated and dried *in vacuo* to yield a yellow oil (24.8 g, 60%); ν_{max}/cm^{-1} (neat) 3200 (OH), 1679 (C=O), 1379 (^tBu CH_3); (Anal. Calc. for $C_{24}H_{41}NO_2$: C, 76.8; H, 11.0; N, 3.7. Found: C, 76.5; H, 11.3; N, 4.0%); ^1H NMR (250 MHz, $CDCl_3$) δ 10.35 (s, 1H, C*H*O), 7.58 (d, 1H, *J* 2.6 Hz, Ar*H*), 7.20 (s, 1H, Ar*H*), 3.73 (s, 2H, ArCH_2N), 2.45 (t, 4H, *J* 7.6 Hz, 2 x NC$H_2$$CH_2$), 1.48-1.44 (m, 4H, 2 x NCH_2CH_2), 1.26-1.17 (m, 21H, C(CH_3)$_3$, 2 x $NCH_2CH_2(CH_2)_3CH_3$), 0.80 (t, 6H, *J* 3.3 Hz, 2 x $N(CH_2)_5CH_3$); ^{13}C NMR (250 MHz, $CDCl_3$) δ 196.5 (*C*HO), 159.9 (Ar*C*), 141.3 (Ar*C*), 132.3 (Ar*C*), 123.6 (Ar*C*), 123.3 (Ar*C*), 122.1 (Ar*C*), 56.9 ($CH_2N(CH_2)_5CH_3$), 53.3 (2 x NCH_2CH_2), 33.9 ($C(CH_3)_3$), 31.4 (2 x NCH_2CH_2), 31.2 ($C(CH_3)_3$), 26.8 (2 x $N(CH_2)_2CH_2(CH_2)_2CH_3$), 25.9 (2 x $N(CH_2)_3CH_2CH_2CH_3$), 22.4 (2 x $N(CH_2)_4CH_2CH_3$), 13.8 (2 x $N(CH_2)_5CH_3$); FAB MS, *m/z* 376 (MH^+).

Ligand 2

4-*t*-Butyl-2-{[(*E*)-5-*t*-butyl-2-hydroxy-phenylimino]-methyl}-6-dihexylaminomethyl-phenol

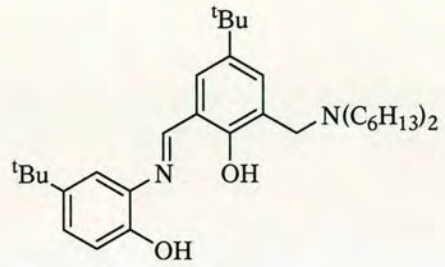

A solution of 2-amino-4-*t*-butylphenol (1.10 g, 6.70 mmol) and 2-hydroxy-3-dihexylaminomethyl-5-*t*-butyl-benzaldehyde (2.50 g, 6.70 mmol) in methanol (100 ml) was stirred for 2 hours. The resulting solution was concentrated and dried *in vacuo* to give a viscous red oil (3.40 g, 96%); ν_{max}/cm^{-1} (nujol) 3398 (OH), 1619 (N=C), 1363 (^tBu CH_3); ^1H NMR (250 MHz, $CDCl_3$) δ 9.03 (s, 1H, ArC*H*N), 7.21-7.19 (m, 2H, 2 x Ar*H*), 7.14-7.10 (m, 2H, 2 x Ar*H*), 6.86 (d, 1H, *J* 8.5 Hz, Ar*H*), 3.72 (s, 2H, ArCH_2N), 2.46 (t, 4H, *J* 7.6 Hz, 2 x NC$H_2$$CH_2$), 1.50-1.49 (m, 4H, 2 x NCH_2CH_2), 1.26-1.18 (m, 30H, C(CH_3)$_3$, 2 x $NCH_2CH_2(CH_2)_3CH_3$), 0.82-0.77 (m, 6H, 2 x $N(CH_2)_5CH_3$); ^{13}C NMR (250 MHz, $CDCl_3$) δ 160.0 (Ar*C*HN), 157.3 (Ar*C*), 149.2 (Ar*C*), 142.9 (Ar*C*), 141.5 (Ar*C*), 135.8 (Ar*C*), 129.5 (Ar*C*), 124.9 (Ar*C*), 122.9 (Ar*C*), 122.3 (Ar*C*), 121.4 (Ar*C*), 113.9 (Ar*C*), 113.4 (Ar*C*), 57.0 (ArCH_2N), 53.4 (2 x NCH_2CH_2), 34.1 (2 x *C*(CH_3)$_3$), 31.4 (2 x NCH_2CH_2), 31.2 (2 x C(CH_3)$_3$), 26.9 (2 x $N(CH_2)_2CH_2(CH_2)_2CH_3$), 26.0 (2 x $N(CH_2)_3CH_2CH_2CH_3$), 22.5 (2 x $N(CH_2)_4CH_2CH_3$), 13.9 (2 x $N(CH_2)_5CH_3$); FAB MS, *m/z* 523 (MH^+).

_N_-(_t_-butoxycarbonyl)-2-amino-4-_t_-butyl-phenol

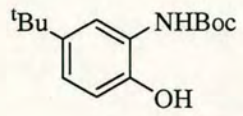

A solution of 2-amino-4-_t_-butylphenol (3.00 g, 18.2 mmol) and di-_t_-butylcarbonate (4.00 g, 18.2 mmol) in THF (100 ml) was stirred at room temperature for 2 hours. The solution was concentrated to *ca.* 10 ml, water (20 ml) added and extracted with ethyl acetate (4 x 50 ml). The solution was dried over magnesium sulfate, filtered and the solvent removed *in vacuo*. The brown powder obtained was recrystallised from hexane to yield a pale brown crystalline material (4.80 g, 99%); ν_{max}/cm^{-1} (nujol) 3391 (OH), 1696 (C=O), 1604 (NH), 1376 (^{t}Bu CH_3); (Anal. Calc. for $C_{15}H_{23}NO_3$: C, 67.9; H, 8.7; N, 5.3. Found: C, 68.1; H, 9.0; N, 5.3%); ^{1}H NMR (250 MHz, $CDCl_3$) δ 8.06 (br s, 1H, N*H*), 7.10 (dd, 1H, *J* 8.4, 2.0 Hz, Ar*H*), 6.84 (d, 1H, *J* 8.4 Hz, Ar*H*), 6.57 (br s, 1H, Ar*H*), 1.45 (s, 9H, $OC(CH_3)_3$), 1.19 (s, 9H, $ArC(CH_3)_3$); ^{13}C NMR (250 MHz, $CDCl_3$) δ 155.2 (*C*=O), 145.2 (Ar*C*), 143.7 (Ar*C*), 124.5 (Ar*C*), 122.7 (Ar*C*), 118.5 (2 x Ar*C*), 81.9 ($OC(CH_3)_3$), 33.9 ($ArC(CH_3)_3$), 31.3 ($OC(CH_3)_3$), 28.2 ($ArC(CH_3)_3$); FAB MS, *m/z* 266 (MH^+).

N-(*t*-butoxycarbonyl)-2-amino-4-*t*-butyl-6-dihexylaminomethyl-phenol

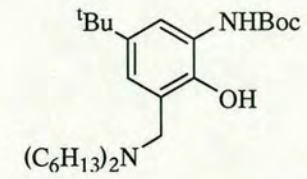

A solution of *N*-(*t*-butoxycarbonyl)-2-amino-4-*t*-butyl-phenol (4.60 g, 17.5 mmol) and *N*-ethoxymethyldihexylamine (4.30 g, 17.5 mmol) was stirred at reflux in acetonitrile (50 ml) for 7 days. The resulting solution was concentrated and dried *in vacuo* to yield an orange oil and used without further purification in the following synthesis ν_{max}/cm^{-1} (nujol) 3430 (OH), 1731 (C=O), 1606 (NH), 1528 (Ar C=C), 1366 (^tBu CH_3); (Anal. Calc. for $C_{28}H_{50}N_2O_3$: C, 72.7; H, 10.9; N, 6.1. Found: C, 72.9; H, 11.2; N, 6.0%); ^1H NMR (250 MHz, $CDCl_3$) δ 6.99 (s, 1H, Ar*H*), 6.53 (d, 1H, *J* 2.3 Hz, Ar*H*), 3.65 (s, 2H, ArCH_2N), 2.41 (t, 4H, *J* 7.6 Hz, 2 x NCH_2CH_2), 1.44-1.39 (m, 13H, 2 x NCH_2CH_2, $OC(CH_3)_3$), 1.24-1.18 (m, 21H, $ArC(CH_3)_3$, 2 x $NCH_2CH_2(CH_2)_3CH_3$), 0.82-0.78 (m, 6H, 2 x $N(CH_2)_5CH_3$); ^{13}C NMR (250 MHz, $CDCl_3$) δ 152.9 (*C*=O), 143.7 (Ar*C*), 141.6 (Ar*C*), 126.2 (Ar*C*), 119.8 (Ar*C*), 118.1 (Ar*C*), 114.1 (Ar*C*), 67.9 ($OC(CH_3)_3$), 58.3 (ArCH_2N), 53.3 (2 x NCH_2CH_2), 34.2 ($ArC(CH_3)_3$), 31.4 ($OC(CH_3)_3$), 28.3 ($ArC(CH_3)_3$), 26.9 (2 x NCH_2CH_2), 26.2 (2 x $N(CH_2)_2CH_2(CH_2)_2CH_3$), 25.4 (2 x $N(CH_2)_3CH_2CH_2CH_3$), 22.4 (2 x $N(CH_2)_4CH_2CH_3$), 13.9 (2 x $N(CH_2)_5CH_3$); FAB MS, *m/z* 462 (MH^+).

2-Amino-4-*t*-butyl-6-dihexylaminomethyl-phenol

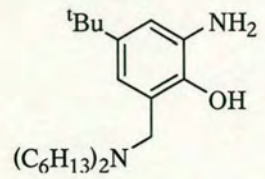

N-(*t*-butoxycarbonyl)-2-amino-4-*t*-butyl-6-dihexylaminomethyl-phenol (2.00 g, 4.30 mmol) was treated with a 1:1 mixture of chloroform and trifluoroacetic acid (50 ml). After stirring for 2 hours, the mixture was reduced to minimum volume and dried *in vacuo*. The resulting oil was resuspended in ethyl acetate (50 ml) and washed with 0.1 M NaOH solution (4 x 50 ml). The organic layer was separated, dried over magnesium sulfate, concentrated and dried *in vacuo* to yield an orange oil (0.80 g, 52%); ν_{max}/cm^{-1} (nujol) 3397 (OH), 1512 (Ar C=C), 1377 (^tBu CH_3); 1H NMR (250 MHz, $CDCl_3$) δ 7.95 (s, 2H, NH_2) 6.60 (d, 1H, *J* 2.3 Hz, Ar*H*), 6.31 (d, 1H, *J* 2.2 Hz, Ar*H*), 3.62 (s, 2H, $ArCH_2N$), 2.42 (t, 4H, *J* 7.2 Hz, 2 x NCH_2CH_2), 1.45-1.39 (m, 4H, 2 x NCH_2CH_2), 1.21-1.17 (m, 21H, $C(CH_3)_3$, 2 x $NCH_2CH_2(CH_2)_3CH_3$), 0.83-0.77 (m, 6H, 2 x $N(CH_2)_5CH_3$); 13C NMR (250 MHz, $CDCl_3$) δ 143.2 (Ar*C*), 141.6 (Ar*C*), 133.7 (Ar*C*), 120.6 (Ar*C*), 114.9 (Ar*C*), 111.7 (Ar*C*), 58.3 ($ArCH_2N$), 53.3 (2 x NCH_2CH_2), 33.8 ($C(CH_3)_3$), 31.5 (2 x NCH_2CH_2), 31.3 ($C(CH_3)_3$), 26.8 (2 x $N(CH_2)_2CH_2(CH_2)_2CH_3$), 26.1 (2 x $N(CH_2)_3CH_2CH_2CH_3$), 22.4 (2 x $N(CH_2)_4CH_2CH_3$), 13.9 (2 x $N(CH_2)_5CH_3$); FAB MS, m/z 363 (MH^+).

Ligand 3

4-*t*-Butyl-2-{[(*E*)-5-*t*-butyl-2-hydroxy-phenylimino]-methyl}-6-dihexylaminomethyl-phenol

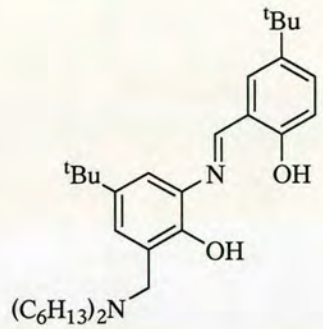

A solution of 2-amino-4-*t*-butyl-6-dihexylaminomethyl-phenol (1.90 g, 5.20 mmol) and 2-hydroxy-5-*t*-butylbenzaldehyde (0.90 g, 5.20 mmol) was stirred in methanol (100 ml) for 2 hours. The resulting solution was concentrated and dried *in vacuo* to yield a viscous red oil (2.40 g, 89%); ν_{max}/cm^{-1} (nujol) 3379 (OH), 1617 (N=C), 1365 (^tBu CH_3); ^1H NMR (250 MHz, $CDCl_3$) δ 8.86 (s, 1H, ArC*H*N), 7.51 (dd, 1H, *J* 8.7, 2.5 Hz, Ar*H*), 7.44 (d, 1H, *J* 2.5 Hz, Ar*H*), 7.06 (d, 1H, *J* 2.4 Hz, Ar*H*), 6.87 (dd, 1H, *J* 3.7, 2.1 Hz, Ar*H*), 6.79 (d, 1H, *J* 2.4 Hz, Ar*H*), 3.71 (s, 2H, ArCH_2N), 2.44 (t, 4H, *J* 7.7 Hz, 2 x NC$H_2$$CH_2$), 1.57-1.47 (m, 4H, 2 x NCH_2CH_2), 1.26-1.17 (m, 30H, 2 x $C(CH_3)_3$, 2 x $NCH_2CH_2(CH_2)_3CH_3$), 0.81-0.78 (m, 6H, 2 x $N(CH_2)_5CH_3$); ^{13}C NMR (250 MHz, $CDCl_3$) δ 159.4 (Ar*C*HN), 149.2 (Ar*C*), 141.5 (Ar*C*), 134.1 (Ar*C*), 129.6 (Ar*C*), 128.1 (Ar*C*), 123.4 (Ar*C*), 122.6 (Ar*C*), 119.9 (Ar*C*), 118.8 (Ar*C*), 118.0 (Ar*C*), 117.1 (Ar*C*), 116.2 (Ar*C*), 58.4 (ArCH_2N), 53.3 (2 x NCH_2CH_2), 33.9 (2 x $C(CH_3)_3$), 31.5 (2 x NCH_2CH_2), 31.2 (2 x $C(CH_3)_3$), 26.9 (2 x $N(CH_2)_2CH_2(CH_2)_2CH_3$), 25.9 (2 x $N(CH_2)_3CH_2CH_2CH_3$), 22.4 (2 x $N(CH_2)_4CH_2CH_3$), 13.9 (2 x $N(CH_2)_5CH_3$); FAB MS, *m/z* 523 (MH^+).

Ligand 4

4-*t*-Butyl-2-{[(*E*)-5-*t*-butyl-3-dihexylaminomethyl-2-hydroxy-phenylimino]-methyl}-6-dihexylaminomethyl-phenol

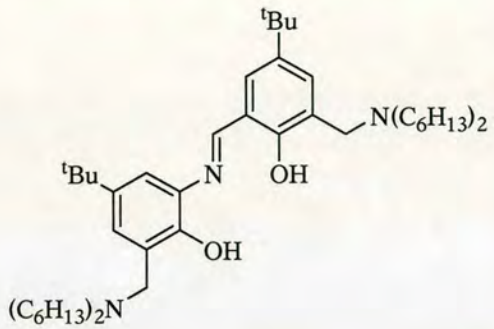

A solution of 2-amino-4-*t*-butyl-6-dihexylaminomethyl-phenol (0.50 g, 1.40 mmol) and 2-hydroxy-3-dihexylaminomethyl-5-*t*-butyl-benzaldehyde (0.52 g, 1.40 mmol) was stirred in methanol (60 ml) for 2 hours. The resulting solution was concentrated and dried *in vacuo* to yield a viscous red oil (0.80 g, 81%); ν_{max}/cm^{-1} (nujol) 3367 (OH), 1604 (N=C), 1364 (^tBu CH_3); ^1H NMR (250 MHz, $CDCl_3$) δ 8.88 (s, 1H, ArC*H*N), 7.58 (d, 1H, *J* 2.5 Hz, *ArH*), 7.26 (d, 1H, *J* 2.3 Hz, *ArH*), 7.05 (d, 1H, *J* 2.5 Hz, Ar*H*), 6.76 (d, 1H, *J* 2.3 Hz, Ar*H*), 3.72 (s, 4H, 2 x ArCH_2N), 2.42 (t, 8H, *J* 7.6 Hz, 4 x NCH_2CH_2), 1.46-1.45 (m, 8H, 4 x NCH_2CH_2), 1.32-1.17 (m, 42H, 2 x $C(CH_3)_3$, 4 x $NCH_2CH_2(CH_2)_3CH_3$), 0.82-0.77 (m, 12H, 4 x $N(CH_2)_5CH_3$); ^{13}C NMR (250 MHz, $CDCl_3$) δ 162.5 (Ar*C*HN), 160.0 (Ar*C*), 157.8 (Ar*C*), 149.1 (Ar*C*), 141.4 (Ar*C*), 141.2 (Ar*C*), 140.4 (Ar*C*), 132.0 (Ar*C*), 123.4 (Ar*C*), 122.5 (Ar*C*), 122.2 (Ar*C*), 118.7 (Ar*C*), 118.0 (Ar*C*), 53.3 (4 x N*C*H_2CH_2), 33.9 (2 x *C*$(CH_3)_3$), 31.5 (4 x NCH_2CH_2), 31.2 (2 x $C(CH_3)_3$), 26.9 (4 x $N(CH_2)_2CH_2(CH_2)_2CH_3$), 26.1 (4 x $N(CH_2)_3CH_2CH_2CH_3$), 22.4 (4 x $N(CH_2)_4CH_2CH_3$), 13.9 (4 x $N(CH_2)_5CH_3$); FAB MS, *m/z* 720 (MH^+).

1-Ethoxymethylpiperidine

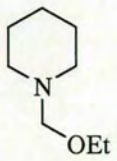

To a stirred suspension of paraformaldehyde (12.1 g, 400 mmol) and potassium carbonate (59.5 g, 430 mmol) in ethanol (1.5 l) at 0 °C was added piperidine (27.4 g, 320 mmol). The suspension was allowed to warm to room temperature and stirred for 3 days. The product was filtered and the solvent removed *in vacuo*. Distillation (0.5 mm Hg, 138 °C) gave the product as a colourless liquid (19.8 g, 43%); ^{1}H NMR (250 MHz, $CDCl_3$) δ 3.94 (s, 2H, NCH_2O), 3.37 (q, 2H, *J* 7.0 Hz, OCH_2CH_3), 2.53 (t, 4H, *J* 5.2 Hz, 2 x $NCH_2CH_2CH_2$), 1.50-1.42 (m, 4H, 2 x $NCH_2CH_2CH_2$), 1.36-1.30 (m, 2H, $NCH_2CH_2CH_2$), 1.08 (t, 3H, *J* 7.0 Hz, CH_3); ^{13}C NMR (250 MHz, $CDCl_3$) δ 88.5 (NCH_2O), 63.5 (OCH_2CH_3), 50.0 (2 x $NCH_2CH_2CH_2$), 25.0 (2 x $NCH_2CH_2CH_2$), 23.0 ($NCH_2CH_2CH_2$), 17.5 (OCH_2CH_3); FAB MS, *m/z* 144 (MH^+).

2-Hydroxy-3-piperidinyl-5-*t*-butyl-benzaldehyde

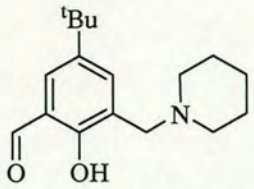

A solution of 2-hydroxy-5-*t*-butylbenzaldehyde (12.1 g, 84.0 mmol) and 1-ethoxymethylpiperidine (15.0 g, 84.0 mmol) in acetonitrile (400 ml) was stirred at reflux under a flow of nitrogen for 5 days. The product was obtained as a colourless powder after drying *in vacuo*. The colourless powder was purified by recrystallisation from hexane to yield a colourless crystalline material (16.2 g, 71%); ν_{max}/cm^{-1} (nujol) 3198 (OH), 1687 (C=O), 1377 (^tBu CH_3); (Anal. Calc. for $C_{17}H_{25}NO_2$: C, 74.1; H, 9.2; N, 5.1. Found: C, 74.4; H, 9.3; N, 5.2%); ^1H NMR (250 MHz, $CDCl_3$) δ 10.45 (s, 1H, C*H*O), 7.70 (d, 1H, *J* 2.6 Hz, Ar*H*), 7.31 (s, 1H, Ar*H*), 3.77 (s, 2H, ArCH_2N), 2.61 (s, 4H, 2 x NCH_2CH_2), 1.72 (t, 4H, *J* 5.4 Hz, 2 x NCH$_2$CH_2), 1.56 (d, 2H, *J* 8.4 Hz, NCH$_2$CH$_2$CH_2), 1.33 (s, 9H, C(CH_3)$_3$); ^{13}C NMR (250 MHz, $CDCl_3$) δ 191.6 (*C*HO), 160.3 (Ar*C*), 141.9 (Ar*C*), 132.8 (Ar*C*), 124.3 (Ar*C*), 123.1 (Ar*C*), 122.7 (Ar*C*), 61.7 (Ar*C*H$_2$N), 54.3 (2 x NCH_2CH$_2$), 34.5 (*C*(CH$_3$)$_3$), 31.7 (C(*C*H$_3$)$_3$), 26.1 (2 x NCH$_2$CH_2), 24.2 (NCH$_2$CH$_2$CH_2); FAB MS, *m/z* 276 (MH^+).

Ligand 5

4-*t*-Butyl-2-{[(*E*)-5-*t*-butyl-2-hydroxy-phenylimino]-methyl}-6-piperidinyl-phenol

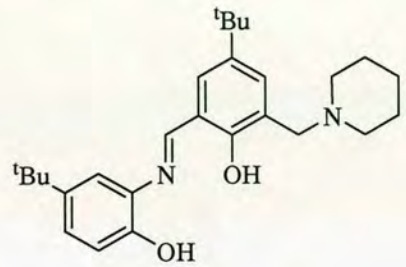

A solution of 2-amino-4-*t*-butylphenol (0.27 g, 1.60 mmol) and 2-hydroxy-3-piperidinylaminomethyl-5-*t*-butyl-benzaldehyde (0.45 g, 1.60 mmol) in methanol (75 ml) was stirred for 24 hours. The resulting solution was concentrated and dried *in vacuo* to give yellow solid. The solid was recrystallised from methanol to give yellow/orange crystals (0.48 g, 72%); ν_{max}/cm^{-1} (nujol) 3212 (OH), 1617 (N=C), 1377 (^tBu CH_3); (Anal. Calc. for $C_{27}H_{38}N_2O_2$: C, 76.7; H, 9.1; N, 6.6. Found: C, 76.5; H, 9.1; N, 6.8%); ^1H NMR (250 MHz, $CDCl_3$) δ 9.02 (s, 1H, ArC*H*N), 7.81 (d, 2H, *J* 2.5 Hz, 2 x Ar*H*), 7.14 (d, 2H, *J* 2.3 Hz, 2 x Ar*H*), 6.85 (d, 1H, *J* 8.4 Hz, Ar*H*), 3.64 (s, 2H, ArCH_2N), 2.48 (br s, 4H, 2 x NC$H_2$$CH_2$), 1.64-1.41 (m, 4H, 2 x NCH_2CH_2), 1.45-1.41 (m, 2H, $NCH_2CH_2CH_2$), 1.26 (s, 9H, C(CH_3)$_3$), 1.25 (s, 9H, (CH_3)$_3$C); ^{13}C NMR (250 MHz, $CDCl_3$) δ 157.2 (Ar*C*HN), 155.3 (Ar*C*), 149.2 (Ar*C*), 142.9 (Ar*C*), 141.5 (Ar*C*), 135.8 (Ar*C*), 129.6 (Ar*C*), 124.9 (Ar*C*), 123.2 (Ar*C*), 122.2 (Ar*C*), 121.4 (Ar*C*), 113.9 (Ar*C*), 113.4 (Ar*C*), 61.2 (ArCH_2N), 53.8 (2 x NCH_2CH_2), 34.2 (*C*(CH_3)$_3$), 34.0 (*C*(CH_3)$_3$), 31.5 (C(*C*H_3)$_3$), 31.3 (C(*C*H_3)$_3$), 25.6 (2 x NCH_2CH_2), 23.8 (N $CH_2CH_2CH_2$); FAB MS, *m/z* 423 (MH^+).

N-(*t*-butoxycarbonyl)-2-amino-4-*t*-butyl-6-piperidinyl-phenol

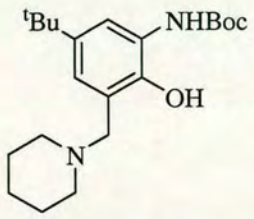

A solution of *N*-(*t*-butoxycarbonyl)-2-amino-4-*t*-butyl-phenol (1.80 g, 6.90 mmol) and 1-ethoxymethylpiperidine (1.00 g, 6.90 mmol) was stirred at reflux in acetonitrile (30 ml) for 5 days. The resulting solution was concentrated *in vacuo* then recrystallised from ethanol to yield a colourless crystalline material suitable for crystallography (1.80 g, 71%); ν_{max}/cm^{-1} (nujol) 3423 (OH), 1730 (C=O), 1531 (Ar C=C), 1377 (^tBu CH_3); (Anal. Calc. for $C_{21}H_{34}N_2O_3$: C, 69.6; H, 9.5; N, 7.7. Found: C, 69.6; H, 9.8; N, 7.5%); ^1H NMR (250 MHz, $CDCl_3$) δ 7.92 (s, 1H, N*H*), 6.99 (s, 1H, Ar*H*), 6.54 (d, 1H, *J* 2.3 Hz, Ar*H*), 3.57 (s, 2H, ArCH_2N), 2.45-2.41 (m, 4H, 2 x NCH_2CH_2), 1.57-1.53 (m, 4H, 2 x NCH_2CH_2), 1.48-1.43 (m, 11H, $NCH_2CH_2CH_2$, $OC(CH_3)_3$), 1.20 (s, 9H, $ArC(CH_3)_3$); ^{13}C NMR (250 MHz, $CDCl_3$) δ 153.4 (*C*=O), 144.2 (Ar*C*), 142.2 (Ar*C*), 126.7 (Ar*C*), 119.9 (Ar*C*), 118.8 (Ar*C*), 114.9 (Ar*C*), 80.2 ($OC(CH_3)_3$), 62.7 ($ArCH_2N$), 54.3 (2 x NCH_2CH_2), 34.7 ($ArC(CH_3)_3$), 32.0 ($OC(CH_3)_3$), 28.8 ($ArC(CH_3)_3$), 26.2 (2 x NCH_2CH_2), 24.3 ($NCH_2CH_2CH_2$); FAB MS, *m/z* 363 (MH^+).

2-Amino-4-*t*-butyl-6-piperidinyl-phenol trifuoroacetic acid salt

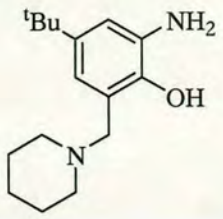

N-(*t*-butoxycarbonyl)-2-amino-4-*t*-butyl-6-piperidinyl-phenol (310 mg, 0.86 mmol) was dissolved in dichloromethane (10 ml). Trifluoroacetic acid was added (3.18 ml, 42.8 mmol) and the mixture stirred for 5 days. The reaction was quenched with a saturated solution of sodium carbonate (10 ml) and extracted with dichloromethane (3 x 15 ml). The combined organics were washed with saturated sodium chloride solution (10 ml) and dried over magnesium sulfate. The solution was concentrated and dried *in vacuo* to yield a colourless powder as the di-TFA salt (252 mg, 78%); ν_{max}/cm^{-1} (nujol) 3471 (OH), 1502 (Ar C=C), 1377 (^tBu CH_3); (Anal. Calc. for $C_{16}H_{26}N_2O.2(C_2HO_2F_3)$: C, 49.0; H, 5.8; N, 5.7. Found: C, 49.4; H, 5.8; N, 6.0%); ^1H NMR (250 MHz, MeOD) δ 6.61 (d, 1H, *J* 2.4 Hz, Ar*H*), 6.32 (d, 1H, *J* 2.4 Hz, Ar*H*), 3.55 (s, 2H, ArCH_2N), 2.75-2.05 (m, 2H, NCH_2CH_2), 1.60-1.56 (m, 2H, NCH_2CH_2), 1.42-1.32 (m, 6H, 2 x NCH_2CH_2, $NCH_2CH_2CH_2$), 1.16 (s, 9H, Ar$C(CH_3)_3$); ^{13}C NMR (250 MHz, MeOD) δ 147.5 (Ar*C*), 146.6 (Ar*C*), 128.2 (Ar*C*), 127.9 (Ar*C*), 122.4 (Ar*C*), 120.1 (Ar*C*), 56.9 (ArCH_2N), 54.4 (2 x NCH_2CH_2), 35.6 (Ar$C(CH_3)_3$), 32.1 (Ar$C(CH_3)_3$), 24.4 (2 x NCH_2CH_2), 23.1 ($NCH_2CH_2CH_2$); FAB MS, *m/z* 263 (MH^+).

Ligand 6

4-*t*-Butyl-2-{[(*E*)-5-*t*-butyl-2-hydroxy-phenylimino]-methyl}-6-piperidinyl-phenol

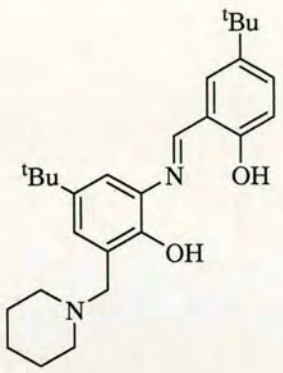

A solution of 2-Amino-4-*t*-butyl-6-piperidinyl-phenol trifuoroacetic acid salt (131 mg, 0.27 mmol) and 2-hydroxy-5-*t*-butylbenzaldehyde (47.6 mg, 0.27 mmol) was stirred in methanol (15 ml) for 24 hours. The resulting solution reduced to small volume, recrystallised from methanol, concentrated and dried *in vacuo* to yield an orange powder. (114 mg, 83%); ν_{max}/cm^{-1} (nujol) 3371 (OH), 1667 (N=C), 1377 (^tBu CH_3); (Anal. Calc. for $C_{27}H_{38}N_2O_2$: C, 76.7; H, 9.1; N, 6.6. Found: C, 76.7; H, 8.8; N, 6.9%); ^1H NMR (360 MHz, MeOD) δ 8.81 (s, 1H, ArC*H*N), 7.58 (d, 1H, *J* 2.5 Hz, Ar*H*), 7.43 (dd, 1H, *J* 8.7, 2.5 Hz, Ar*H*), 7.32-7.27 (m, 2H, 2 x Ar*H*), 6.83 (d, 1H, *J* 8.7 Hz, Ar*H*), 4.27 (s, 2H, ArCH_2N), 3.41 (br d, 2H, *J* 11.8 Hz, NCH_2CH_2), 2.94 (br t, 2H, *J* 11.8 Hz, NCH_2CH_2), 1.89-1.70 (m, 4H, 2 x NCH_2CH_2), 1.25 (s, 9H, $C(CH_3)_3$); ^{13}C NMR (360 MHz, MeOD) δ165.5 (Ar*C*HN), 159.2 (Ar*C*), 148.6 (Ar*C*), 145.0 (Ar*C*), 143.0 (Ar*C*), 138.7 (Ar*C*), 131.8 (Ar*C*), 130.1 (Ar*C*), 128.5 (Ar*C*), 119.9 (Ar*C*), 119.2 (Ar*C*), 117.8 (Ar*C*), 117.0 (Ar*C*), 56.6 (ArCH_2N), 53.7 (2 x $NCH_2CH_2CH_2$), 35.0 ($C(CH_3)_3$), 34.6 ($C(CH_3)_3$), 31.6 ($C(CH_3)_3$), 31.5 ($C(CH_3)_3$), 23.6 (2 x $NCH_2CH_2CH_2$), 22.3 ($NCH_2CH_2CH_2$);FAB MS, *m/z* 422 (MH^+).

Ligand 7

4-*t*-Butyl-2-{[(*E*)-5-*t*-butyl-3-piperidinyl-2-hydroxy-phenylimino]-methyl}-6-piperidinyl-phenol

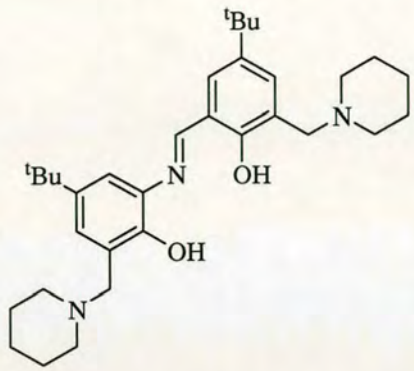

A solution of 2-amino-4-*t*-butyl-6-piperidinyl-phenol (260 mg, 0.53 mmol) and 2-hydroxy-3-piperidinyl-5-*t*-butyl-benzaldehyde (150 mg, 0.54 mmol) was stirred in methanol (60 ml) for 4 hours. The resulting solution was recrystallised from methanol, concentrated and dried *in vacuo* to yield a yellow/orange powder (331 mg, 100%); ν_{max}/cm^{-1} (nujol) 3392 (OH), 1621 (N=C), 1377 (^tBu CH_3); (Anal. Calc. for $C_{33}H_{49}N_3O_2$: C, 76.3; H, 9.5; N, 8.1. Found: C, 76.3; H, 9.3; N, 8.3%); ^1H NMR (360 MHz, MeOD) δ 8.99 (s, 1H, ArC*H*N), 7.81 (d, 1H, *J* 2.5 Hz, Ar*H*), 7.68 (d, 1H, *J* 2.5 Hz, Ar*H*), 7.43 (d, 1H, *J* 2.3 Hz, Ar*H*), 7.35 (d, 1H, *J* 2.3 Hz, Ar*H*), 4.41 (s, 2H, ArCH_2N), 4.26 (s, 2H, ArCH_2N), 3.19-3.15 (m, 8H, 4 x NCH_2CH$_2$), 1.91-1.85 (m, 8H, 4 x NCH$_2$CH_2), 1.70 (br s, 4H, 2 x NCH$_2$CH$_2$CH_2), 1.40 (s, 18H, 2 x C(CH_3)$_3$); ^{13}C NMR (360 MHz, MeOD) δ 164.3 (Ar*C*HN), 161.0 (Ar*C*), 149.6 (Ar*C*), 144.9 (Ar*C*), 142.9 (Ar*C*), 136.6 (Ar*C*), 135.3 (Ar*C*), 133.1 (Ar*C*), 128.5 (Ar*C*), 120.4 (Ar*C*), 120.0 (Ar*C*), 118.7 (Ar*C*), 118.2 (Ar*C*), 58.5 (Ar*C*H$_2$N), 56.5 (ArCH$_2$N), 54.2 (4 x N*C*H$_2$CH$_2$CH$_2$), 35.3 (*C*(CH$_3$)$_3$), 35.1 (*C*(CH$_3$)$_3$), 31.8 (C(*C*H$_3$)$_3$), 31.7 (C(*C*H$_3$)$_3$), 24.8 (2 x NCH$_2$*C*H$_2$CH$_2$), 24.0 (2 x NCH$_2$*C*H$_2$CH$_2$), 23.3 (NCH$_2$CH$_2$*C*H$_2$), 22.7 (NCH$_2$CH$_2$*C*H$_2$); FAB MS, *m/z* 520 (MH^+).

1-*t*-Butyl-4-(piperidinyl)methylbenzene

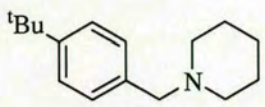

To an excess of piperidine (8.70 ml, 88.0 mmol) in dichloromethane (100 ml) at 0 °C was added 4-*t*-butylbenzylbromide (5.00 g, 22.0 mmol) and the resulting solution stirred overnight at room temperature. The solution was concentrated *in vacuo*. The residue was washed with an aqueous solution of sodium hydroxide (30 ml, 4 M) and then extracted with diethyl ether (3 x 100 ml). The combined organics were dried over magnesium sulfate, concentrated and dried *in vacuo* to give a colourless oil (4.15 g, 82%); ^{1}H NMR (250 MHz, D_2O) δ 6.98 (d, 2H, *J* 8.2 Hz, 2 x Ar*H*), 6.82 (d, 2H, *J* 8.2 Hz, 2 x Ar*H*), 3.62 (s, 2H, CH_2), 2.82 (br d, 2H, *J* 12.6 Hz, NCH_2), 2.26 (br t, 2H, *J* 12.6 Hz NCH_2), 1.40-0.96 (m, 6H, 2 x $NCH_2CH_2CH_2$, $NCH_2CH_2CH_2$), 0.69 (s, 9H, $C(CH_3)_3$); ^{13}C NMR (360 MHz, D_2O) δ 154.5 (Ar*C*), 131.9 (2 x Ar*C*), 127.0 (2 x Ar*C*), 126.6 (Ar*C*), 60.8 ($ArCH_2N$), 53.4 (2 x NCH_2CH_2), 34.9 ($ArC(CH_3)_3$), 31.1 ($ArC(CH_3)_3$), 23.4 (2 x NCH_2CH_2), 21.9 ($NCH_2CH_2CH_2$); FAB MS, *m/z* 230 (MH^+).

1-*t*-Butyl-4-(dihexylamino)methylbenzene

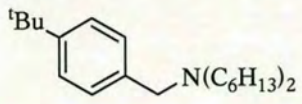

To an excess of dihexylamine (30.0 g, 162 mmol) in dichloromethane (150 ml) at 0 °C 4-*t*-butylbenzylbromide (11.9 g, 52.5 mmol) was added and the resulting solution stirred overnight at room temperature. The solution was concentrated *in vacuo*. The residue was washed with an aqueous solution of sodium hydroxide (150 ml, 4 M) and then extracted with diethyl ether (3 x 50 ml). The combined organics were dried over magnesium sulfate, concentrated and purified by column chromatography on silica gel, eluting with 10% methanol in dichloromethane to give a brown oil (10.8 g, 62%); ^{1}H NMR (250 MHz, $CDCl_3$) δ 7.24 (d, 2H, *J* 7.9 Hz, 2 x Ar*H*), 7.16 (d, 2H, *J* 7.9 Hz, 2 x Ar*H*), 3.47 (s, 2H, ArCH_2N), 2.37 (t, 4H, *J* 7.3 Hz, 2 x N$CH_2(CH_2)_4CH_3$), 1.48-1.36 (m, 4H, 2 x $NCH_2CH_2(CH_2)_3CH_3$), 1.27-1.16 (m, 21H, 2 x $NCH_2CH_2(CH_2)_3CH_3$, $C(CH_3)_3$), 0.81-0.76 (m, 6H, 2 x $N(CH_2)_5CH_3$); ^{13}C NMR (250 MHz, $CDCl_3$) δ 150.2 (Ar*C*), 136.1 (Ar*C*), 132.3 (Ar*C*), 129.2 (Ar*C*), 126.3 (Ar*C*), 125.4 (Ar*C*), 58.2 (2 x $NCH_2(CH_2)_4CH_3$), 53.8 ($ArCH_2N$), 34.8 ($C(CH_3)_3$), 32.1 (2 x $N(CH_2)_3CH_2CH_2CH_3$), 31.7 ($C(CH_3)_3$), 27.4 (2 x $NCH_2CH_2(CH_2)_3CH_3$), 26.8 (2 x $N(CH_2)_2CH_2(CH_2)_2CH_3$), 23.0 (2 x $N(CH_2)_4CH_2CH_3$), 14.4 (2 x $N(CH_2)_5CH_3$);

3-*iso*-Propyl-2-pyrazol-5-one

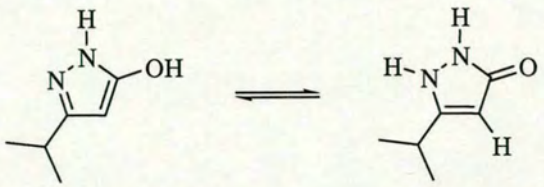

To a solution of hydrazine monohydrate (7.7 ml, 160 mmol) in methanol (150 ml) at 0 °C was added ethyl-*iso*-butyrylacetate (25.5 ml, 160 mmol) dropwise. The solution was stirred at 0 °C for 4 h before heating at reflux for 24 h. The solution was concentrated *in vacuo,* the solid washed with hot hexane and dried *in vacuo* to give a cream solid (18.8 g, 98%); ν_{max}/cm^{-1} (nujol) 2964 (NH), 1628 (C=O); (Anal. Calc. for $C_6H_{10}N_2O$: C 57.1; H 8.0; N 22.2. Found: C, 57.2; H, 8.0; N, 22.0%); ^1H NMR (250 MHz, MeOD) δ 4.45 (s, 1H, C*H*C=O), 2.00 (sept, 1H, *J* 7.0 Hz, C*H*$(CH_3)_2$), 0.37 (d, 6H, *J* 7.0 Hz, CH(C*H*$_3)_2$); ^{13}C NMR (360 MHz, MeOD) δ 164.3 (Ar*C*), 155.6 (Ar*C*), 88.2 (*C*HC=O), 27.6 (*C*H$(CH_3)_2$), 22.0 (CH(*C*$H_3)_2$); FAB MS, *m/z* 127 (MH^+).

2-Hydroxy-3-piperidinyl-5-nonyl-benzaldehyde

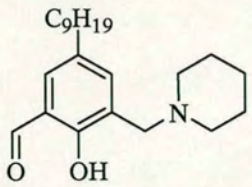

A solution of 2-hydroxy-5-nonylbenzaldehyde (12.5 g, 50.4 mmol) and 1-ethoxymethylpiperidine (7.90 g, 55.2 mmol) in acetonitrile (100 ml) was stirred at reflux under a flow of nitrogen for 6 days. The solution was concentrated and dried *in vacuo* to yield an orange oil (12.7 g, 73%); ν_{max}/cm^{-1} (neat) 3396 (OH), 1683 (C=O); ^1H NMR (250 MHz, $CDCl_3$) δ 10.40 (s, 1H, C*H*O), 7.61-7.51 (m, 1H, Ar*H*), 7.22-7.14 (m, 1H, Ar*H*), 3.71 (s, 2H, ArCH_2N), 2.53 (br s, 4H, 2 x NCH_2CH_2), 1.71-1.64 (m, 4H, NCH_2CH_2), 1.27-1.19 (m, 2H, NCH_2CH_2CH_2), 0.81-0.74 (m, 19H, C_9H_{19}); FAB MS, *m/z* 346 (MH^+);

4-Nonyl-2-nitrophenol

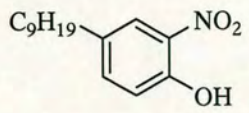

To a solution of 4-nonylphenol (5.00 g, 22.7 mmol) in chloroform (46 ml) was added $Fe(NO_3)_3.9H_2O$ (9.17 g, 22.7 mmol) and the solution heated at 40 °C for 3 hours. The reaction was quenched by addition of HCl (100 ml, 1 M) and the organics separated. The aqueous was extracted with $CHCl_3$ (3 x 50 ml), the combined organics were washed with saturated sodium chloride solution (50 ml), dried over magnesium sulfate and concentrated *in vacuo* to yield a brown oil (6.00 g, 99%); ν_{max}/cm^{-1} (neat) 3251 (OH), 1537 (NO_2), 1322 (NO_2); ^1H NMR (250 MHz, $CDCl_3$) δ 10.40 (s, 1H, O*H*), 7.95-7.86 (m, 1H, Ar*H*), 7.52-7.43 (m, 1H, Ar*H*), 7.00 (d, 1H, *J* 8.8 Hz, Ar*H*), 1.78-0.55 (m, 19H, C_9H_{19}); FAB MS, *m/z* 266 (MH^+).

4-Nonyl-2-aminophenol

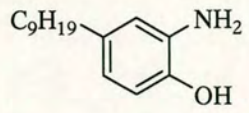

To a solution of 4-nonyl-2-nitrophenol (5.90 g, 22.3 mmol) in methanol (50 ml) was added 10% Pd/C (500 mg), the solution was vigorously stirred under an atmosphere of hydrogen (1 atm) for 24 hours. The solution was filtered through celite (pre-washed with methanol) and the celite pad thoroughly washed with methanol (100 ml). The filtrate was concentrated *in vacuo* to give the product as a red solid (5.18 g, 100%); ν_{max}/cm^{-1} (nujol) 3242 (OH), 1517 (Ar C=C); (Anal. Calc. for $C_{15}H_{25}NO$: C 76.6; H 10.7; N 6.0. Found: C, 76.7; H, 10.7; N, 5.9%); ^1H NMR (250 MHz, $CDCl_3$) δ 7.45-7.41 (m, 1H, Ar*H*), 7.01-6.83 (m, 2H, 2 x Ar*H*), 6.70 (br s, 3H, NH_2, O*H*), 1.61-0.66 (m, 19H, C_9H_{19}); FAB MS, *m/z* 236 (MH^+).

Ligand 9

4-Nonyl-2-{[(*E*)-5-*t*-butyl-2-hydroxy-phenylimino]-methyl}-6-piperidinyl-phenol

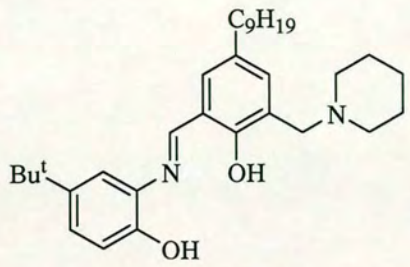

A solution of 2-amino-4-*t*-butyl-phenol (283 mg, 1.72 mmol) and 2-hydroxy-3-piperidinyl-5-nonyl-benzaldehyde (591 mg, 1.72 mmol) was stirred in methanol (25 ml) for 4 hours. The resulting solution was concentrated and dried *in vacuo* to yield a yellow/orange oil (850 mg, 100%); ν_{max}/cm^{-1} (nujol) 3405 (OH), 1620 (N=C), 1377 (^{t}Bu CH_3); ^{1}H NMR (250 MHz, MeOD) δ 9.07 (s, 1H, ArC*H*N), 7.62-7.44 (m, 3H, 3 x Ar*H*), 7.29 (dd, 1H, *J* 8.5, 2.4 Hz, Ar*H*), 6.98 (d, 1H, *J* 8.5 Hz, Ar*H*), 3.81 (br s, 2H, ArCH_2N), 2.69 (br s, 4H, 2 x NCH_2CH$_2$), 1.75-1.73 (m, 4H, 2 x NCH$_2$CH_2), 1.61-1.60 (m, 2H, NCH$_2$CH$_2$CH_2), 1.46 (s, 9H, C(CH_3)$_3$), 1.46-0.65 (m, 19H, C$_9$H$_{19}$); FAB MS, *m/z* 493 (MH$^+$).

Ligand 10

4-Nonyl-2-{[(*E*)-5-nonyl-2-hydroxy-phenylimino]-methyl}-6-piperidinyl-phenol

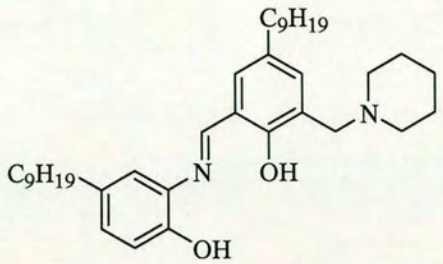

A solution of 2-amino-4-nonylphenol (250 mg, 1.06 mmol) and 2-hydroxy-3-piperidinyl-5-nonyl-benzaldehyde (366 mg, 1.06 mmol) was stirred in methanol (20 ml) for 4 hours. The resulting solution was concentrated and dried *in vacuo* to yield a red oil (596 mg, 100%); ν_{max}/cm^{-1} (nujol) 3410 (OH), 1620 (N=C), 1504 (Ar C=C); ^1H NMR (250 MHz, MeOD) δ 9.02 (s, 1H, ArC*H*N), 7.56-7.29 (m, 3H, 3 x Ar*H*), 7.31-7.20 (m, 1H, Ar*H*), 6.89 (d, 1H, *J* 8.5 Hz, Ar*H*), 4.06 (br s, 2H, ArCH_2N), 2.95 (br s, 4H, 2 x NCH_2CH$_2$), 1.76-0.69 (m, 44H, 2 x NCH$_2$CH_2, NCH$_2$CH$_2$CH_2, 2 x C$_9H_{19}$); FAB MS, *m/z* 563 (MH^+).

.

5.3 Metal complex synthesis

General complex synthesis

For the synthesis of each "metal-only" complex, methanol solutions of the ligand and the appropriate metal acetate were combined and left to stir for 2 hours. In some cases a precipitate was formed which was collected and dried before redissolving in dichloromethane and washing with aqueous ammonia to remove any residual acetic acid. When no precipitate was formed, the solution was concentrated and dried *in vacuo* before redissolving and washing as before. The washed organic solution was dried over magnesium sulfate, concentrated and dried *in vacuo* to yield the metal complex. Complexes were recrystallised from methanol. The maximum yield is calculated assuming a 1: 1 ligand to metal ratio. The complexes were analysed by ICP-OES and CHN analysis, IR and FAB mass spectrometry, and the mass shown is for the 2 : 2 complex, unless otherwise stated.

$[Ni_2(\mathbf{1}\text{-}2H)_2]$ was prepared as described above from ligand **1** (1.0 g, 3.08 mmol) in methanol (10 ml) and $Ni(CH_3COO)_2.4H_2O$ (0.77 g, 3.08 mmol) in methanol (5 ml) to yield a yellow/brown solid (0.80 g, 68%); ν_{max}/cm^{-1} (nujol) 1616 (N=C), 1376 (^tBu CH_3); (Ni-content by ICP-OES for a 0.00025M solution in butan-1-ol: found 19.71 ppm, $C_{21}H_{25}NO_2Ni$ requires 18.21 ppm); (Anal. Calc. for $C_{21}H_{25}NO_2Ni.CH_3O$: C 64.0; H 6.8; N 3.4. Found: C, 63.8; H, 6.7; N, 3.7%); FAB MS, *m/z* 763 (MH^+).

$[Cu_2(\mathbf{1}\text{-}2H)_2]$ was prepared as described above from ligand **1** (1.0 g, 3.08 mmol) in methanol (10 ml) and $Cu(CH_3COO)_2.H_2O$ (0.61 g, 3.08 mmol) in methanol (5 ml) to yield a yellow solid (1.08 g, 91%); ν_{max}/cm^{-1} (nujol) 1617 (N=C), 1376 (^tBu CH_3); (Cu-content by ICP-OES for a 0.00025M solution in butan-1-ol: found 19.58 ppm, $C_{21}H_{25}NO_2Cu$ requires 19.60 ppm); (Anal. Calc. for $C_{21}H_{25}NO_2Cu.CH_3O$: C, 63.2; H, 6.8; N, 3.4. Found: C 63.0; H 6.7; N 3.7%); FAB MS, *m/z* 773 (MH^+).

$[Ni_2(\mathbf{5}\text{-}2H)_2]$ was prepared as described above from ligand **5** (1.0 g, 2.37 mmol) in methanol (5 ml) and $Ni(CH_3COO)_2.4H_2O$ (0.58 g, 2.37 mmol) in methanol (5 ml) to yield a dark brown solid (0.79 g, 70%); ν_{max}/cm^{-1} (nujol) 1612 (N=C), 1377 (^tBu CH_3); (Ni-content by ICP-OES for a 0.00025M solution in butan-1-ol: found 18.43 ppm, $C_{27}H_{36}N_2O_2Ni$ requires 18.21 ppm); (Anal. Calc. for $C_{27}H_{36}N_2O_2Ni.CH_3O$: C 65.9; H 7.7; N 5.5. Found: C, 65.6; H, 7.9; N, 5.8%); FAB MS, *m/z* 957 (MH^+).

$[Cu_2(\mathbf{5}\text{-}2H)_2]$ was prepared as described above from ligand **5** (1.0 g, 2.37 mmol) in methanol (5 ml) and $Cu(CH_3COO)_2.H_2O$ (0.47 g, 2.37 mmol) in methanol (5 ml) to yield a yellow solid (1.06 g, 92%); ν_{max}/cm^{-1} (nujol) 1613 (N=C), 1377 (^tBu CH_3); (Cu-content by ICP-OES for a 0.00025M solution in butan-1-ol: found 19.61 ppm, $C_{27}H_{36}N_2O_2Cu$ requires 19.60 ppm); (Anal. Calc. for $C_{27}H_{36}N_2O_2Cu.CH_3O$: C 65.3; H 7.6; N 5.4. Found: C, 65.0; H, 7.9; N, 5.7%); FAB MS, *m/z* 969 (MH^+).

$[Ni_2(\mathbf{7}\text{-}2H)_2]$ was prepared as described above from ligand **7** (1.0 g, 1.93 mmol) in methanol (5 ml) and $Ni(CH_3COO)_2.4H_2O$ (0.48 g, 1.93 mmol) in methanol (5 ml) to yield a yellow/brown solid (0.93 g, 84%); ν_{max}/cm^{-1} (nujol) 1617 (N=C), 1377 (^tBu CH_3); (Ni-content by ICP-OES for a 0.00025M solution in butan-1-ol: found 17.97 ppm, $C_{33}H_{47}N_3O_2Ni$ requires 18.21 ppm); (Anal. Calc. for $C_{33}H_{47}N_3O_2Ni.CH_3O$: C 67.2; H 8.3; N 6.9. Found: C, 67.0; H, 8.5; N, 7.2%); FAB MS, *m/z* 1151 (MH^+).

$[Cu(\mathbf{7}\text{-}2H)]^*$ was prepared as described above from ligand **7** (1.0 g, 1.93 mmol) in methanol (5 ml) and $Cu(CH_3COO)_2.H_2O$ (0.39 g, 1.93 mmol) in methanol (5 ml) to yield a brown solid (0.81 g, 72%); ν_{max}/cm^{-1} (nujol) 1616 (N=C), 1377 (^tBu CH_3); (Cu-content by ICP-OES for a 0.00025M solution in butan-1-ol: found 19.47 ppm, $C_{33}H_{47}N_3O_2Cu$ requires 19.60 ppm); (Anal. Calc. for $C_{33}H_{47}N_3O_2Cu.CH_3O$: C 67.0; H 8.2; N 6.9. Found: C, 66.8; H, 8.2; N, 7.1%); FAB MS, *m/z* 582 (MH^+).

---

* No evidence for 2:2 structure, 1:1 complex mass quoted.

$[Ni_2(\mathbf{8}\text{-}2H)_2]$ was the product of recrystallisation of $[Ni_2(\mathbf{2}\text{-}2H)_2]$ from ethanol and yielded crystals suitable for X-ray analysis (section 3.3).

$[Cu_2(\mathbf{10}\text{-}2H)_2]$ was prepared as described above from ligand **10** (1.0 g, 1.78 mmol) in methanol (15 ml) and $Cu(CH_3COO)_2.H_2O$ (0.36 g, 1.78 mmol) in methanol (20 ml) to yield a red/brown solid (1.06 g, 95%); ν_{max}/cm^{-1} (nujol) 1613 (N=C), 1504 (Ar C=C); (Cu-content by ICP-OES for a 0.00025M solution in butan-1-ol: found 19.63 ppm, $C_{37}H_{56}N_2O_2Cu$ requires 19.60 ppm); (Anal. Calc. for $C_{37}H_{56}N_2O_2Cu.CH_3O$: C 69.6; H 9.1; N 4.3. Found: C, 69.3; H, 9.1; N, 4.3%); FAB MS, *m/z* 1249 (MH^+).

5.4 Liquid : liquid extraction experiments

All extractions were carried out at least twice to ensure reproducibility and confirm validity of results. Aqueous phases were also analysed to ensure an overall mass balance for the metal, allowing us to account for 95% ± 5% at all point in the extraction.

5.4.1 Stripping

Generally experiments were carried out in sealed glass jars containing a solution of the "metal-only" complex $[M(\mathbf{L}\text{-}2H)]_n$ (0.00250 M) in chloroform (5.0 ml) and an acid in water (5.0 ml) at constant anion concentration (0.800 M) and a chosen pH. The pH solutions were made using H_2SO_4 / Na_2SO_4, or HCl / NaCl, adding volumes of each to reach the desired pH in the range 0-7. The mixtures were stirred for 16 hours at room temperature, and the organic and aqueous layers allowed to separate. A 1.00 ml aliquot was removed from the organic layer, evaporated *in vacuo* and redissolved and made up to 10.0 ml in butan-1-ol. The metal and sulphur content were analysed using ICP-OES. The equilibrium pH of the aqueous layer was measured and the loading in the organic phase was expressed as the percentage of the total metal/sulphur in the system present in the organic.

In order to measure the chloride concentration of the organic solutions, a "back-extraction" had to be performed since chloride cannot be determined quantitatively by ICP-OES. A 2.00 ml aliquot of the organic solution was contacted with 10 ml of HNO_3 solution (0.1 M) for 2 hours to transfer all chloride anions to the aqueous phase. 5.0 ml portions of the resulting aqueous solutions were transferred to 10.0 ml volumetric flasks, diluted with NaOH solution (0.1 M) to ensure a pH in the range suitable for use of the chloride-selective electrode (2 – 12) and then made up to volume. The chloride concentration was determined by a chloride-selective electrode.

If the chloride to ligand to copper ratio in the metal chloride complex is 1 : 1 : 1 then 100% loading in the extraction experiments will generate an aqueous solution, after

back stripping as above, with a chloride concentration of 0.00025 M. The chloride-selective electrode was therefore calibrated in the concentration range of 0.0025 M to 0.000025 M. This was performed before each analysis by preparing a series of solutions of known chloride concentration. Each solution's potential (mV) was recorded using the chloride-selective electrode, using solutions of known chloride concentration to plot the straight line graph shown in Figure 5.1. The concentration was the determined using the following equation,

$$[Cl^-]_{sample} = \exp((P - I)/S)$$

where $[Cl^-]_{sample}$ is the unknown chloride concentration, P is the potential (mV) recorded by the chloride electrode, I is the intercept of the calibration graph and S is the slope of the calibration graph.

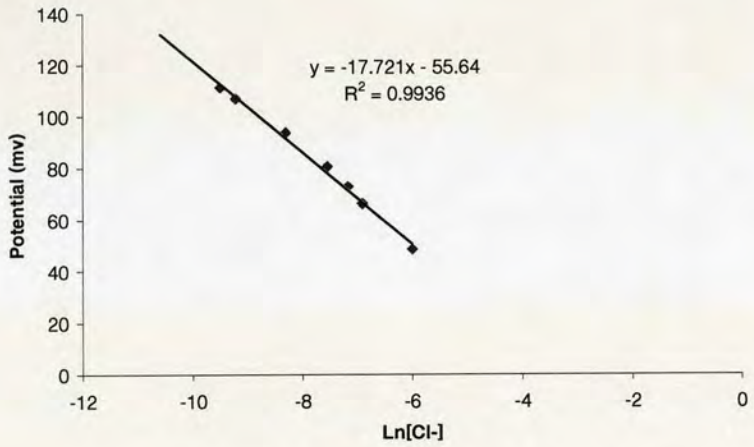

Figure 5.1: Calibration of the chloride electrode.

5.4.2 Loading

Loading experiments were also carried out in sealed glass jars. A solution of known concentration (0.00250 M) of the ligand in chloroform (5.0 ml) was contacted with a metal salt ($CuSO_4$ or $CuCl_2$, 0.003125 M) in water (5.0 ml). The aqueous solution contained 4.0 ml of the metal salt and 1.0 ml of varied concentrations of NaOH or H_2SO_4 solutions to obtain the desired pH and a constant metal salt concentration

equivalent to that of the ligand. The solutions were then stirred, separated and analysed as in the stripping experiment.

5.4.3 Load/Strip Cycles

Load: A solution of known concentration (0.0025 M) of ligand in chloroform was contacted with an aqueous solution of $CuSO_4$ (1.0 M). The extraction was stirred for 1 hour then separated. A 1.00 ml aliquot was removed from the organic layer, evaporated *in vacuo* and redissolved and made up to 10.0 ml in butan-1-ol. The metal and sulphur content were analysed using ICP-OES and the equilibrium pH of the aqueous layer was measured.

Strip: The remaining organic layer separated from the $CuSO_4$ solution, contacted with H_2SO_4 (150 g l^{-1}) and stirred for 1 hour. The layers were separated and analysed as before.

The load/strip cycle was repeated 2-4 times.

5.4.4 Selectivity of copper(II)/ iron(III)

Loading experiments were carried out as in section 5.4.2, with the addition of iron(III) sulfate (0.003125 M) to the aqueous phase.

5.4.5 Selectivity of sulfate/chloride

Stripping experiments were carried out as in section 5.4.1. The aqueous layer consisted of equal volumes (2.50 ml) of the stock sulfate and chloride solutions of similar pH to obtain a range of pH solutions at constant and equal anion concentration (0.800 M).

5.5 X-ray Crystallography

The structure of Ligand **1** was determined by Dr Stephen Moggach, the Ligand **1** nickel cubane by Dr Simon Parsons and all other structures by Mr Fraser White. All files can be found on the appendix CD. Data were collected on a Bruker SMART Apex CCD diffractometer equipped with an Oxford Cryosystems low temperature device operating at 150 K, using Mo-Kα radiation.

All structures were solved by direct methods (SHELXTL) (patterson dirdif) and refined by interative cycles of least squares refinement against F^2 and difference Fourier synthesis (SHELXTL). Most H-atoms were idealized, being placed geometrically and treated by riding methods. All hydrogen atoms attached to hetero-atoms were placed using difference maps. All non-H atoms were modelled with anisotropic displacement parameters. Refinement parameters for all crystal structures can be found in the attached files in the appendices.

5.6 EPR

Following determination of loading of copper by ICP-OES, a number of points (usually seven) that represented an even distribution between the highest and lowest copper(II) extractions were selected for EPR analysis. Samples from the organic phase were analysed and these were taken directly from the freshly separated extraction experiments. Each spectrum was recorded with a modulation of 4, the variable parameters used for each ligand system are shown in Table 5.1.

Ligand System	Centre Field (G)	Sweep Width (G)	Gain	Frequency (GHz)	Power (mW)	Sweep Time (s)
Ligand **1**	3365	1000	400000	9.7	32	100
Ligand **1** + L_{aux}	3320	500	100000	9.72	32	100
Ligand **5**	3320	300	200000	9.71	32	100
Ligand **10**	3350	300	250000	9.72	32	100

Table 5.1: EPR parameters.

The parameters obtained from a copper(II) EPR spectrum give an insight into the bonding and donor environment. The copper and nitrogen hyperfine coupling

constants (A^{Cu} and A^{N}) can be used to predict the location of the unpaired electron of the copper(II) ion in the system. The spectroscopic splitting factor (g) varies from that of a free electron (2.0023) with respect to the coupling environment. Coupling to unoccupied orbitals results in a decrease in g, whilst coupling to filled orbitals such as with copper(II) causes an increase in g.

Ligand System	g	A^{Cu} (G)	A^{N} (G)
Ligand **1** + L_{aux}	2.108	91.7	10.3 and 21.7
Ligand **5**	2.214	80.0	-
Ligand **10**	2.214	80.0	-

Table 5.2: EPR parameters from modelled spectra.

CHAPTER 6

Conclusions

The main objective of the work described in this thesis was to design, synthesise and investigate the properties of a series of ligands capable of improving the metal transport efficiency of solvent extraction, and also of extracting metal salts. Such extractants could provide circuits with improved environmental impact and be able to address feed solutions of higher tenors than those currently used with commercial extractants.

It was first necessary to consider design features for ligands capable of multiloading divalent metals. A fundamental parameter in design is the preferred geometry of the loaded metal and this is clearly metal-dependent. Nickel and copper, which show a preference for planar donor sets were chosen, being of considerable current interest to the metallurgical industries. Imine ligands derived from substituted salicylaldehydes and 2-aminophenols with a dianionic planar O, N, O metal binding site were synthesised. Whilst this type of ligand (**1**) gave very interesting coordination chemistry with nickel(II), a 4 : 4 ligand to nickel species with unusual magnetic properties, the "strength" of binding was far weaker than that required from a commercial extractant, and its $pH_{½}$ was too high for industrial use. Therefore, no further studies were carried out with nickel. The observation that high nuclearity complexes can be formed by these diphenolate ligands provides an avenue for interesting research outwith the remit of the current thesis but also could present problems in metal recovery because the rates of extraction and stripping are likely to be low if complicated, high molecular weight assemblies are involved. Also, the solubilities of such species might be low in water-immiscible media.

Copper extractions with ligand **1** proved more promising than with nickel, with a significantly lower $pH_{½}$, and using EPR spectroscopy to probe the solution stoichiometry of extracted species suggested that multinuclear complexes were present. The ligand was also capable of forming mononuclear copper species, when an additional ligand, 3-*iso*-propyl-2-pyrazol-5-one (L_{aux}) was introduced into the extraction experiment. This species was interpreted to be a ternary complex with 1 : 1 : 1 ligand to copper to L_{aux} stoichiometry and formed at a lower $pH_{½}$, suggesting

that it is more stable than binary complexes. EPR studies supported this interpretation, with the presence of a copper signal displaying hyperfine coupling to two individual nitrogen donors which increased in intensity with an increase of copper concentration. Comparing the mass transport efficiency of the commercial copper extractant, P50 to ligand **1** and the **1** + L_{aux} blend indicates that an improvement was achieved, although the actual strength of binding was only comparable in the case of the ternary complex.

Having established that ligand **1** was capable of the multiloading extraction behaviour it had been designed to perform; analogues capable of binding the cation and its attendant anion were investigated. Initial studies suggested that the monosubstituted piperidino ligand, **5**, showed the desired properties. A decrease of two pH units in the $pH_{½}$ of copper-binding was observed, indicating the presence of a more stable complex. The sulfate-loading was also studied, which showed anomalous behaviour compared to previous metal salt extraction studies at Edinburgh. At low pH sulfate and copper are stripped from the organic phase. This suggested some form of cooperative binding, where loss of copper results in simultaneous sulfate loss. Increasing the sulfate concentration in the aqueous phase resulted in a decrease in $pH_{½}$ for copper loading, again suggesting that the copper-sulfate loading is cooperative. EPR studies indicated the presence of different species in different pH ranges: 1 : 1 : 1 ligand to copper to hydrogen sulfate at low pH and 2 : 2 : 1 stoichiometry of ligand to copper to sulfate at high pH.

In order to investigate whether the structure of **5** in which an anion binding site is chemically attached to the salicylaldimine metal binding site was key to the successful extraction of both copper and sulfate, a "dual-host" comparison experiment was carried out in which 1-*t*-butyl-4-dihexylaminomethylbenzene was used in a mixture with **1**. This showed that the mixture of the individual components was less efficient than the combination in one structure, and further supported the presence of cooperative binding being key to the successful loading of copper and sulfate.

Having established that ligand **5** may provide a new process for the extraction of copper and sulfate from sulfate feeds, further experiments were carried out to probe the solubility, stability and selectivity of these types of ligands under conditions similar to those which would be used in an industrial process. Ligand **10** was synthesised, which had higher solubility in non-polar solvents and lower solubility in water, imparted by the addition of hydrophobic nonyl groups. This reagent proved to have a lower $pH_{½}$ for copper-loading than **5** and displayed very promising simultaneous sulfate-loading, with both being loaded at > 90% between pH 1.5-5. This is ideal behaviour for a potential industrial copper sulfate extractant.

Investigations into the stability of ligands were less promising, showing almost complete hydrolysis of ligand **5** after just one stripping cycle and more gradual but still significant hydrolysis of **10** over several cycles. Selectivity tests were performed with **10** with copper(II)/iron(III) mixed solutions and sulfate/chloride solutions. Again, these were not at all promising, with preference of iron over copper and chloride over sulfate.

Since the concept of using ligand design to enhance the efficiency of copper transport and to develop reagents which can extract both copper(II) and sulfate ions from aqueous feed solutions has been established in this thesis, it would be of considerable scientific interest and industrial importance to consider how to achieve these properties *and* appropriate selectivity of cation and anion transport and stability to hydrolysis. As the latter is very compound-type dependent, the logical approach to this would be to tackle the selectivity challenge first. Designing the metal binding site while focussing on selectivity for copper over iron is a key feature and very challenging. Using ligands which do not contain "hard" phenolate donors which show a high affinity for iron(III) may be essential. The design of ligands which can selectively bind sulfate in the presence of chloride is also an extremely challenging task because it requires a reversal of the Hofmeister bias. A highly preorganised site with size and shape which makes it difficult to accommodate two chloride ions could favour uptake of one dianionic sulfate unit. However, very elaborate structures of this type may make the cost of the extractant prohibitively high.

CHAPTER 7

7 CHAPTER 7 189

7.1 Chapter 2 Extraction Data 191

7.2 Chapter 3 Extraction Data 195

7.3 Chapter 4 Extraction Data 203

7.4 Piperidino amine distribution coefficient studies 206

7.5 $pH_{½}$ calculations 208

7.5.1 Chapter 2 $pH_{½}$ graphs 208

7.5.2 Chapter 3 $pH_{½}$ graphs 210

7.5.3 Chapter 4 $pH_{½}$ graphs 214

Also on disk:

cif files and crystal data for

Ligand **1**

Ligand **1** + Ni cubane

Ligand **5**

Ligand **8** + Ni

Protected pip amine

Literature crystal

RJG crystal